



**THESIS APPROVAL**  
**GRADUATE SCHOOL, KASETSART UNIVERSITY**

Master of Science (Chemistry)

DEGREE

Chemistry

FIELD

Chemistry

DEPARTMENT

**TITLE:** Experimental and Theoretical Studies of 2-Methoxy-5-(2'-ethylhexyloxy)-  
1,4-phenylene-vinylene Derivatives

**NAME:** Miss Suphawarat Phalinyot

**THIS THESIS HAS BEEN ACCEPTED BY**

THESIS ADVISOR

( Mr. Songwut Suramitr, Ph.D. )

THESIS CO-ADVISOR

( Associate Professor Supa Hannongbua, Dr.rer.nat. )

THESIS CO-ADVISOR

( Miss Pimpa Hormnirun, Ph.D. )

ACTING

DEPARTMENT HEAD

( Associate Professor Supa Hannongbua, Dr.rer.nat. )

**APPROVED BY THE GRADUATE SCHOOL ON**

DEAN

( Associate Professor Gunjana Theeragool, D.Agr. )

THESIS

EXPERIMENTAL AND THEORETICAL STUDIES OF  
2-METHOXY-5-(2'-ETHYLHEXYLOXY)-1,4-PHENYLENE-  
VINYLENE DERIVATIVES

The seal of Kasetsart University is a large, light green circular emblem. It features a central figure of a deity or guardian spirit, possibly a Ganesha-like figure, standing on a lotus. The figure is surrounded by a decorative border. The words "KASETSART UNIVERSITY" are written in a semi-circle at the top, and "1943" is at the bottom. There are also small floral motifs on the sides.

SUPHAWARAT PHALINYOT

A Thesis Submitted in Partial Fulfillment of  
the Requirements for the Degree of  
Master of Science (Chemistry)  
Graduate School, Kasetsart University  
2010

Suphawarat Phalinyot 2010: Experimental and Theoretical Studies of 2-Methoxy-5-(2'-ethylhexyloxy)-1,4-phenylene-vinylene Derivatives. Master of Science (Chemistry), Major Field: Chemistry, Department of Chemistry. Thesis Advisor: Mr. Songwut Suramitr, Ph.D. 110 pages.

The light-emitting organic materials are prepared as the emissive layer to improve OLEDs device. Thus, the main objective of this work are to synthesize and characterize the organic molecules of [1',4'-Bis(thienyl-vinyl)]-2-methoxy-5-(2'-ethylhexyloxy)-1,4-phenylene-vinylene with and without cyano group on the vinylene moiety and the two thiophene rings are linked with a conjugated phenylene group through -C=C- double bond *via* Knoevenagel condensation. The characteristic of its structures were confirmed with  $^1\text{H}$ -NMR,  $^{13}\text{C}$ -NMR, FTIR, TGA, LC-MS, EA, UV-vis and fluorescence spectrometre. Thermal stability of MEH-ThV and MEH-ThV-CN ( $T_d > 300\text{ }^\circ\text{C}$ ) enough to be used as electroluminescence materials in light-emitting devices. The absorption spectrum of PTVMEH-ThV is red-shifted and broadened in comparison with that of MEH-ThV-CN. The photophysical properties of both structures exhibited as green light emission. It is noteworthy that can be used as new luminescence materials in the fabrication of OLED-based full-color displays.

Moreover, quantum chemical calculations are investigated the structural, electronic, optical and emission properties of MEH-ThV and MEH-ThV-CN molecules by HF and DFT methods. The effect of substituents on structures with electron donating (thiophene ring) and withdrawing groups (cyano group) are compared between the experimental and theoretical results. The calculated ground state geometry of *EE*-MEH-ThV-CN is non-planar because of the sterical hindrance of the electron-withdrawing cyano groups effect. The optical and emission properties of *EE*-MEH-ThV is red-shifted, as compared to the *EE*-MEH-ThV-CN, due to there is stronger interchain interactions in *EE*-MEH-ThV, which leads to more coplanar backbone structure than that *EE*-MEH-ThV-CN molecule.

\_\_\_\_\_  
Student's signature

\_\_\_\_\_  
Thesis Advisor's signature

\_\_\_\_ / \_\_\_\_ / \_\_\_\_

## ACKNOWLEDGEMENTS

I would like to thank my advisor, Dr. Songwut Suramitr for his kindness, valuable suggestions, encouragement, continuous support and constant inspiration the course of my degree. I would sincerely like to thank Associate Professor Supa Hannongbua for kindly providing valuable suggestions and helpful guidance. I also wish to express my appreciation to Dr. Pimpa Homnirun and Dr. Titinun Karpkird for valuable suggestions and comments to make my experimental part. Furthermore, I am also grateful to Miss Chuleeporn Luadthong who I spent time discussing in my experimental work. Special thanks are due to my graduate committees, Dr. Potjaman Poolmee and Dr. Jakkapan Sirijarensre for their helpful comments and suggestions.

This work was supported in part by the Thailand Research Fund (RTA5080005), Kasetsart University Research and Development Institute (KURDI), the National Center of Excellence in Petroleum, Petrochemicals Technology and Advanced Materials (NCE-PPAM), office of the Higher Education Commission, Ministry of Education, Large Scale Simulation Research Laboratory (LSR) and the Center of Nanotechnology, Kasetsart University.

Special thanks are the Laboratory for Computational and Applied Chemistry (LCAC) at Kasetsart University are also gratefully acknowledge for computational resource, software facilities and research facilities.

Finally, I would like to dedicate this thesis to my parents and my colleagues at LCAC for their encouragement and understanding me. They also support me with love and sincerity throughout the entire study.

Suphawarat Phalinyot  
April, 2010.



## TABLE OF CONTENTS

	<b>Page</b>
TABLE OF CONTENTS	i
LIST OF TABLES	ii
LIST OF FIGURES	iv
LIST OF ABBREVIATIONS	ix
INTRODUCTION	1
OBJECTIVES	8
LITERATURE REVIEW	9
MATERIALS AND METHODS	14
RESULTS AND DISCUSSION	27
CONCLUSION	77
LITERATURE CITED	79
APPENDICES	88
Appendix A Supporting information	89
Appendix B Presentations	98
CURRICULUM VITAE	110

## LIST OF TABLES

Table		Page
1	Optical data of MEH-ThV-CN and MEH-ThV measured in chloroform solution	32
2	Electrochemical data from MEH-ThV-CN and MEH-ThV as obtained from cyclic voltammetry (CV)	36
3	Structural parameters of MEH-ThV obtained from fully optimization by HF and B3LYP methods at 6-31G(d,p) level of basis set (bond length in angstrom (Å), angle in degrees).	40
4	The lowest excitation energies in eV and oscillator strength ( <i>f</i> ) (values in parentheses) using TD-B3LYP/6-31G(d,p) method based HF/6-31G(d,p) and B3LYP/6-31G(d,p) optimize geometry and absorption spectra of experimental data in CHCl <sub>3</sub> solution for the MEH-ThV geometry.	45
5	Fully optimization of structural parameters of <i>EE</i> -, <i>EZ</i> - and <i>ZZ</i> -MEH-ThV with the S <sub>0</sub> and S <sub>1</sub> geometries obtained from HF/6-31G(d,p) and TD-B3LYP/dft-SV(P) methods, respectively (bond length in angstrom and angle in degrees).	48
6	The lowest excitation energies in eV and oscillator strength ( <i>f</i> ) (values in parentheses) both in gas phase and solvent phase (in CHCl <sub>3</sub> ) using TD-B3LYP/6-31G(d,p) method and absorption spectra of experimental data in CHCl <sub>3</sub> solution for the <i>EE</i> -, <i>EZ</i> - and <i>ZZ</i> -MEH-ThV geometries.	54
7	Fully optimization of structural parameters of <i>EE</i> -, <i>EZ</i> - and <i>ZZ</i> -MEH-ThV-CN with the S <sub>0</sub> and S <sub>1</sub> geometries obtained from HF/6-31G(d,p) and TD-B3LYP/dft-SV(P) methods, respectively (bond length in angstrom and angle in degrees).	59

## LIST OF TABLES (Continued)

Table		Page
8	The lowest excitation energies in eV and oscillator strength ( $f$ ) (values in parentheses) in gas phase and solvent phase (in CHCl <sub>3</sub> ) using TD-B3LYP/6-31G(d,p) method and absorption spectra of experimental data in CHCl <sub>3</sub> solution for the <b><i>EE</i></b> -, <b><i>EZ</i></b> - and <b><i>ZZ</i></b> - <b>MEH-ThV-CN</b> geometries.	66
9	The emission energies in eV and oscillator strength (values in parentheses) for <b><i>EE</i></b> - <b>MEH-ThV</b> and <b><i>EE</i></b> - <b>MEH-ThV-CN</b> geometries. The values written in italics stand for the excitation contributions in percentage involved in each calculated transition (H denoted HOMO and L is LUMO) using TD-B3LYP/dft-SV(P) method.	74
10	The calculation absorption ( $\lambda_{\text{abs}}$ ), emission wavelength ( $\lambda_{\text{em}}$ ) in gas phase and Stoke shift of the <b><i>EE</i></b> - <b>MEH-ThV</b> and <b><i>EE</i></b> - <b>MEH-ThV-CN</b> as obtained from TD-B3LYP/6-31G(d,p) and TD-B3LYP/dft-SV(P) methods, respectively.	75
11	Calculated fluorescence energies ( $E_{\text{flu}}$ ), oscillator strength and radiative lifetime of the <b><i>EE</i></b> - <b>MEH-ThV</b> and <b><i>EE</i></b> - <b>MEH-ThV-CN</b> as obtained from TD-B3LYP/dft-SV(P) calculations. Geometries first singlet excited stated ( $S_1$ ) were optimized at TD-B3LYP/dft-SV(P) level.	76

## LIST OF FIGURES

Figure		Page
1	Structure of organic light-emitting diodes (OLED)	1
2	Process of organic light-emitting diodes (OLED)	2
3	Structures of conjugated polymers	3
4	Molecular structure of poly[2-methoxy-5-(2'-ethylhexyloxy)-1,4-phenylene-vinylene] copolymer (MEH-PPV) <sub>n</sub>	5
5	Schematic diagram of <i>EE</i> -, <i>EZ</i> - and <i>ZZ</i> -MEH-ThV structures	24
6	Schematic diagram of <i>EE</i> -, <i>EZ</i> - and <i>ZZ</i> -MEH-ThV-CN structures	25
7	Thermogravimetric curve of MEH-ThV-CN and MEH-ThV monomer at a heating rate of 10 °C/min under nitrogen atmosphere	30
8	Absorption spectra of MEH-ThV-CN and MEH-ThV in CHCl <sub>3</sub> solution	31
9	Emission spectra of MEH-ThV-CN and MEH-ThV in CHCl <sub>3</sub> solution	33
10	Light emitting in chloroform solution. (a) MEH-ThV and (b) MEH-ThV-CN.	34
11	Cyclic voltammograms of MEH-ThV-CN in 0.1 mol/l TBAP acetonitrile, scan rate 20 mV/s	37
12	Cyclic voltammograms of MEH-ThV in 0.1 mol/l TBAP acetonitrile, scan rate 20 mV/s	38
13	Schematic represent the bond number on backbone structure of MEH-ThV molecule	39
14	Optimized bond length of MEH-ThV obtained from HF/6-31G(d,p) and B3LYP/6-31G(d,p) methods.	41

## LIST OF FIGURES (Continued)

Figure		Page
15	Aromatic system on backbone structure of MEH-ThV geometry as obtained from HF/6-31G(d,p) method.	42
16	Optimized torsion angle of MEH-ThV obtained from HF/6-31G(d,p) (green line) and B3LYP/6-31G(d,p) (red line) methods.	43
17	Absorption spectra of MEH-ThV obtained from the experimental in CHCl <sub>3</sub> solution and calculated using TD-B3LYP/6-31G(d,p) in gas phase (black line) and PCM model in CHCl <sub>3</sub> solution (red line) with optimization at HF/6-31G(d,p) and B3LYP/6-31G(d,p) methods.	46
18	Optimized bond length and bond length alternation (BLA) of <i>EE</i> -MEH-ThV of the S <sub>0</sub> and S <sub>1</sub> geometries as obtained from HF/6-31G(d,p) and TD-B3LYP/dft-SV(P) methods, respectively.	49
19	Optimized bond length and bond length alternation (BLA) of <i>EZ</i> -MEH-ThV of the S <sub>0</sub> and S <sub>1</sub> geometries as obtained from HF/6-31G(d,p) and TD-B3LYP/dft-SV(P) methods, respectively.	49
20	Optimized bond length and bond length alternation (BLA) of <i>ZZ</i> -MEH-ThV of the S <sub>0</sub> and S <sub>1</sub> geometries as obtained from HF/6-31G(d,p) and TD-B3LYP/dft-SV(P) methods, respectively.	50
21	Optimized torsion angle of <i>EE</i> -, <i>EZ</i> - and <i>ZZ</i> -MEH-ThV of the ground state (S <sub>0</sub> ) (green line) and the first singlet excited state (S <sub>1</sub> ) geometries (red line) as obtained from HF/6-31G(d,p) and TD-B3LYP/dft-SV(P) methods, respectively.	51



## LIST OF FIGURES (Continued)

Figure		Page
22	Absorption spectra of <i>EE</i> -MEH-ThV obtained from the experimental in chloroform solution and calculated using TD-B3LYP/6-31G(d,p) in gas phase (black line) and PCM model (red line).	55
23	Absorption spectra of <i>EZ</i> -MEH-ThV obtained from the experimental in chloroform solution and calculated using TD-B3LYP/6-31G(d,p) in gas phase (black line) and PCM model (red line).	56
24	Absorption spectra of <i>ZZ</i> -MEH-ThV obtained from the experimental in chloroform solution and calculated using TD-B3LYP/6-31G(d,p) in gas phase (black line) and PCM model (red line).	57
25	Schematic represents the bond number on backbone structure of MEH-ThV-CN molecule.	58
26	Optimized bond length and bond length alternation (BLA) of <i>EE</i> -MEH-ThV-CN of the $S_0$ and $S_1$ geometries as obtained from HF/6-31G(d,p) and TD-B3LYP/dft-SV(P) methods, respectively.	60
27	Optimized bond length and bond length alternation (BLA) of <i>EZ</i> -MEH-ThV-CN of the $S_0$ and $S_1$ geometries as obtained from HF/6-31G(d,p) and TD-B3LYP/dft-SV(P) methods, respectively.	60
28	Optimized bond length and bond length alternation (BLA) of <i>ZZ</i> -MEH-ThV-CN of the $S_0$ and $S_1$ geometries as obtained from HF/6-31G(d,p) and TD-B3LYP/dft-SV(P) methods, respectively.	61



## LIST OF FIGURES (Continued)

Figure		Page
29	Optimized torsion angle of <i>EE</i> -, <i>EZ</i> - and <i>ZZ</i> -MEH-ThV-CN of the ground state ( $S_0$ ) (green color) and first singlet excited state ( $S_1$ ) geometries (red color) as obtained from HF/6-31G(d,p) and TD-B3LYP/dft-SV(P) methods, respectively.	62
30	Aromatic system on backbone structures of <i>EE</i> -MEH-ThV-CN geometry as obtained from HF/6-31G(d,p) method.	64
31	Absorption spectra of <b><i>EE</i>-MEH-ThV-CN</b> obtained from the experimental in chloroform solution and calculated using TD-B3LYP/6-31G(d,p) in gas phase (black line) and PCM model (red line).	67
32	Absorption spectra of <b><i>EZ</i>-MEH-ThV-CN</b> obtained from the experimental in chloroform solution and calculated using TD-B3LYP/6-31G(d,p) in gas phase (black line) and PCM model (red line).	68
33	Absorption spectra of <b><i>ZZ</i>-MEH-ThV-CN</b> obtained from the experimental in chloroform solution and calculated using TD-B3LYP/6-31G(d,p) in gas phase (black line) and PCM model (red line).	69
34	Plots of the TD-B3LYP/6-31G(d,p) molecular orbitals contributing significantly to the lowest energy transitions of studied molecules in <i>EE</i> -MEH-ThV conformation. H denotes HOMO and L is LUMO.	71
35	Plots of the TD-B3LYP/6-31G(d,p) molecular orbitals contributing significantly to the lowest energy transitions of studied molecules in <i>EE</i> -MEH-ThV-CN conformation. H denotes HOMO and L is LUMO.	72

**LIST OF FIGURES (Continued)**

<b>Appendix</b>	<b>Figure</b>	<b>Page</b>
A1	$^1\text{H}$ -NMR and $^{13}\text{C}$ -NMR spectrum of C2	89
A2	$^1\text{H}$ -NMR and $^{13}\text{C}$ -NMR spectrum of C3	90
A3	$^1\text{H}$ -NMR and $^{13}\text{C}$ -NMR spectrum of C4	91
A4	$^1\text{H}$ -NMR and $^{13}\text{C}$ -NMR spectrum of C5	92
A5	$^1\text{H}$ -NMR and $^{13}\text{C}$ -NMR spectrum of MEH-ThV	93
A6	$^1\text{H}$ -NMR and $^{13}\text{C}$ -NMR spectrum of MEH-ThV-CN	94
A7	FTIR spectrum of MEH-ThV (red line) and Nujol mulls (blue line).	95
A8	FTIR spectrum of MEH-ThV-CN compound	95
A9	MS spectrum of MEH-ThV compound.	96
A10	MS spectrum of MEH-ThV-CN compound.	96

## LIST OF ABBREVIATIONS

Å	=	Angstrom
AM1	=	Semiempirical Austin Model1
B3LYP	=	Beck's three parameter hybrid functional using the LYP Correlation functional
CNDO	=	Complete Neglect of Differential Overlap
<sup>13</sup> C-NMR	=	Carbon nuclear magnetic resonance
CV	=	Cyclic voltammetry
DFT	=	Density function theory
E <sub>g</sub>	=	Energy gap
E <sub>ox</sub>	=	Onset oxidation potentials
E <sub>red</sub>	=	Onset reduction potentials
EL	=	Electroluminescence
FETs	=	Field effect transistors
FT	=	Flourene-thiophene
HF	=	Hartree Fock theory
HOMO	=	Highest occupied molecular orbitals
<sup>1</sup> H-NMR	=	Proton nuclear magnetic resonance
LCDs	=	Liquid crystal displays
LUMO	=	Lowest unoccupied molecular orbitals
OLED	=	Organic light emitting diodes
OPV <sub>N</sub>	=	poly( <i>para</i> -phenylene vinylene) oligomers
MEH-PPV	=	2-Methoxy-5-(2'-ethylhexyloxy)-1,4-phenylene- vinylene
MEH-ThV	=	[1',4'-Bis(thienyl-vinyl)]-2-methoxy-5-(2'- ethylhexyloxy)-1,4-phenylene vinylene
MEH-ThV-CN	=	1',4'-Bis[2-cyano-(thienyl-vinyl)]-2-methoxy-5-(2'- ethylhexyloxy)-1,4-phenylene vinylene

## LIST OF ABBREVIATIONS (Continued)

PBBPTDEHP	=	Poly{1,4-bis[3-(4'-butylphenyl)thienyl]-2,5-di(ethylhexyloxy)phenylene}
PES	=	Potential energy surfaces
PL	=	Photoluminescence
ppm	=	Parts per million
PPV	=	Poly( <i>p</i> -phenylene vinylene)s
PPVCs	=	Polymer photovoltaic cells
PPV-DT	=	<i>p</i> -Phenylene-vinylene-dithienylene
PTVMEH-PPV	=	Poly{[1',4'-bis-(thienyl-vinyl)]-2-methoxy-5-(2'-ethylhexyloxy)-1,4-phenylene-vinylene}
T <sub>d</sub>	=	Decomposition temperature
TDDFT	=	Time-dependent density functional theory
ThV	=	Thienylene-vinylene
TGA	=	Thermogravimetric analysis

## EXPERIMENTAL AND THEORETICAL STUDIES OF 2-METHOXY-5-(2'-ETHYLHEXYLOXY)-1,4-PHENYLENE- VINYLENE DERIVATIVES

### INTRODUCTION

In 1987, Tang and Van Slyke, together with their groups, used organic material as the emitting source for organic light-emitting diodes (OLEDs). The OLED composed of two layers of a hole-transporting layer and emitting material which are sandwich between an indium-tin-oxide anode and an alloyed Mg:Ag (Van Slyke, 1987). Electron-hole recombination is emitted as green electroluminescent. After that, the performances of OLED devices have been extensively improved such as turn-on voltage (Cao *et al.*, 1999), external efficiency (Malinsky *et al.*, 1999), current density (Cleave *et al.*, 1999) and luminescence (Ogundare *et al.*, 2008). The OLED component is composed of a cathode, an emissive layer, a conductive layer, an anode and a substrate (Figure 1).

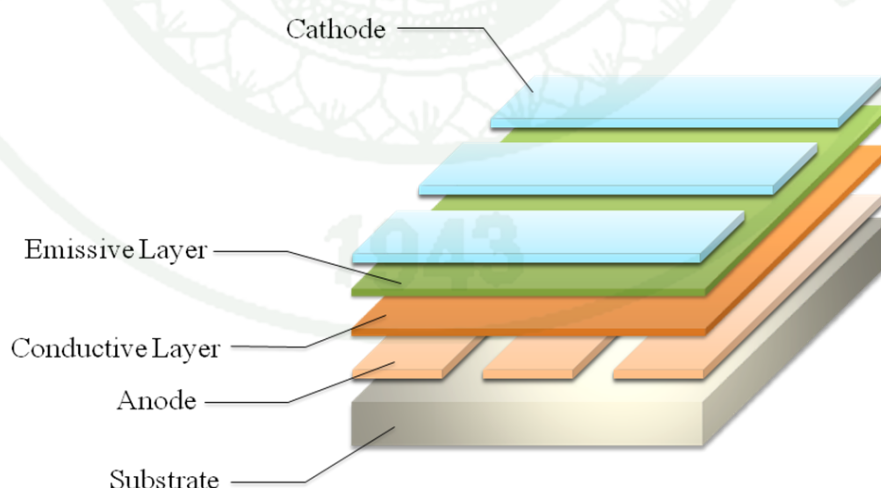


**Figure 1** Structure of organic light-emitting diodes (OLED).

Organic light-emitting diodes (OLEDs) are fabricated as electroluminescent organic film sandwiched between a high work function anode and a low function cathode. When a voltage is applied between anode and cathode, electrons are injected from the cathode into the  $\pi^*$ -band (lowest unoccupied molecular orbital, LUMO) of the organic materials, and holes are injected from the anode into the  $\pi$ -band (highest occupied molecular orbital, HOMO). The injected electrons and holes interact within the organic materials film and radiatively decay to produce electroluminescence, which causes electroluminescent light (Figure 2). The emissive organic materials, supplied with an electrical current, can produce full-color display and panel light sources (Sheats *et al.*, 1999). For full-color application, it is necessary to have red (620-700 nm), green (500-550 nm) and blue (430-500 nm) emitters with sufficiently high light-emitting efficiencies, low operating voltages and high external quantum efficiency. These three colors of light depend on the type of emissive organic material. The emissive organic materials have  $\pi$ -conjugated system in the structures and they have smaller hole injection barrier than electron injection barrier. Furthermore, the conjugated organic materials or conjugated polymer with low HOMO-LUMO energy level, by increasing the electron affinity, have been used as materials for OLED device.

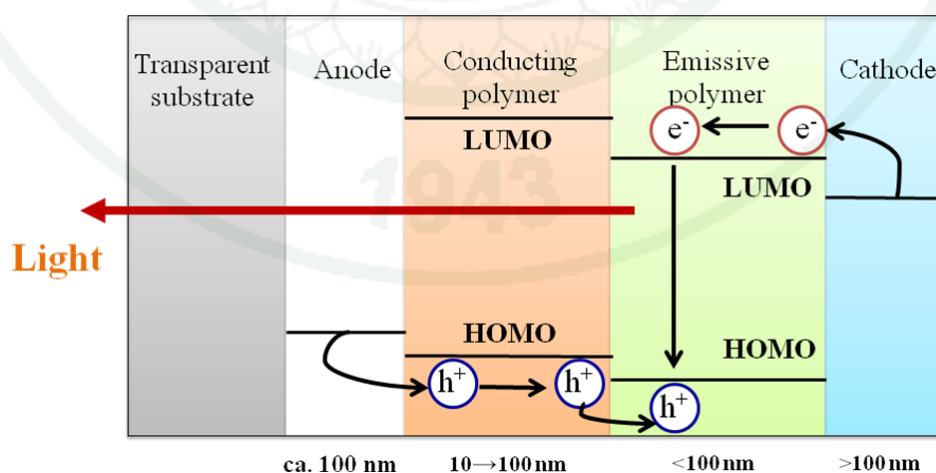


**Figure 2** Process of organic light-emitting diodes (OLED).



Conjugated polymers derive their semiconducting properties by having delocalized  $\pi$ -electron bonding along the polymer chain. The  $\pi$  (bonding) and  $\pi^*$  (antibonding) orbitals form delocalized valence and conduction orbitals, which support mobile charge carriers. Indeed, most of the conjugated polymers are colored as a consequence of their band gaps in the 1.5-4.0 eV range. The first study of conducting polymers on the doping effect of polyacetylene which the conductivity of doped-polymer increasing 109 times is compared to those on undoped one (Heeger *et al.*, 1977). This research area was initiated by Alan J. Heeger, Alan G. MacDiarmid and Hideki Shirakawa who got the Nobel Prize awards in 2000. After that conducting polymers have been extensively investigated for various technological application such as organic solar cells (Miller *et al.*, 2001), organic light-emitting diodes (OLEDs) (Vardeny *et al.*, 2005), field effect transistors (FETs) (Liu *et al.*, 2001) and liquid crystal displays (LCDs) (Choi *et al.*, 2004).

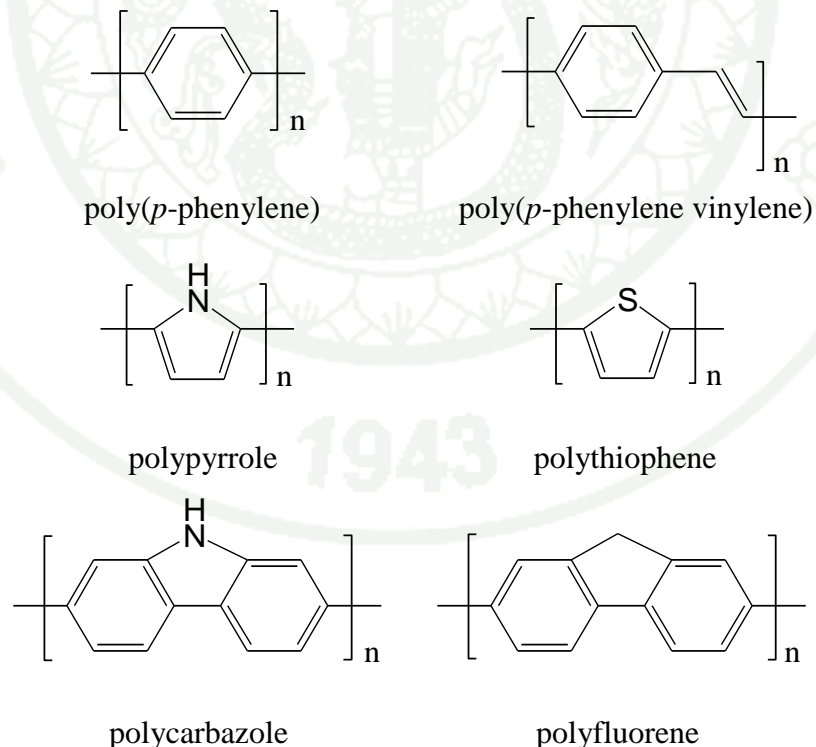


**Figure 3** Structures of conjugated polymers.

In the past decade, many conjugated polymers, such as poly(*p*-phenylene)s, poly(*p*-phenylene vinylene)s, polythiophene, polypyrrole, polyfluorene and polycarazole have become the promising materials for the optoelectronic applications, as shown in Figure 3.

Among the numerous conducting polymers, poly(*p*-phenylene vinylene) (PPV) is the most extensively studied with energy gap of 2.5 eV. Moreover, PPV is a polymer with attractive properties such as high electrical conductivity, electroluminescence, photoluminescence and photoconductivity. The particular application of the organic light-emitting diodes (OLED) based on poly(*p*-phenylene vinylene) (PPV) is reported in 1990 (Burroughes *et al.*, 1990). PPV structure has  $\pi$ -conjugation system, high thermal stability and good film forming properties. There are also future advantages on device fabrication such as high quantum efficiencies, long lifetime and easily fabricate devices (Heeger *et al.*, 1977). Therefore, the properties of this conducting polymer are still challenging for development.

Structure of 2-methoxy-5-(2'-ethylhexyloxy)-1,4-phenylene-vinylene (MEH-PPV) structure is depicted in Figure 4. MEH-PPV copolymer is a class of conjugated polymers which the alkoxy side groups attached onto the phenylene ring at the C<sub>2</sub> and C<sub>5</sub>, leading to an increase of solubility in common organic solvent such as chloroform, tetrahydrofuran, hexane, dichloromethane and so on. This copolymer shows high efficiency in the OLEDs application due to their high efficient red emission in both photoluminescence (PL) and electroluminescence (EL) (Wu *et al.*, 2003). In addition, MEH-PPV emits red light color and shows other good characteristics such as high thermal stability, high molecular weight, large current density, low band gap, easy electrochemical preparations and also high PL quantum yield. The advantages of this polymer are that their solubility properties and HOMO and LUMO energy levels can be adjusted by varying the molecular structures of the polymer. So their derivatives might be combined with donor-acceptor groups or fused with other conjugated ring for enhancing the electronic properties and thermal stability.

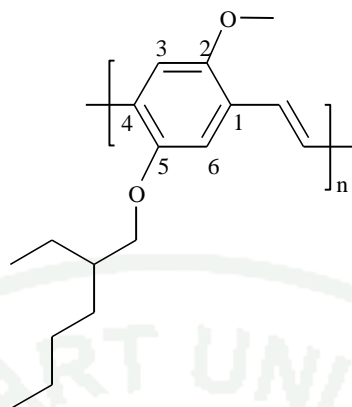


**Figure 4** Molecular structure of poly[2-methoxy-5-(2'-ethylhexyloxy)-1,4-phenylene-vinylene] copolymer (MEH-PPV)<sub>n</sub>

The synthetic efforts have been made toward a decrease in bandgap of conjugated polymers by adding electron donor or electron acceptor groups. The energy gaps ( $E_g$ ) of conjugated polymers can be reduced to below 1 eV while the good stability is maintained. Theoretical calculations have also proved to be of importance for these studies because of the experimental limitations. Due to the high level of disorder associated with most of these materials, structural information could not be obtained easily by experiments. Therefore, theoretical studies are used to investigate energy gap control.

Theoretical investigations have been proven to be an important tool for studying the relationships between electronic structures and optical properties of the  $\pi$ -conjugated materials. This helps in understand a fundamental of the conformational analysis, electronic and optical characteristics of known materials and in guiding the experimental efforts toward novel compound with enhanced characteristics. The theoretical quantity of energy gap for direct comparison with the experimental energy gap ( $E_g$ ) should be the transition (or excitation) energy from the ground state to the first dipole-allowed excited state (Zhu *et al.*, 2004). The energy gap ( $E_g$ ) in an extended system is defined as the difference between the highest occupied molecular orbital (HOMO) and the lowest unoccupied molecular orbital (LUMO). Theoretical approaches are available to calculate the extrapolation energy gap for increasing

longer oligomers, and extrapolation to infinite chain length is followed. A distinct advantage of this approach is that it can provide the convergence behavior of the structural and electronic properties of oligomers. In practice both the oligomers extrapolation and the polymer approaches are generally considered to be complementary to each other in our understanding of the properties of polymers.

For the quantum chemical calculation on both the ground states and excited states, theoretical methods have been applied to different conjugated polymer systems (Huang *et al.*, 2001; Corral *et al.*, 2000; Poolmee *et al.*, 2005; Meeto *et al.*, 2008). In particular, the density function theory (DFT) method is able to describe the geometry molecules, as well as their energetic, in a satisfactory manner (Grozema *et al.*, 2005). Hybrid exchange correlation functionals are widely used in the DFT formalism, to get a better fit with experiments. Popular forms of hybrid DFT methods, including Becke's three parameter hybrid functional (Becke., 1993) using the Lee Yang Parr (LYP) (Lee *et al.*, 1988) correlation functional (B3LYP). There are many applications of hybrid DFT in conjugated polymers, which gives acceptable results for the geometry and HOMO-LUMO gaps of oligomers for some hetero-type conjugated polymers (Hutchison *et al.*, 2002). Many researchers focus on TDDFT method in order to investigate the electronic properties with geometry relaxation effects in excited states (Jacquemin and Perpète, 2006). In 2006, Saha and coworker pointed out that conventional TDDFT with the B3LYP functional should be used carefully, because it can provide inaccurate estimates of the chain length dependence of  $\pi$ - $\pi^*$  excitation energies for these molecules with long  $\pi$ -conjugated chains. Nowadays, TDDFT still has some limitations, even though it can be helpful in understanding fundamentals of the electronic and optical characteristics of conjugated polymers and guiding the experimental efforts toward compounds with enhanced characteristics.

Thus, the main objectives of this work are to synthesize and characterize [1',4'-Bis(thienyl-vinyl)]-2-methoxy-5-(2'-ethylhexyloxy)-1,4-phenylene vinylene (MEH-ThV) with and without cyano group on the vinylene moiety and the two thiophene rings are linked with a conjugated phenylene group through -C=C- double bond. Moreover, quantum chemical calculations are investigated on the structural,

electronic and optical properties of MEH-ThV and MEH-ThV-CN monomers by density functional theory method. The effect of substituents on oligomeric structures with electron donating and withdrawing groups are compared between the experimental and theoretical results.





## OBJECTIVES

1. To synthesize and characterize [1',4'-Bis(thienyl-vinyl)]-2-methoxy-5-(2'-ethylhexyloxy)-1,4-phenylene vinylene (MEH-ThV) and [1',4'-Bis[2-cyano-(thienyl-vinyl)]]-2-methoxy-5-(2'-ethylhexyloxy)-1,4-phenylene vinylene (MEH-ThV-CN).
2. To investigate conformational analysis, optical and electronic properties with electron donating and accepting groups substitution onto the MEH-PPV-base molecules by quantum chemical calculations.
3. To compare the absorption and emission properties between the quantum chemical calculations molecules and experimental results of MEH-ThV and MEH-ThV-CN.



## LITERATURE REVIEW

Electroluminescence from conjugated polymers was first reported in 1990 (Burroughes *et al*). Poly(*p*-phenylene) (PPV) was used as an active layer of light-emitting device. In addition, organic materials show attractive device characteristics, including efficient light generation, low-cost manufacturing.

The full-color (red, blue and green) materials are still challenging to develop the organic materials for organic-emitting diodes (OLEDs) devices. Researchers have improved the organic molecule in color emissions for OLEDs. Xue and Luo (2004) reported red-emitting materials of *p*-phenylene vinylene dithienylene type copolymer (PPV-DT) with or without cyano group on the vinylene moiety and synthesized by Wittig-Horner Emmons reaction and palladium-catalyzed homo-coupling reaction. The results showed that the structure with a cyano group gave 632 nm as red shifts for in emission spectra in CH<sub>2</sub>Cl<sub>2</sub> solution and as red light wavelength (600-700 nm) while the structure without a cyano group revealed an emission maximum at 595 nm.

In addition, a new yellow-green light emissive conjugated polymer of poly{1,4-bis[3-(4'-butylphenyl)thienyl]-2,5-di(ethylhexyloxy)phenylene} (PBBPTD-EHP) has been synthesized using FeCl<sub>3</sub> as the oxidizing reagent and characterized by thermal analysis, UV-Vis and fluorescence spectroscopy techniques. The PBBPTDEHP polymer was shown to have good thermal stability that it decomposed as two steps. The first step from 280 to 450 °C corresponds to the degradation of the side chain. The second from 450 to 580 °C is attributed to the breakdown of the backbone that this polymer can be used as an electroluminescent material. The polymer exhibited an absorption maximum at 435 nm in CHCl<sub>3</sub> solution and the photoluminescence spectra for the solution is 525 nm, which corresponds to yellow-green emission (500-600 nm) (Ding *et al.*, 2000).

Recently, 2-methoxy-5-(2'-ethylhexyloxy)-1,4-phenylene-vinylene (MEH-PPV) have received attention as polymer photovoltaic cells (PPVCs) and photodetectors because of its advantages of low cost, light weight, good film-forming

property, high absorption coefficient centered at *ca.* 500 nm and good charge transport properties. Moreover, this polymer can improve the utilization of sunlight and increase the absorption in longer wavelength region. Therefore, MEH-PPV copolymer was investigated for optical and electronic properties and most widely synthesized as well. For instance, in 2005, Hou and coworker synthesized two random copolymers of 2-methoxy-5-(2'-ethylhexyloxy)-1,4-phenylene-vinylene (MEH-PVV) and 2,5-thienylene-vinylene (ThV) with the molar ratio of ThV as 10% and 18% by Gilch method, the alternate copolymer of MEH-PV and ThV was synthesized by Horner-Emmons reaction. Poly(3-hexyl-thienylene-vinylene) (P3HTV) was synthesized by Stille coupling reaction. The results were shown the increase of the ratio of ThV in the copolymer, the thermal decomposition temperature decreases and the absorption spectra of the copolymers containing ThV broadened and red-shifted in comparison with that of MEH-PPV. The more the ThV units contained in the copolymer as red-shifted of the absorption and it should be very important for better utilization of solar light. The result of cyclic voltammetry revealed that the HOMO energy level of the copolymers moved upward with the copolymerization of ThV. The change of the HOMO level could enhance easily to release electron and increase the donor ability for the copolymer. Santos *et al* (2007) studied electroluminescent polymers. They found that MEH-PPV appoints as a good alternative for application in LEDs and LECs because MEH-PPV is soluble in common organic solvents, and can be promptly prepared as a spin-cast film without using the precursor approach, usually required for PPV.

The substitutions of donor groups and acceptor groups on poly(*p*-phenylene vinylene) (PPV) have an impact on the optical and electronic properties. In 2005, Huo and coworker investigated the two thiophene rings linked with MEH-PPV through trans -C=C- the double bond by the Horner-Emmons reaction. The molecular structure of the poly{[1',4'-bis-(thienyl-vinyl)]-2-methoxy-5-(2'-ethylhexyloxy)-1,4-phenylene-vinylene} (PTVMEH-PPV) obtained by Universal Grignard metathesis Polymerization (GRIM). The properties of PTVMEH-PPV were investigated and compared with those of MEH-PPV and MEH-ThV (Hou *et al.*, 2005). The thermal stability of PTVMEH-PPV is 246 °C which is lower than that of MEH-PPV due to the

structure of MEH-ThV has the thiophene ring through vinylene linkage on main chain of conjugated polymers. The absorption peak of PTVMEH-PPV covered a absorption wavelength in the visible range (380-680 nm). The absorption edge of PTVMEH-PPV is 657 nm, which is red shift as compared to MEH-PPV (550 nm) and MEH-ThV (630 nm), is presumably due to the PTVMEH-PPV have thiophene ring in the polymer main chains. The onset oxidation potentials ( $E_{ox}$ ) and onset reduction potentials ( $E_{red}$ ) of the polymer from the electrochemical measurement is -1.70 V and 0.12 V (versus Ag/Ag<sup>+</sup>), respectively, and its have been estimated to be -3.01 eV and -4.83 eV. The band gap of the polymer (1.82 eV) is lower than that of MEH-PPV (2.17 eV). In 2006, Peres and coworker designed and synthesized structures of the halogen substitution on poly(*p*-phenylene vinylene) (PPV) copolymer via Wessling and Witting reaction. The observed optical absorption and emission peaks are red shifted due to the presence of halogen substituent.

Since the quantum chemical calculations became the excellent tools for investigating structures and properties in many chemical systems. There are large amounts of researches topic which performed by quantum calculations. In 1994, Cornil and coworker calculated the optical absorption spectra of oligomers of *p*-phenylene vinylene) and their methoxy-substituted derivatives on the basis of geometries optimized by semiempirical AM1 method couple with a single CI technique. The results were in good agreement with experimental UV-Vis absorption spectra of oligomers and polymers, and provided a detail interpretation of the electronic transition involved for example distinguishing the role of localized and delocalized  $\pi$  electron bonding. In addition, the lowest energy transition from highest occupied molecular orbital to lowest unoccupied with molecular orbital at higher energies associated with the delocalized  $\pi$  orbitals. These match well the measured absorption features in PPV compounds, at 4.5 eV (tetramer), 4.1 eV (pentamer) and 3.8 eV (hexamer, polymer).

In 2003, Correia and Ramos investigated poly(*p*-phenylene vinylene) (PPV) and its derivative, which cyano groups substitution were induced in the PPV chains and a charge rearrangement among the polymer atom. The self-consistent quantum

chemistry at Complete Neglect of Differential Overlap (CNDO) level have been used to study the static properties of the cyano-substituted PPV molecule with 16 repeat units in its neutral and charge states, and charge mobility along the polymer molecule. The mono-cyano substitution of PPV chains leads to an asymmetric increase of ionization potential and electron affinity, but it does not seem to affect the position of the charge-induced effects in the absence of an applied electric field. When an electric field greater than the threshold is applied, the injected charges move along the cyano-substituted molecules. The value of charge mobility depends on the strength of the electric field as well as on charge sign and substitution position.

In 2005, Suramitr and coworker investigated the geometries and energy gaps of poly(*para*-phenylene vinylene) oligomers (OPV<sub>N</sub>) and their alkoxy derivatives using quantum chemical calculations. This oligomer series includes poly(*para*-methoxy)-PV, (DMO-OPV<sub>N</sub>) and poly(2-methoxy,5-(2'-ethyl-hexyloxy)-PV), (MEH-OPV<sub>N</sub>). Potential energy hypersurfaces of all OPV<sub>2</sub> and OPV<sub>2</sub>-alkoxy derivatives were calculated by the semiempirical AM1 and *ab-initio* method at the HF/3-21G and HF/6-31G levels. OPV<sub>2</sub> provide two conformational structures. There are coplanar and twisted conformers. For its alkoxy derivatives, the stable conformation was found to be that in which the two adjacent phenylene rings were coplanar. An intramolecular weak hydrogen bond interaction was also found to occur between the oxygen atom of the alkoxy derivatives and the hydrogen atom of the vinylene linkage. By using these linear relationships, they can be employed to semiquantitatively estimate the first excitation energy. The relationships with the working function of  $E_{\text{expt}} = 0.604E_{\text{TDDFT-B3LYP/6-31G}} + 0.947$  and  $E_{\text{expt}} = 0.604E_{\text{TDDFT-B3LYP/6-31G}^*} + 0.983$  were proposed, based on the geometry obtained from HF/3-21G for corrected the extrapolated energy gaps of DMO-OPV<sub>N</sub>, DHO-OPV<sub>N</sub> and MEH-OPV<sub>N</sub>. It was found that satisfactory linear relationship and TDDFT method can be used to predict the lowest excitation energies for compounds in these systems and applicable to the design of new conducting polymer.

The time-dependent density functional theory (TD-DFT) is a powerful tool to determine the excitation energy; therefore, it was widely common used to investigate



the excited state properties of conjugated polymer which is quite large system. Poolmee *et al.* (2005) reported the bonding character between LUMO of Flourene-thiophene, FT units from TD-DFT calculations. It is anticipated that the excitation spectrum depends on the torsional angle and the high accuracy method. From the SAC-CI calculation, the results show that excitation from HOMO to LUMO in all torsional angles and the  $S_1$  state is located apart from other two states. The excited states are mainly described by the linear combination of the transition from next HOMO and HOMO to LUMO and next LUMO. Therefore using SAC-CI method, fine analysis of the excited states of the FT and also FMT, which are important fragment of the light-emitting devices have been achieved.

In 2004, Han and Lee investigated the geometry and electronic properties using time-dependent density-theory (TD-DFT) methods of oligo(*p*-phenylene-vinylene) (PPV $n$ ), where  $n$  is the number of monomers. To minimize the errors due to the calculations for oligomers, they employed long-chain models, up to PPV30 and various equations for extrapolation to infinity. The absorption ( $S_0 \rightarrow S_1$ ) and emission ( $S_1 \rightarrow S_0$ ) transition energies obtained from TD-DFT//DFT methods are 2.44 and 2.16 eV, respectively. Comparisons with available experimental data demonstrated that TDDFT is a very reliable tool for investigating the electronic transitions of PPV.

From the literatures, there is no available theoretical investigation on the 2-methoxy-5-(2'-ethylhexyloxy)-1,4-phenylene-vinylene (MEH-PPV) and its derivatives system. So, it is a good opportunity to start on this research topic and the detail knowledge of the relationship between structure, optical properties and electronic properties. It can be a useful guide for comparison with synthetic processes.

## MATERIALS AND METHODS

### Synthesis and Characterization

#### 1. Materials

Sodium methoxide, formaldehyde, magnesium sulfate anhydrous ( $\text{MgSO}_4$ ) and potassium *tert*-butoxide were purchased from Fluka Chemical Company (Buchs, Switzerland). 4-Methoxyphenol, 3-bromomethyl heptanes, triphenyl phosphine and *N,N*-dimethylformamide (DMF) were purchased from Aldrich Chemical Company (Steinheim, Germany). 2-Thiophene carboxaldehyde and potassium carbonate were purchased from Acros Organics (Geel, Belgium). Methanol, 1,4-dioxane and sodium cyanide were purchased from Carlo Erba Reagent (Milan, Italy). Hexane, dichloromethane and diethyl ether were purchased from Labscan (Dublin, Ireland). Hydrochloric acid (HCl) and tetrahydrofuran (THF) were purchased from Fisher Scientific (Leicester, England). Tetrahydrofuran (THF) was dried over sodium metal and benzophenone under nitrogen atmosphere until the dark blue colour and distilled immediately before use. *N,N*-dimethylformamide (DMF) and methanol (MeOH) were dried over Type 3Å molecular sieve for 72 hours.

#### 2. Instruments

$^1\text{H}$ -NMR and  $^{13}\text{C}$ -NMR analyses were carried out using a VARIAN UNITY INOVA spectrometer which operated at 400 MHz for  $^1\text{H}$  and 100.5 MHz for  $^{13}\text{C}$  nuclei in deuterated chloroform ( $\text{CDCl}_3$ ) with tetramethylsilane (TMS) as an internal reference. FT-IR analysis was carried out using a Perkin Elmer system 2000 Fourier transform infrared spectrometer. FT-IR of MEH-ThV was recorded with Nujol mulls, whereas MEH-ThV-CN was measured with KBr pellet. UV analysis was done with Perkin Elmer Lambda 35 UV-Vis spectrophotometer, using a quartz cell with 1 cm path length. Fluorescence analysis was obtained using Perkin Elmer Instruments LS55 fluorescence spectrophotometer. Mass spectroscopy (MS) was determined on a micrOTOF 72 LC-MS spectrometer. Thermogravimetric analysis (TGA) was

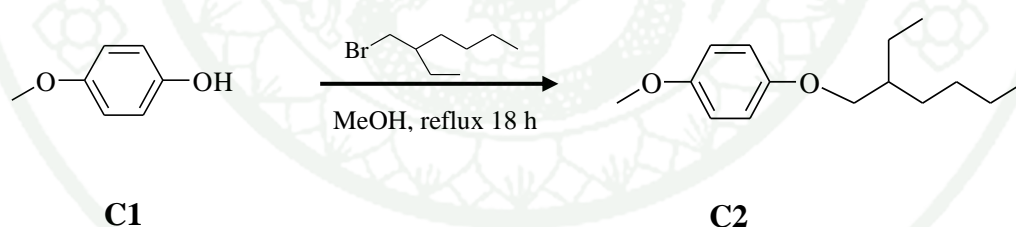


performed under nitrogen atmosphere at heating rate of 10 °C/min on a Perkin Elmer TGA-7 thermal analyzer. Cyclic voltammograms were recorded under nitrogen atmosphere using Autolab Potentiostat Galvanostat running Autolab GPES software. The electrochemical cyclic voltammetry was performed in a 0.1 M *tetra*-butylammonium perchlorate (TBAP) in acetonitrile solution at a scan rate of 20 mV/s. Platinum electrode was used as working electrode, platinum electrode as counter electrode and Ag/Ag<sup>+</sup> electrode as reference electrode. An elemental analysis (EA) was performed with a LECO CHNS-932 elemental analyzer. The energy levels were calculated using the ferrocence (FOC) value of -4.8 eV with respect to vacuum level, which is defined as zero (Liu *et al.*, 1999).

### 3. Methods

All compounds were performed under a nitrogen atmosphere using standard techniques and the synthetic processes adapted literature procedure (Hou *et al.*, 2006).

#### 3.1 1-((2-Ethylhexyl)oxy)-4-methoxybenzene (C2)

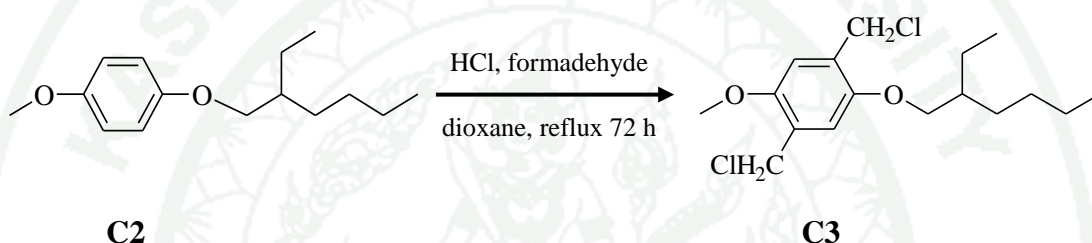


Sodium methoxide (13.50 g, 0.25 mol) and 4-methoxyphenol (**C1**) (29.30 g, 236 mmol) were dissolved in 250 ml of dry methanol. The reaction mixture was heated to reflux for 30 min. Then the mixture was stirred at room temperature and 3-bromomethyl heptanes (46.50 g, 259 mmol) in 150 ml of dry methanol was added dropwise and then refluxed for 18 h. The solvent was removed by rotary evaporation and the residue was extracted with diethyl ether (200 ml) and 10% w/v NaOH. The organic layer was dried over anhydrous magnesium sulfate and evaporated. It was obtained with a yield of 30.13 g, 53.87% as bright yellow oil.

$^1\text{H}$ -NMR (400 MHz,  $\text{CDCl}_3$ ): 6.77-6.84 (m, 4H, Ar-*H*), 3.76 (d,  $^3J_{\text{HH}} = 5.46$  Hz, 2H, - $\text{OCH}_2$ -), 3.71 (s, 3H, - $\text{OCH}_3$ ), 1.68 (m, 1H, -*CH*-), 1.53-1.28 (m, 8H, - $\text{CH}_2$ -), 0.93-0.87 (m, 6H, - $\text{CH}_3$ )

$^{13}\text{C}$ -NMR (100.5 MHz,  $\text{CDCl}_3$ ): 153.54, 153.50, 115.23, 114.41, 70.94, 55.35, 39.41, 30.47, 29.02, 23.78, 22.98, 13.94, 10.96

### 3.2 1,4-Bis(chloromethyl)-2-((2'-ethylhexyl)oxy)-5-methoxybenzene) (C3)

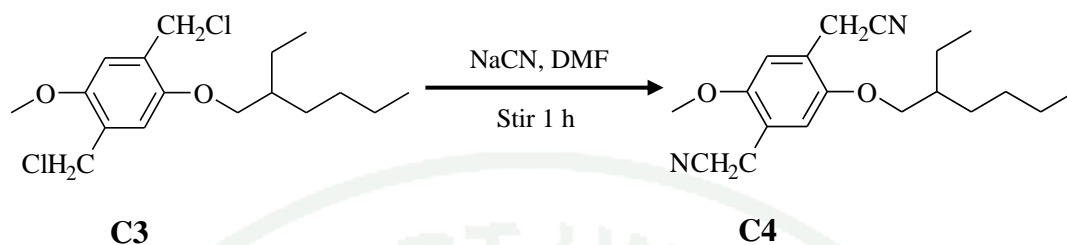


A solution of hydrochloric acid (90 ml), dioxane (120 ml) and **C2** (24.20 g, 101 mmol) was saturated with hydrochloric acid for 30 min and formaldehyde (70 ml) was then added dropwise at 0 °C. After the solution was stirred for 3 h at room temperature, formaldehyde (50 ml) was added dropwise again at 0 °C with an ice bath. Hydrochloride acid was bubbled into the solution. The reaction mixture was stirred at room temperature for 12 hours and then was heated to reflux for 72 hours. After removal of the solvent, the residue was dissolved in hot hexane (75 ml). This mixture was poured into ice-cold methanol (250 ml) and filtered under suction. The precipitate was washed with ice-cold methanol (150 ml) and dried to give a white solid (yield 6.11 g, 17.97%).

$^1\text{H}$ -NMR (400 MHz,  $\text{CDCl}_3$ ): 6.92 (s, 1H, Ar-*H*), 6.91 (s, 1H, Ar-*H*), 4.64 (s, 2H, - $\text{CH}_2\text{Cl}$ -), 4.63 (s, 2H, - $\text{CH}_2\text{Cl}$ -), 3.88 (d,  $^3J_{\text{HH}} = 5.07$  Hz, 2H, - $\text{OCH}_2$ -), 3.85 (s, 3H, - $\text{OCH}_3$ ), 1.74 (m, 1H, -*CH*-), 1.57-1.29 (m, 8H, - $\text{CH}_2$ -), 0.96-0.89 (m, 6H, - $\text{CH}_3$ )

$^{13}\text{C}$ -NMR (100.5 MHz,  $\text{CDCl}_3$ ): 150.93, 150.85, 127.02, 126.80, 114.02, 113.36, 71.11, 56.30, 41.31, 39.58, 30.60, 29.09, 23.99, 23.03, 14.05, 11.20

## 3.3 1,4-Bis(cyanomethyl)-2-((2'-ethylhexyl)oxy)-5-methoxybenzene) (C4)



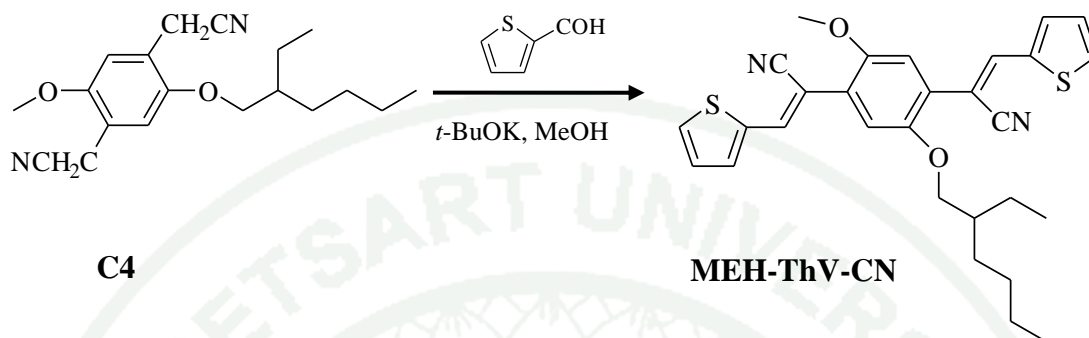
A mixture of **C3** (1.00 g, 4.20 mmol) and sodium cyanide (0.83 g, 16.90 mmol) was dissolved in 100 ml of dry *N,N*-dimethylformamide (DMF). The mixture was heated at 110 °C with vigorous stirring for 1 h and poured into crushed ice. To obtain brown solid precipitates, the solid was filtrated by suction filtration and washed with hexane. The residue was recrystallized with hexane to afford as a white solid (0.70 g, 74.79%).

$^1\text{H}$ -NMR (400 MHz,  $\text{CDCl}_3$ ): 6.86 (s, 1H, Ar-*H*), 6.85 (s, 1H, Ar-*H*), 3.81 (d,  $^3J_{\text{HH}} = 5.46$  Hz, 2H,  $-\text{OCH}_2-$ ), 3.78 (s, 3H,  $-\text{OCH}_3$ ), 3.63 (s, 4H,  $-\text{CH}_2\text{CN}$ ), 1.67 (m, 1H,  $-\text{CH}-$ ), 1.49-1.18 (m, 8H,  $-\text{CH}_2-$ ), 0.89-0.82 (m, 6H,  $-\text{CH}_3$ )

$^{13}\text{C}$ -NMR (400 MHz,  $\text{CDCl}_3$ ): 150.42, 150.30, 119.09, 119.00, 117.76, 117.70, 112.48, 111.81, 71.13, 56.12, 39.49, 30.59, 29.08, 23.98, 22.98, 18.63, 18.57, 14.04, 11.15

1943

3.4 [1,4-Bis(thienyl-1,1'-cyanovinylene)]-2-methoxy-5-(2'-ethylhexyloxy) benzene (MEH-ThV-CN)



Compound 4 (**C4**) (2.00 g, 6.40 mmol), 2-thiophene carboxaldehyde (1.80 g, 15.40 mmol) and potassium *tert*-butoxide (7.20 g, 64 mmol) were dissolved in 100 ml of dry methanol. Then the reaction mixture was heated to reflux for 24 h. The resulting yellow precipitates were collected by filtration and washed with ice-cold methanol to obtain as a yellow solid of MEH-ThV-CN (yield 1.23 g, 38.28%).

<sup>1</sup>H-NMR (400 MHz, CDCl<sub>3</sub>): 8.06 (s, 1H, =CH), 7.88 (s, 1H, =CH), 7.67 (t, <sup>3</sup>J<sub>HH</sub> = 3.51 Hz, 2H, Th-CH), 7.56 (d, <sup>3</sup>J<sub>HH</sub> = 5.07 Hz, 2H, Th-CH-), 7.16 (ddd, <sup>3</sup>J<sub>HH</sub> = 3.90 Hz, <sup>3</sup>J<sub>HH</sub> = 2.73 Hz, <sup>4</sup>J<sub>HH</sub> = 1.17 Hz, 2H, S-CH-), 7.14 (s, 1H, Ar-H), 7.10 (s, 1H, Ar-H), 3.90 (d, <sup>3</sup>J<sub>HH</sub> = 5.07 Hz, 2H, -OCH<sub>2</sub>-), 3.87 (s, 3H, -OCH<sub>3</sub>), 1.74-1.68 (m, 1H, -CH-), 1.48-1.19 (m, 8H, -CH<sub>2</sub>-), 0.88 (t, <sup>3</sup>J<sub>HH</sub> = 7.41 Hz, 3H, -CH<sub>3</sub>), 0.80 (t, <sup>3</sup>J<sub>HH</sub> = 7.02 Hz, 3H, -CH<sub>3</sub>)

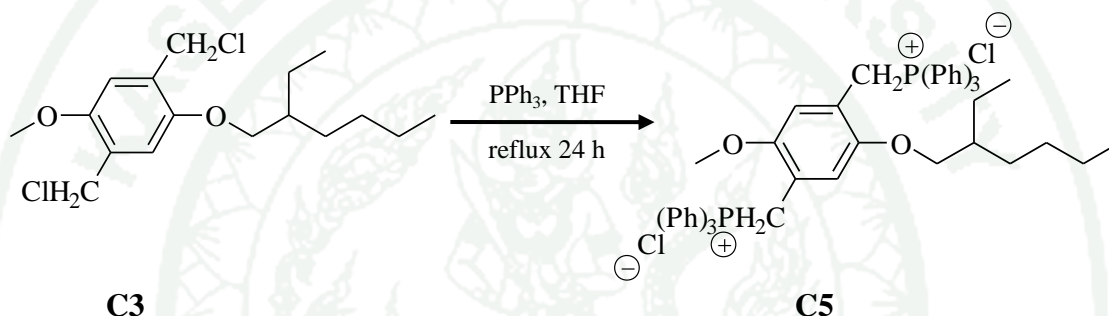
<sup>13</sup>C-NMR (100.5 MHz, CDCl<sub>3</sub>): 150.91, 150.83, 138.89, 138.77, 138.13, 138.04, 132.51, 132.14, 130.18, 130.11, 127.82, 127.73, 124.20, 124.16, 118.37, 118.16, 113.93, 113.41, 104.61, 104.52, 71.82, 56.52, 39.66, 30.79, 29.14, 24.10, 22.98, 14.00, 11.21

Elemental analysis for C<sub>29</sub>H<sub>30</sub>N<sub>2</sub>O<sub>2</sub>S<sub>2</sub> (F.W. 502.69): C, 69.29; H, 6.02; N, 5.57; O, 6.37; S, 12.76% Found C, 70.57; H, 6.43; N, 5.62; S, 14.34

FT-IR (KBr,  $\text{cm}^{-1}$ ): 3076 ( $=\text{C}-\text{H}$ , stretching); 2954, 2925 ( $-\text{C}-\text{H}$ , stretching); 2212 ( $\text{C}\equiv\text{N}$ , stretching); 1576 ( $\text{C}=\text{C}$ , stretching), 1422 ( $-\text{C}-\text{H}$ , bending); 1215 ( $\nu_{\text{as}}\text{C}-\text{O}$ , stretching); 1033 ( $\nu_{\text{s}}\text{C}-\text{O}$ , stretching)

LC-MS ( $m/z$ ) 525 ( $\text{M}+\text{Na}$ )<sup>+</sup>

### 3.5 1,4-Bis(triphenylphosphine)-2-methoxy-5-(2'-ethylhexyloxy) benzene salt (C5)



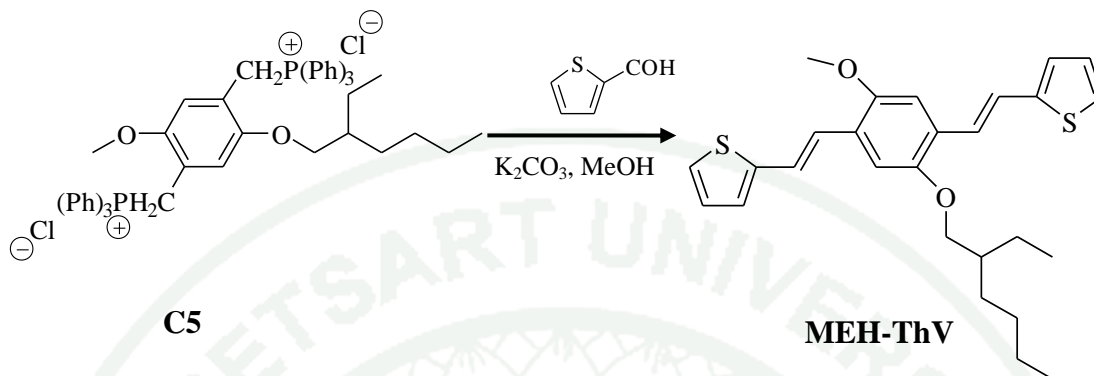
Compound 3 (**C3**) (3.00 g, 9 mmol) and triphenyl phosphine (7.10 g, 27 mmol) were dissolved in 60 ml of anhydrous tetrahydrofuran. This mixture was stirred for 24 h at reflux temperature. Upon cooling, a white solid precipitates were filtered and washed with tetrahydrofuran (50 ml) and diethyl ether (50 ml). A white solid was obtained with a yield of 5.22 g, 68.25%.

<sup>1</sup>H-NMR (400 MHz,  $\text{CDCl}_3$ ): 7.77-7.59 (m, 30H,  $-\text{P}^+(\text{Ph})_3\text{Cl}^-$ ), 6.81 (s, 1H, Ar-H), 6.69 (s, 1H, Ar-H), 5.34 (d,  $^3J_{\text{HH}} = 13.26$  Hz, 4H,  $-\text{CH}_2\text{P}^+(\text{Ph})_3\text{Cl}^-$ ), 2.90 (d,  $^3J_{\text{HH}} = 6.24$  Hz, 2H,  $-\text{OCH}_2-$ ), 2.56 (s, 3H,  $-\text{OCH}_3$ ), 2.29-1.19 (m, 1H,  $-\text{CH}-$ ), 1.11-1.08 (m, 8H,  $-\text{CH}_2-$ ), 0.89 (t,  $^3J_{\text{HH}} = 7.41$  Hz, 3H,  $-\text{CH}_3$ ), 0.69 (t,  $^3J_{\text{HH}} = 7.41$  Hz, 3H,  $-\text{CH}_3$ )

<sup>13</sup>C-NMR (400 MHz,  $\text{CDCl}_3$ ): 150.94, 150.79, 134.80, 134.77, 134.68, 134.65, 134.34, 134.25, 134.25, 134.19, 130.05, 129.96, 129.84, 118.60, 118.45, 117.75, 117.59, 116.28, 115.30, 70.73, 55.13, 38.94, 30.18, 28.97, 23.32, 22.92, 14.08, 11.03



### 3.6 [1,4-Bis(thienyl-vinyl)]-2-methoxy-5-(2-methylhexyloxy)benzene (MEH-ThV)



A mixture of compound 5 (**C5**) (5.23 g, 6 mmol) and 2-thiophenecarboxaldehyde (2.13 g, 0.19 mol) were dissolved in 100 ml of dry methanol and potassium carbonate (1.70 g, 12 mmol) was added at 0 °C. The mixture was heated to reflux for 24 h. After that the solvent was removed and the residue crude product was purified by column chromatography on silica gel using dichloromethane/hexane (4:1) as eluent. Evaporation of the eluent afforded MEH-ThV as pale yellow oil. (0.94 g, yield 33.66%).

<sup>1</sup>H-NMR (400 MHz, CDCl<sub>3</sub>): 7.28 (d, <sup>3</sup>J<sub>HH</sub> = 14.03 Hz, 2H, -CH=CH-), 7.27 (d, <sup>3</sup>J<sub>HH</sub> = 15.20 Hz, 2H, -CH=CH-), 7.19 (s, 1H, Ar-H), 7.18 (s, 1H, Ar-H), 7.09-6.99 (m, 6H, Th-CH-), 3.94 (d, <sup>3</sup>J<sub>HH</sub> = 5.46 Hz, 2H, -OCH<sub>2</sub>), 3.91 (s, 3H, -OCH<sub>3</sub>), 1.85-1.77 (m, 1H, -CH-), 1.61-12.7 (m, 8H, -CH<sub>2</sub>-), 0.99 (t, <sup>3</sup>J<sub>HH</sub> = 7.41 Hz, 3H, -CH<sub>3</sub>), 0.94-0.87 (m, 3H, -CH<sub>3</sub>)

<sup>13</sup>C-NMR (400 MHz, CDCl<sub>3</sub>): 151.35, 151.23, 127.56, 125.78, 125.64, 124.23, 124.17, 123.35, 123.15, 122.24, 122.10, 110.40, 109.13, 71.77, 56.29, 39.81, 31.58, 30.94, 24.27, 22.65, 14.10, 11.36

Elemental analysis for C<sub>27</sub>H<sub>32</sub>O<sub>2</sub>S<sub>2</sub> (F.W. 452) : C, 71.64; H, 7.13; O, 7.07; S, 14.17%  
Found C, 73.30; H, 7.30; S, 14.34

FT-IR (nujol mulls,  $\text{cm}^{-1}$ ) : 3033 (=C-H, stretching), 2954 (-C-H, stretching), 1491 (C=C, stretching), 1454 (-C-H, bending), 1207 ( $\nu_{\text{as}}$  C-O, stretching), 1034 ( $\nu_{\text{s}}$  C-O, stretching)

LC-MS ( $m/z$ ) 453 ( $\text{M}^+$ )



## Quantum Chemical Calculations

Quantum chemical calculation is the application of chemical, mathematical and computational skills to approximate the chemistry problems. It uses computers to generate information such as properties of electronic structure determinations, geometry optimizations, frequency calculations, transition structures, protein calculations, electron and charge distributions, potential energy surfaces (PES), rate constants for chemical reactions (kinetics), thermodynamic calculations heat of reactions and energy of activation of molecular system with common computer software. It also helps to predict before running the actual experiments so that they can be better prepared for making observations. In addition, the experimental cannot be explained with the electron term. Computational quantum chemistry is one of the challenging tasks in calculating predicting the properties of variety of molecules. This approach can be provided molecular models and guide the design of novel molecules.

### 1. Models of Calculation

Starting geometries of [1,4-bis(thienyl-vinyl)]-2-methoxy-5-(2'-ethylhexyloxy)benzene (MEH-ThV) and [1,4-bis(thienyl-1,1'-cyanovinylene)]-2-methoxy-5-(2'-ethylhexyloxy)benzene (MEH-ThV-CN) were constructed by molecular modeling. The molecular structure of MEH-ThV-CN composed of the two thiophene rings linking with a phenylene vinylene group and a cyano groups were substituted on vinylene unit. MEH-ThV is similar structure to that of MEH-ThV-CN but it is not replaced by cyano group on vinylene linkages. The vinylene units between the phenylene ring is twisted by about 15-30° off-planar and torsion angle close to 180° is more stable conformation corresponding to *cis*- (*Z*) and *trans*- (*E*) forms, respectively (Suramitr *et al.*, 2005). So these structures show three possibility isomers that *EE*-, *EZ*- and *ZZ*- forms in both the structures, as shown in Figures 5 and 6. Then, the ground state geometry of their molecules were determined by a fully optimization using the *ab initio* Hartree-Fock (HF) and density function theory (DFT) method. The basis set 6-31G(d,p) has been used for the geometries optimization (Francl *et al.*, 1982) and all calculations were performed using the Gaussian 03 program package

(Frisch *et al.*, 2004). Lowest first singlet excited state geometries of MEH-ThV and MEH-ThV-CN were optimized by using TD-B3LYP/dft-SV(P) method based on the ground state geometries of all molecules (Suramitr *et al.*, 2010). The fully optimization of the first singlet excited state were carried out by means of TURBOMOLE version 5.10 program (Aldrich *et al.*, 1989). It is well-understood that, in this method provides accurate geometries for conjugated system. (Osuna *et al.*, 2007 and Meeto *et al.*, 2008).

## 2. Conformation Analysis

In this study, the MEH-ThV-CN and MEH-ThV conformations were investigated the effect of substituent groups with and without the cyano group based on vinylene unit. The bond length, bond angle and torsion angle were calculated using HF and method with 6-31G(d,p) basis set. The main chain structure (C1-C9 atoms) was considered for conformational analysis of the bond length parameter. The vinylene unit (C4-C5-C6-C7) was studied with the bond angle and torsion angle which was directly connected to backbone for MEH-ThV and MEH-ThV-CN structures. Moreover, the alkyl substituent at C2 and C5 atoms (in Figure 4) play an important role in the thermal stability and solubility and do not affect the electronic structure and optical properties. Therefore, we might neglect the appearance of alkyl group at that position here. Consequently, the models and also the atom number used in this study are shown in Figures 5 and 6.

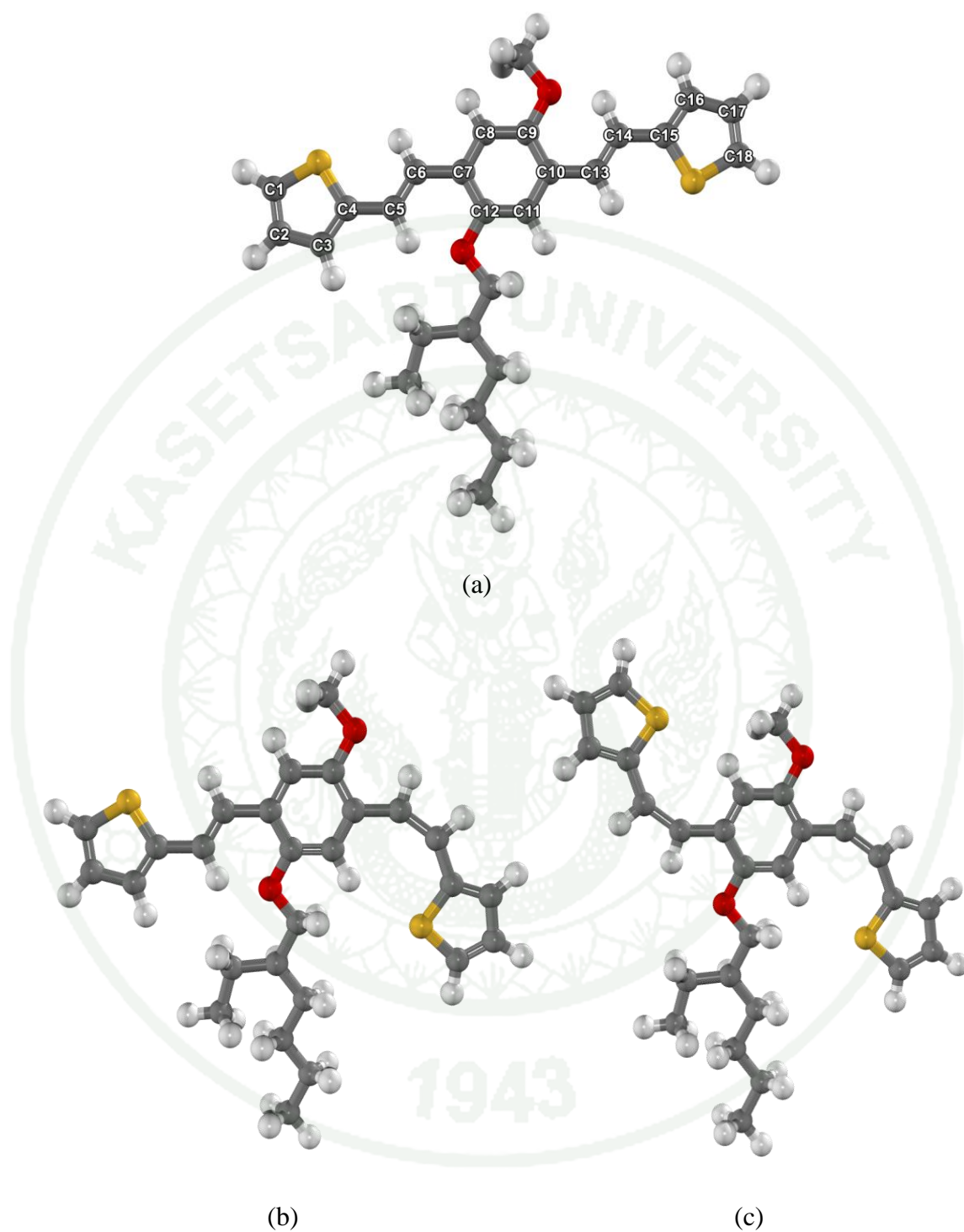


**Figure 5** Schematic diagram of (a) *EE*-, (b) *EZ*- and (c) *ZZ*-MEH-ThV structures.



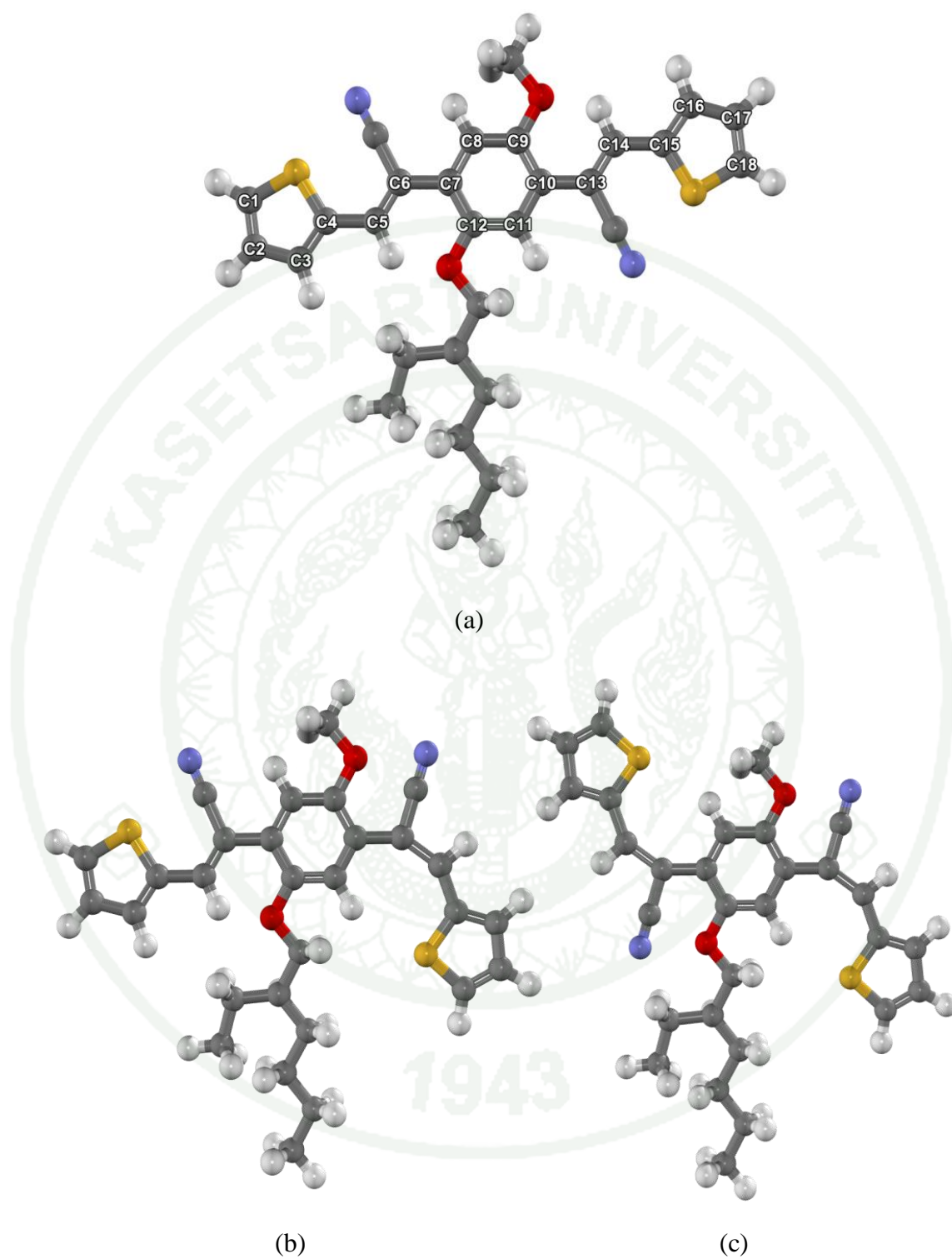


**Figure 6** Schematic diagram of (a) *EE*-, (b) *EZ*- and (c) *ZZ*-MEH-ThV-CN structures.

### 3. Electronic Properties

#### 3.1 Absorption and Emission properties

The electronic transitions were calculated by time-dependent density function theory (TDDFT) method employing the basis set 6-31G(d,p) based on the HF/6-31G(d,p) optimized geometries in the Gaussian 03 program packages. In the DFT calculations were performed using Becke's three parameter hybrid function, B3, with nonlocal correlation of Lee-Yang-Parr, LYP, abbreviated as B3LYP (Beck, 1993). The excitation energies and emission transition energies calculations of all molecules have been carried out at TD-B3LYP/dft-SV(P) level using TURBOMOLE version 5.10 program packages.

#### 3.2 Fluorescence Energy and Radiative lifetime

The fluorescence energy as the emission transition energies was obtained from the vertical de-excitation at the optimized first singlet excite state using TD-B3LYP/dft-SV(P) method. Radiative lifetime can be calculated on the fluorescence energy and oscillator strengths according to the following formula (Bransden and Joachain, 1983).

$$\tau = \frac{c^3}{2(E_{flu})^2 f}$$

Where  $c$  is the velocity of light,  $E_{flu}$  is the fluorescence transition energy and  $f$  is oscillator strength. Fluorescence or radiative lifetime provides information useful in discrimination of particles which the long conjugated system leads to a decrease of lifetime. The effect of electron withdrawing cyano group on vinylene moiety of MEH-ThV and MEH-ThV-CN were investigated of radiative lifetime.

## RESULTS AND DISCUSSION

### Synthesis and Characterization

#### 1. Synthesis

##### 1.1 Synthesis of [1,4-Bis(thienyl-vinyl)]-2-methoxy-5-(2'-ethylhexyloxy) benzene (MEH-ThV)

MEH-ThV was started by *O*-alkylation of 4-methoxyphenol (**C1**) with 2-ethylhexylbromide. Chloromethylation in phenyl ring with electron-donating alkoxy group (**C3**) can be easily obtained by **C2** to bubble with hydrochloric acid at 0 °C. Then, compound 3 (**C3**) was treated with triphenylphosphine to produce the corresponding salt of compound 5 (**C5**) by Wittig's reaction in anhydrous THF. MEH-ThV was obtained *via* the Knoevenagel condensation of a 2-thiophene carboxaldehyde with potassium carbonate in dry methanol to give the product of MEH-ThV as a pale yellow oil in 33.66% yield after chromatographic purification. The long alkoxy side chain on phenylene unit enhanced the solubility in common organic solvent such as tetrahydrofuran, hexane, chloroform, and dichloromethane. This structure was confirmed by  $^1\text{H}$ -NMR,  $^{13}\text{C}$ -NMR, FTIR, LC-MS and element analysis.

The spectrum of  $^1\text{H}$ -NMR,  $^{13}\text{C}$ -NMR and FTIR measurement were shown in Appendix A. The  $^1\text{H}$ -NMR spectrum of MEH-ThV-CN was easily obtained because it can be dissolved in *d*-chloroform ( $\text{CDCl}_3$ ) at room temperature.  $^1\text{H}$ -NMR and  $^{13}\text{C}$ -NMR results on alkyl side chain and alkoxy groups of MEH-ThV were agreed well with the results of MEH-ThV-CN spectra. The  $^1\text{H}$ -NMR spectrum of MEH-ThV remaining as *trans* stereochemistry of the vinylene bridge was confirmed by the coupling constant ( $J=14.03$  Hz) for  $-\text{CH}=\text{CH}-$  proton at 7.28 ppm. To obtain an IR spectrum of MEH-ThV compound, it is combined with Nujol mull. The major peaks of Nujol mull for FTIR analysis are 2950-2800, 1465-1450, and 1380-1370

$\text{cm}^{-1}$  in the salt plates (NaCl plates). The FTIR results indicate that nujol peaks were confused with MEH-ThV peaks which these were  $\text{CH}_2$  and  $\text{CH}_3$  stretching and bending. The symmetric C-O and asymmetric C-O vibrational stretching were assigned at 1207 and 1034  $\text{cm}^{-1}$ , respectively, which it was associated with the alkoxy groups on phenyl moiety. The elemental composition of MEH-ThV showed good agreement between the expected (C, 71.64; H, 7.13; O, 7.07; S, 14.17%) and observed (C, 73.30; H, 7.30; S, 14.34) empirical formula.

## 1.2 Synthesis of [1,4-Bis(thienyl-1,1'-cyanovinylene)]-2-methoxy-5-(2'-ethylhexyloxy) benzene (MEH-ThV-CN)

The synthesis of [1,4-Bis(thienyl-1,1'-cyanovinylene)]-2-methoxy-5-(2-methylhexyloxy)benzene (MEH-ThV-CN) was obtained starting from compound 1, 2 and 3, respectively. The compound 4 (**C4**) was substituted with the electron-withdrawing cyano groups *via* nucleophilic substitution with sodium cyanide in DMF. The MEH-ThV-CN was obtained by a Knoevenagel condensation of 2-thiophene (carboxaldehyde) with potassium *tert*-butoxide to afford the product as orange solid in 38.28% yield. This synthesis method of MEH-ThV-CN was prepared consisting of a central dialkoxyphenylene core *p*-disubstituted with two thiophene rings through a cyanovinylene linker.

The  $^1\text{H}$ -NMR spectrum exhibits the chemical shift of alkyl side chain in the region of 0.85-1.80 *ppm*. The methoxy protons ( $-\text{OCH}_3$ ) signal appears at 3.87 *ppm* and methyleneoxy protons ( $-\text{OCH}_2-$ ) signal occurs at 3.90 *ppm* with a coupling constant of 5.07 Hz. The phenylene-*H* shows two singlets centered at 7.14 and 7.10 *ppm*, while the thiophene-*H* shows doublet of doublet (dd) at 7.67 *ppm* with a coupling constant of 3.51 Hz. The thiophene protons signals are attributed to thienyl proton adjacent sulfur atom on thiophene ring. In  $^{13}\text{C}$ -NMR spectrum, there are clear signals in this spectrum. Together with FTIR results, it is agree closely with the structure. The  $\text{C}\equiv\text{N}$  stretching vibration at 2212  $\text{cm}^{-1}$  has been associated with cyano group on vinylene unit in the main chain structure. The vibrations attributed  $=\text{C}-\text{H}$  stretch at 3076  $\text{cm}^{-1}$  corresponding to thiophene ring and vibrational of phenyl ring

occur overtone in the region  $1616\text{--}1796\text{ cm}^{-1}$ . The elemental composition of MEH-ThV-CN shows good agreement between the expected (C, 69.29; H, 6.02; N, 5.57; O, 6.37; S, 12.76%) and observed (C, 70.57; H, 6.43; S, 12.98) empirical formula.

## 2. Thermal Properties

The thermal stabilities of MEH-ThV and MEH-ThV-CN under nitrogen atmosphere were determined by thermogravimetric analyzer (TGA) ( $50\text{--}550\text{ }^{\circ}\text{C}$ ,  $10\text{ }^{\circ}\text{C}/\text{min}$ ). The TGA thermogram is depicted in Figure 7 and decomposition temperature ( $T_d$ ) is  $349.63$  and  $323.00\text{ }^{\circ}\text{C}$ , respectively. Thermal decomposition of MEH-ThV-CN and MEH-ThV were attributed to the degradation on backbone. However, decomposition temperature ( $T_d$ ) of MEH-ThV was higher than that of MEH-ThV-CN, suggesting that dialkoxy side chain and the main chain structure of MEH-ThV retarded thermal degradation effectively. The maximum rate of weight loss of MEH-ThV and MEH-ThV-CN took place at temperature above  $410.32$  and  $388.92\text{ }^{\circ}\text{C}$ , respectively. The TGA results revealed that MEH-ThV was more stable than MEH-ThV-CN under nitrogen atmosphere. Both compounds are thermally enough stable to be used as electroluminescence materials in light-emitting devices.



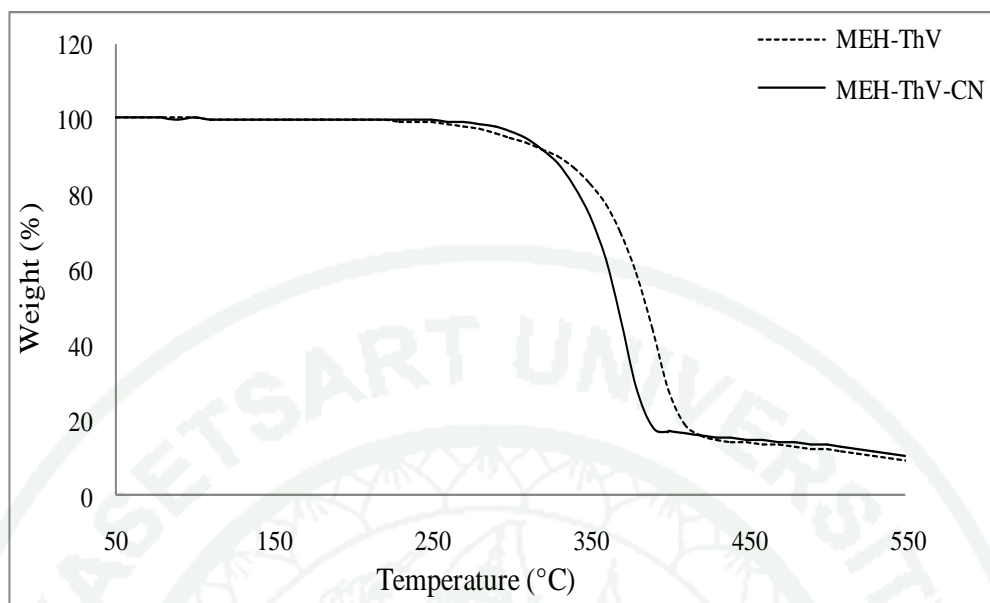


**Figure 7** Thermogravimetric curve of MEH-ThV and MEH-ThV-CN at a heating rate of 10 °C/min under nitrogen atmosphere.

### 3. Absorption Properties

The absorption spectra of MEH-ThV and MEH-ThV-CN in chloroform solution are depicted in Figure 8. The  $\lambda_{\text{max}}$  of UV spectra for MEH-ThV-CN are 281, 335 and 393 nm with absorption edge at 405 nm, whereas the maximum absorption of MEH-ThV occur at 252, 348 and 407 nm as red shifts with a shoulder (423 nm). The compound of MEH-ThV is bathochromic shifts (13 and 14 nm) in absorption, as compared to MEH-ThV-CN, is presumably due to the cyano groups on the vinylene linkages next to the thienyl rings based on molecule and distorted from the electron repulsion. In addition, there are three main peaks in UV-Vis absorption spectra of both compounds. One is due to the  $\pi$ - $\pi^*$  transition of delocalized  $\pi$  electron along the conjugated main chain in long wavelength and another is due to the  $n$ - $\pi^*$  electron transition to the side chain in short wavelength (Gustafsson *et al.*, 1992).

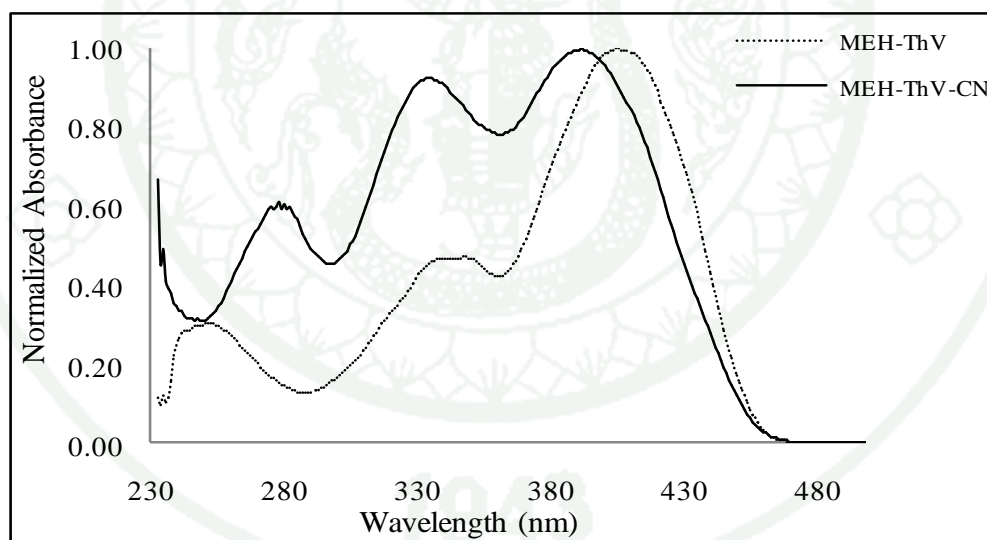


**Figure 8** Absorption spectra of MEH-ThV and MEH-ThV-CN in  $\text{CHCl}_3$  solution.

The low energetic edge of absorption spectrum of MEH-ThV is 423 nm, which corresponds to a band gap ( $E_g$ ) of 2.93 eV. While the absorption onset for MEH-ThV is 405 nm, corresponding to a band gap ( $E_g$ ) of 3.06 eV, as summarized in Table 1. MEH-ThV-CN shows higher band gap than MEH-ThV as increasing disorder in the conjugated system due to steric hindrance of the electron-withdrawing cyano group effect. These results could conclude that there is a stronger interchain interaction in MEH-ThV, which leads to more coplanar backbone structure than that of MEH-ThV-CN structure.

**Table 1** Optical data of MEH-ThV and MEH-ThV-CN measured in chloroform solution.

Compounds	$\lambda_{\max}$ (nm)	$\lambda_{\text{onset}}$ (nm)	$E_g$ (eV)
MEH-ThV	407	423	2.93
MEH-ThV-CN	393	405	3.06

#### 4. Emission Properties

The emission spectra of MEH-ThV and MEH-ThV-CN at room temperature in chloroform solution are shown in Figure 9. The maximum wavelength of emission spectra of MEH-ThV-CN with cyano groups are 383 and 463 nm. In addition, a shoulder peak at 483 nm can be also noticed in the spectrum. However, MEH-ThV without cyano groups in the emission spectra are 403 and 458 nm with edge emission wavelength at 485 nm as slightly blue-shifted (2 nm) than that with electron-withdrawing cyano groups attached on the vinylene moieties.

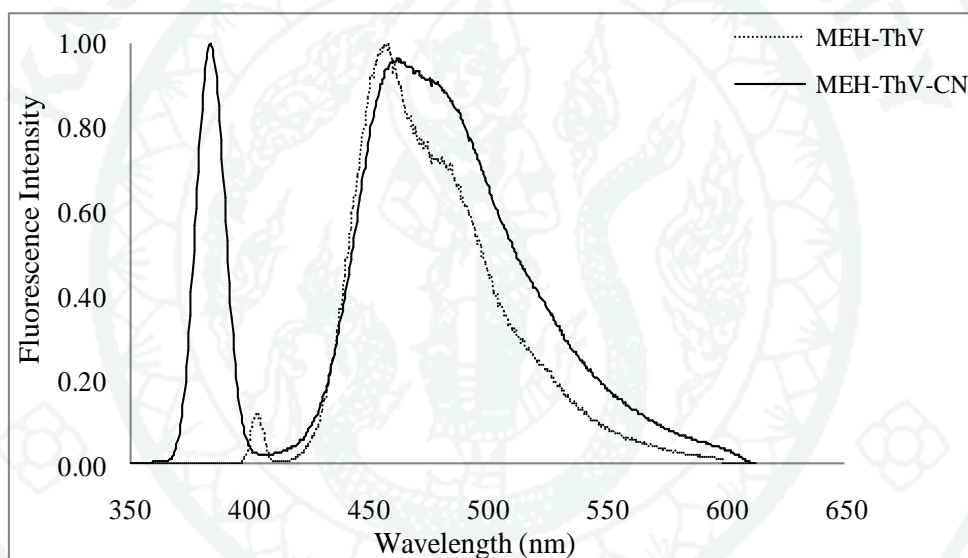


**Figure 9** Emission spectra of MEH-ThV and MEH-ThV-CN in CHCl<sub>3</sub> solution.

Stokes shifts is the difference between of the absorption wavelength and emission wavelength (Stokes, 1958). Stokes shifts of MEH-ThV is 51 nm, whereas MEH-ThV-CN is 70 nm. The results indicated that their main chain structures are rather rigid. However, the photophysical properties of MEH-ThV are green light emission, while MEH-ThV-CN exhibit as green-yellow light emission, and are depicted in Figure 10. It is noteworthy that it can be used as new luminescence materials in the fabrication of OLED based full-color displays.

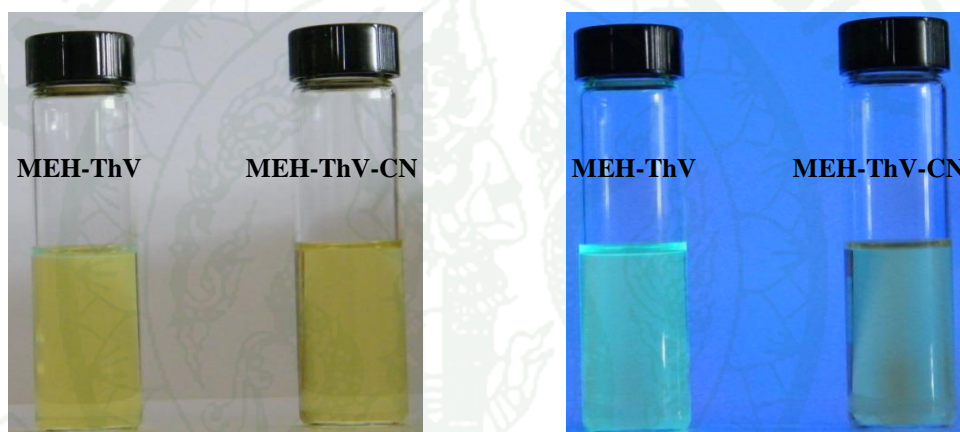


**Figure 10** Light emitting in chloroform solution of MEH-ThV and MEH-ThV-CN measured in (a) short wavelength and (b) long wavelength.



## 5. Electrochemical Properties

Cyclic voltammetry (CV) using 0.1 M TBAP as a supporting electrolyte in acetonitrile was employed to study the electrochemical analysis of the monomers. A platinum electrode was used as the working electrode, platinum electrode as counter electrode and Ag/Ag<sup>+</sup> as reference electrode. The cyclic voltammograms perform quasi-reversible oxidation and reduction processes. Therefore, CV have been applied to investigate their redox behaviors and estimate the highest occupied molecular orbital (HOMO) and the lowest occupied molecular orbital (LUMO) energy levels. The difference between oxidation onset potentials  $E_{onset}^{ox}$  (V) and energy gaps from the onset wavelength of the optical absorption can be used to estimate the energy gap ( $E_g = E_g^{abs} - E_{onset}^{ox}$ ) (Tang *et al.*, 2006). According to Ho *et al.* (2004), the energy levels (in electron volts, eV) corresponding to the electrochemical potentials (vs. Ag/Ag<sup>+</sup>) can be obtained by using the ferrocence (FOC) value of -4.8 eV with respect to vacuum level. The formal potential of Fc/Fc<sup>+</sup> was measured as 0.09 eV against Ag/Ag<sup>+</sup>. Thus, the HOMO and LUMO energies were calculated by using the following equations :

$$E_{HOMO} = -(E_{onset}^{ox} + 4.71)$$

$$E_{LUMO} = (E_{HOMO} + E_g^{abs})$$

The LUMO energy level was not estimated using the onset position of reduction. Energy gap of potential differences between oxidation and reduction onset potentials was not also calculated ( $E_g = E_{HOMO} - E_{LUMO}$ ) because of a discrepancy to the optical energy gap and energy gap from CV curve. The discrepancy is caused by the insulating effect of the side chains during the electrochemical process (Egbe *et al.*, 2004; Chen *et al.*, 2000 and Yamamoto *et al.*, 2002).

The cyclic voltammograms of MEH-ThV and MEH-ThV-CN are depicted in Figures 11 and 12, respectively. The electrochemical properties and band gap ( $E_g$ ) of both compounds are listed in Table 2. The oxidation onset potential of MEH-ThV-CN as 1.25 V was obtained corresponding to HOMO level of -5.96 eV. The LUMO was calculated to be -3.92 eV from the values of the band gap (3.06 eV) and HOMO energy level. The HOMO and the LUMO energies of MEH-ThV are -5.59 and -2.99 eV, respectively.

**Table 2** Electrochemical data from MEH-ThV and MEH-ThV-CN as obtained from cyclic voltammetry (CV)

Compounds	$E_{onset}^{ox}$ (V)	HOMO <sup>a</sup> (eV)	LUMO <sup>b</sup> (eV)	$E_g^c$ (eV)
MEH-ThV	0.85	-5.56	-2.63	2.93
MEH-ThV-CN	1.25	-5.96	-2.90	3.06

<sup>a</sup> HOMO energies estimated from  $E_{HOMO} = -(E_{onset}^{ox} + 4.71)$ .

<sup>b</sup> LUMO energies obtained from  $E_{LUMO} = (E_{HOMO} + E_g^{abs})$ .

<sup>c</sup> Energy gaps estimated from the onset wavelength of the optical absorption.

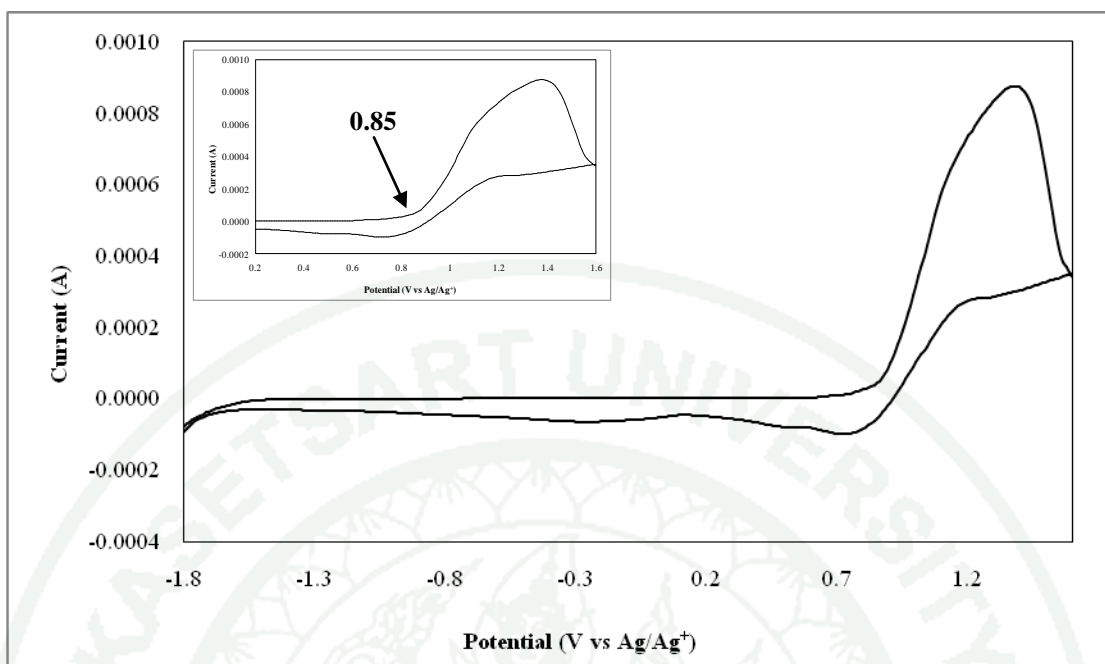


**Figure 11** Cyclic voltammogram of MEH-ThV in 0.1 mol/l TBAP acetonitrile, scan rate 20 mV/s.

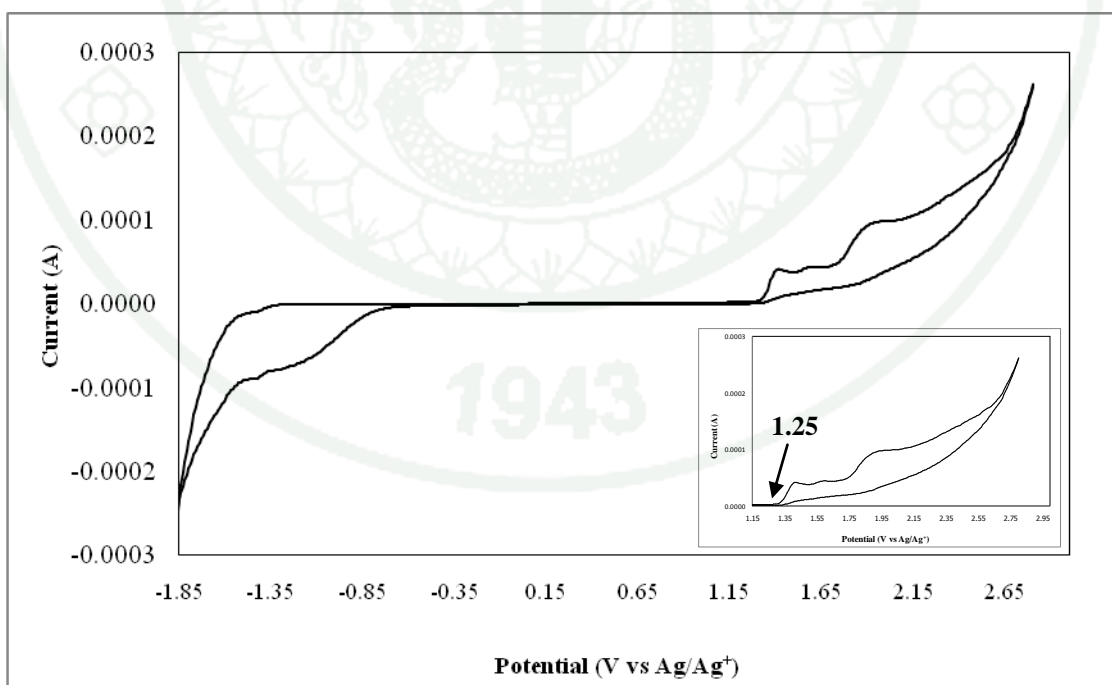


**Figure 12** Cyclic voltammogram of MEH-ThV-CN in 0.1 mol/l TBAP acetonitrile, scan rate 20 mV/s.

## Quantum Chemical Calculations

### 1. Methods Validation

#### 1.1 Comparison on the calculated ground state geometry parameters of MEH-ThV by different theoretical methods

The Hartree Fock (HF) and density functional theory (DFT) methods have been used for the purpose of conformation analysis. Bongini and Bottoni (1999) pointed that the DFT approach provides a good description of the conformation properties of oligomer and polythiophenes, which is agreement with the experimental evidence. Therefore, it will be useful to examine the structural parameters of MEH-ThV geometry (Figure 13) based on molecules. This structure was fully optimized by using *ab initio* method with HF and DFT method with B3LYP hybrid at 6-31G(d,p) level of basis set, as present in Table 3. The structural parameter in term of bond length was considered on backbone structure which this term was investigated only C1-C9 atoms (Figure 13) as symmetry conformation. In 2002, Wong *et al.* studied poly(*p*-phenylene vinylene) (PPV) chain using semiempirical SCF, AM1 and PM3 methods of the ground state optimized geometries, which gave the *cis*-defect (*Z*-) and *trans*-defect (*E*-) in one vinylene group. Therefore, vinylene bridge position of MEH-ThV geometry was considered both the bond angle and torsion angle (C4-C7 atoms). Unfortunately, from our knowledge, there is no X-ray structure of MEH-ThV structure available in literature. Therefore, this structural parameter with the quantum chemical calculations can be predicted the conformational analysis in this study.

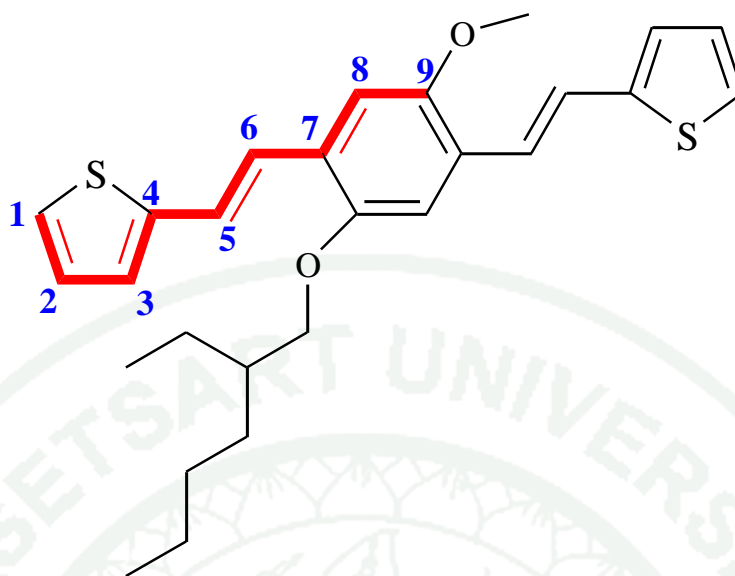


**Figure 13** Schematic represents the bond number on backbone structure of MEH-ThV molecule.



**Table 3** Structural parameters of MEH-ThV obtained from fully optimization by HF and B3LYP methods at 6-31G(d,p) level of basis set (bond length in angstrom (Å), angle in degrees).

Structural parameters	HF/6-31G(d,p)	B3LYP/6-31G(d,p)
Bond length		
C1-C2	1.34	1.37
C2-C3	1.43	1.42
C3-C4	1.35	1.38
C4-C5	1.46	1.44
C5-C6	1.33	1.36
C6-C7	1.47	1.46
C7-C8	1.40	1.41
C8-C9	1.38	1.39
Bond angle		
C4-C5-C6	125.2	125.6
C5-C6-C7	128.9	130.0
Torsion angle		
C4-C5-C6-C7	-178.2	-179.2
BLA	0.0800	0.0475

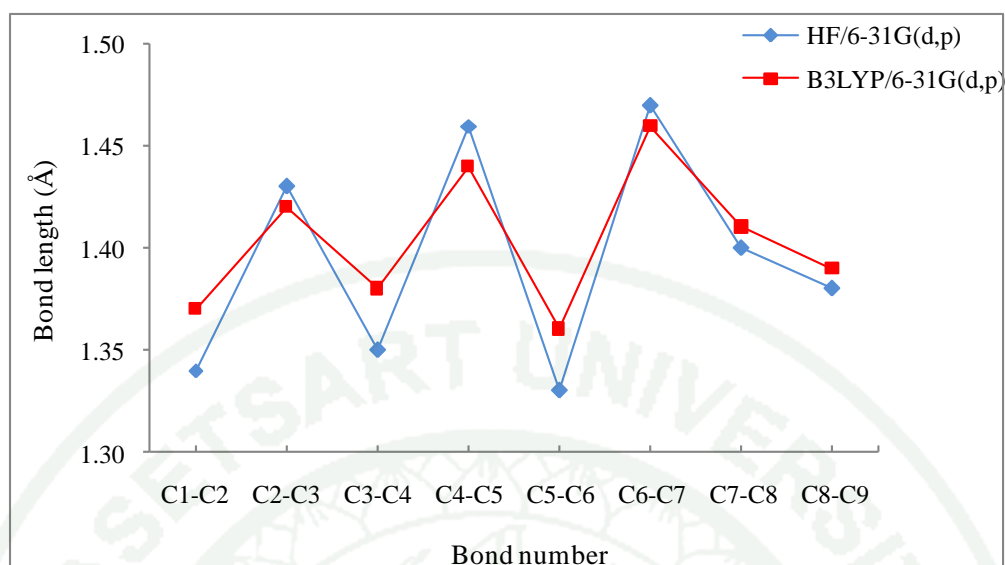


**Figure 14** Optimized bond length of MEH-ThV obtained from HF/6-31G(d,p) and B3LYP/6-31G(d,p) methods.

The bond lengths in the phenylene vinylene and thiophene fragments of MEH-ThV geometry is conjugated chain or double bond alternating with single bond. The C-C and C=C bond lengths of the optimized structure for the MEH-ThV is listed in Table 3. The bond length values were considered as the distance between the carbon atoms on the main chain structure. The bond lengths were compared between HF/6-31G(d,p) and B3LYP/6-31G(d,p) optimized geometry of the ground state ( $S_0$ ). According to the results, in this case the single bond lengths (C-C) became larger, while the double bond lengths (C=C) became shorter in both methods, as presented in Figure 14. Furthermore, these results were found that the smallest C=C bond distance (see bond number C5-C6), it is located on vinylene bridge of 1.33 Å in HF/6-31G(d,p) optimized geometry, while bond distance of B3LYP/6-31G(d,p) optimized geometry is 1.36 Å. The single bond distances (see bond number C4-C5, C6-C7) on vinylene bridge exhibit also the largest distance about 1.45 Å in the both methods. Our calculations indicated that the bond length alterations by electron donating substitutions (thienyl fragments) are significant for vinylene bridge position.

Bond length changes in aromatic systems can also be described by bond length alternation (BLA) (Tretiak *et al.*, 2002). The BLA values for selected molecular fragment can be defined as the differences in the lengths between single bond and double bond between non-hydrogen atoms. The positive and negative sign of BLA indicated that the molecular unit has an aromatic and quinoid isomer, respectively. Thus, the BLA value can be evaluated as following equations :

$$BLA = \left( \frac{\sum d_{single} - \sum d_{double}}{N} \right)$$

Where  $d$  symbols denote the bond determined of single bond and double bond distances on the backbone structure and  $N$  symbol is the number bond. As can be seen from data in Table 3, the HF/6-31G(d,p) optimized geometry lead to increase of the BLA value by 0.0800, whereas the B3LYP/6-31G(d,p) optimized geometry is decreased of 0.0475. From positive sign of BLA of all calculation geometry, it can be concluded that the main chain structure (C1-C18 atoms) are aromatic isomer, as seen clearly in Figure 15.

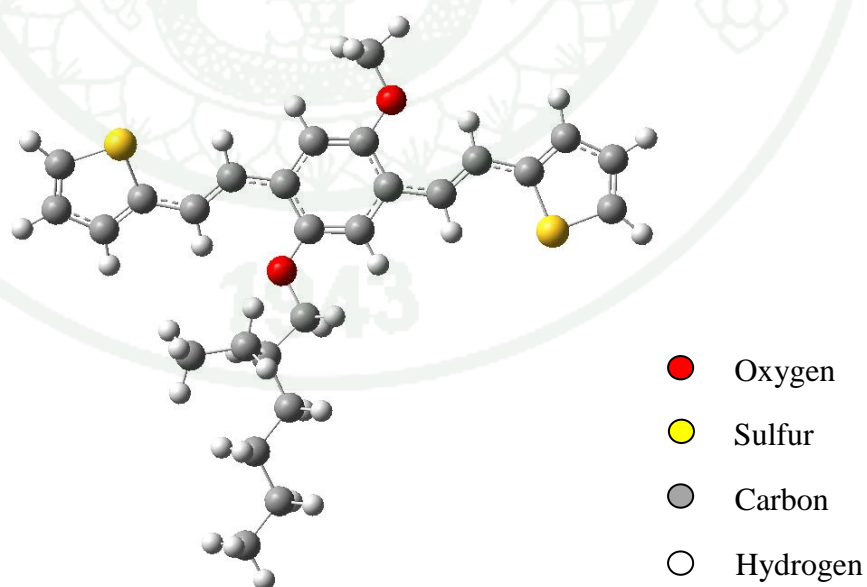


**Figure 15** Aromatic system on backbone structure of MEH-ThV geometry as obtained from HF/6-31G(d,p) method.

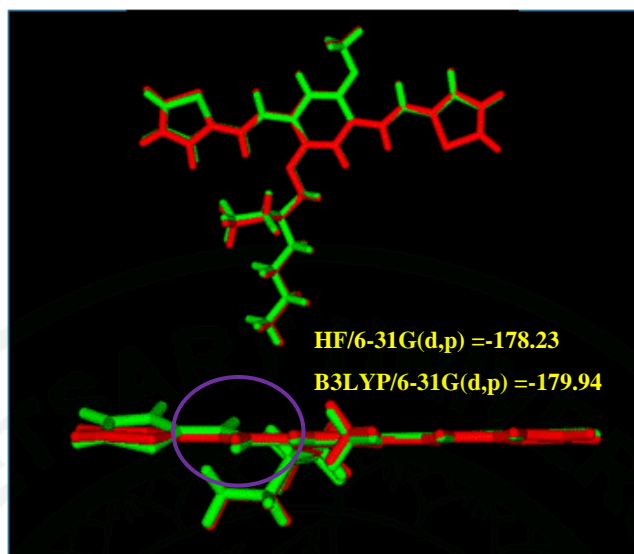


**Figure 16** Optimized torsion angle of MEH-ThV obtained from HF/6-31G(d,p) (green line) and B3LYP/6-31G(d,p) (red line) methods.

The bond angle C4-C5-C6 and C5-C6-C7 in the HF/6-31G(d,p) (125.2 and 128.9 degrees) is similar with B3LYP/6-31G(d,p) (125.6 and 130.0 degrees) optimized geometries. The torsion angles C4-C5-C6-C7 from the HF (-178.2 degree) and DFT (-179.2 degree) methods, the MEH-ThV structure in HF geometry optimization can be considered to be coplanar by having on vinylene bridge twisted within about -1.8 degree from the planar configuration. Conversely, those from the B3LYP geometry optimization are nearly 180.0 degree. The structure can be presented the planar configuration, as shown in Figure 16.

The structural parameters obtained from different theoretical methods are noteworthy because an accurate structure prediction leads to other reliable property calculations. The MEH-ThV structure is optimized using difference level methods of calculation (HF and B3LYP methods). Unfortunately, from our knowledge, there is no x-ray structure of MEH-ThV structure available in literature. Therefore, the absorption properties were then investigated to confirm the configuration of the molecule with different methods.

## 1.2 Comparison on the electronic transition based on ground state geometry optimized of MEH-ThV with HF and B3LYP methods

Electronic transitions of MEH-ThV were investigated to confirm the configuration for ground state geometry optimized with HF and B3LYP methods. The lowest excitation energies and oscillator strengths for the transition from ground state ( $S_0$ ) to excited states ( $S_n$ ) ( $n=1, 2, 3, \dots$ , and 10 states) of the molecule was calculated using TD-DFT calculation in gas phase at the B3LYP/6-31G(d,p) level on HF/6-31G(d,p) and B3LYP/631G(d,p) optimized ground state structures. Comparisons of the predicted values to the absorption band of this molecule in chloroform of MEH-ThV structure was synthesized in this study.

In Table 4, TD-B3LYP calculations on all ground state geometries are used to predict the oscillator strength. It is found that the  $S_0 \rightarrow S_1$  transition corresponding to the excitation from the HOMO (highest occupied molecular orbitals, H denoted) to the LUMO (lowest occupied molecular orbitals, L denoted) is dominant. The polarizable continuum model (PCM) was employed to take the chloroform solvation effect with TD-B3LYP calculation (Tomasi, J. and M. Persico., 1994). The absorption wavelengths of the transition obtained from the ground state geometries optimized using HF was conducted with gas phase (394.89, 324.11 and 252.78 nm), and solvent phase (410.27, 329.91 and 253.82 nm). While the wavelength of the structure from B3LYP method in gas phase is 429.17, 342.98, and 266.55 nm, whereas in solvent phase is 450.73, 349.03, and 267.54 nm. The optical wavelength for experimental data was compared with the TD-DFT excitation spectrum for the MEH-ThV compound, as seen clearly in Figure 17. These results are in qualitative agreement with experimental absorption data. However, the wavelength of the structure from HF method is closer to experimental data of 407, 348, and 252 nm both in gas phase and solvent phase than that of B3LYP method.

From our calculated electronic transitions with TD-B3LYP calculation was compared with the experimental data, the results from the ground state geometries of MEH-ThV molecule using HF/6-31G(d,p) optimization is in better



agreement than B3LYP/6-31G(d,p) method. For the structure accuracy, the HF/6-31G(d,p) method is selected for the ground state geometry optimization.

**Table 4** The lowest excitation energies in eV and oscillator strength ( $f$ ) (values in parentheses) using TD-B3LYP/6-31G(d,p) method based HF/6-31G(d,p) and B3LYP/6-31G(d,p) optimize geometry and absorption spectra of experimental data in  $\text{CHCl}_3$  solution for the MEH-ThV geometry.

Ground State geometry optimization	states	TD-B3LYP/6-31G(d,p)				$\lambda_{\text{abs}}$ (nm) <sup>exp</sup>
		Transition	$E_{\text{ex}}$	$\lambda_{\text{abs}}$	$f$	
		States <sup>a</sup>	(eV)	(nm)		
<b>HF/6-31G(d,p)</b>						
Gas phase	S <sub>0</sub> →S <sub>1</sub>	H→L (81%)	3.14	394.89	1.2454	
	S <sub>0</sub> →S <sub>3</sub>	H-2→L (58%)	3.82	324.11	0.2283	
	S <sub>0</sub> →S <sub>9</sub>	H-2→L+1 (66%)	4.90	252.78	0.2034	
Solvent phase	S <sub>0</sub> →S <sub>1</sub>	H→L (85%)	3.02	410.27	1.4434	407
	S <sub>0</sub> →S <sub>2</sub>	H-1→L (89%)	3.76	329.91	0.3676	348
	S <sub>0</sub> →S <sub>9</sub>	H-2→L+1 (82%)	4.88	253.82	0.2102	252
<b>B3LYP/6-31G(d,p)</b>						
Gas phase	S <sub>0</sub> →S <sub>1</sub>	H→L (78%)	2.89	429.17	1.4416	
	S <sub>0</sub> →S <sub>3</sub>	H-2→L (55%)	3.61	342.98	0.2647	
	S <sub>0</sub> →S <sub>8</sub>	H-4→L+1 (74%)	4.65	266.55	0.1719	
Solvent phase	S <sub>0</sub> →S <sub>1</sub>	H→L (83%)	2.75	450.73	1.6537	407
	S <sub>0</sub> →S <sub>3</sub>	H-2→L (89%)	3.55	349.03	0.2731	348
	S <sub>0</sub> →S <sub>9</sub>	H-1→L+1 (75%)	4.63	267.54	0.1817	252

<sup>a</sup> H = HOMO, L = LUMO, H-1 = next highest occupied molecular orbital, and L+1 = next lowest unoccupied molecular orbital

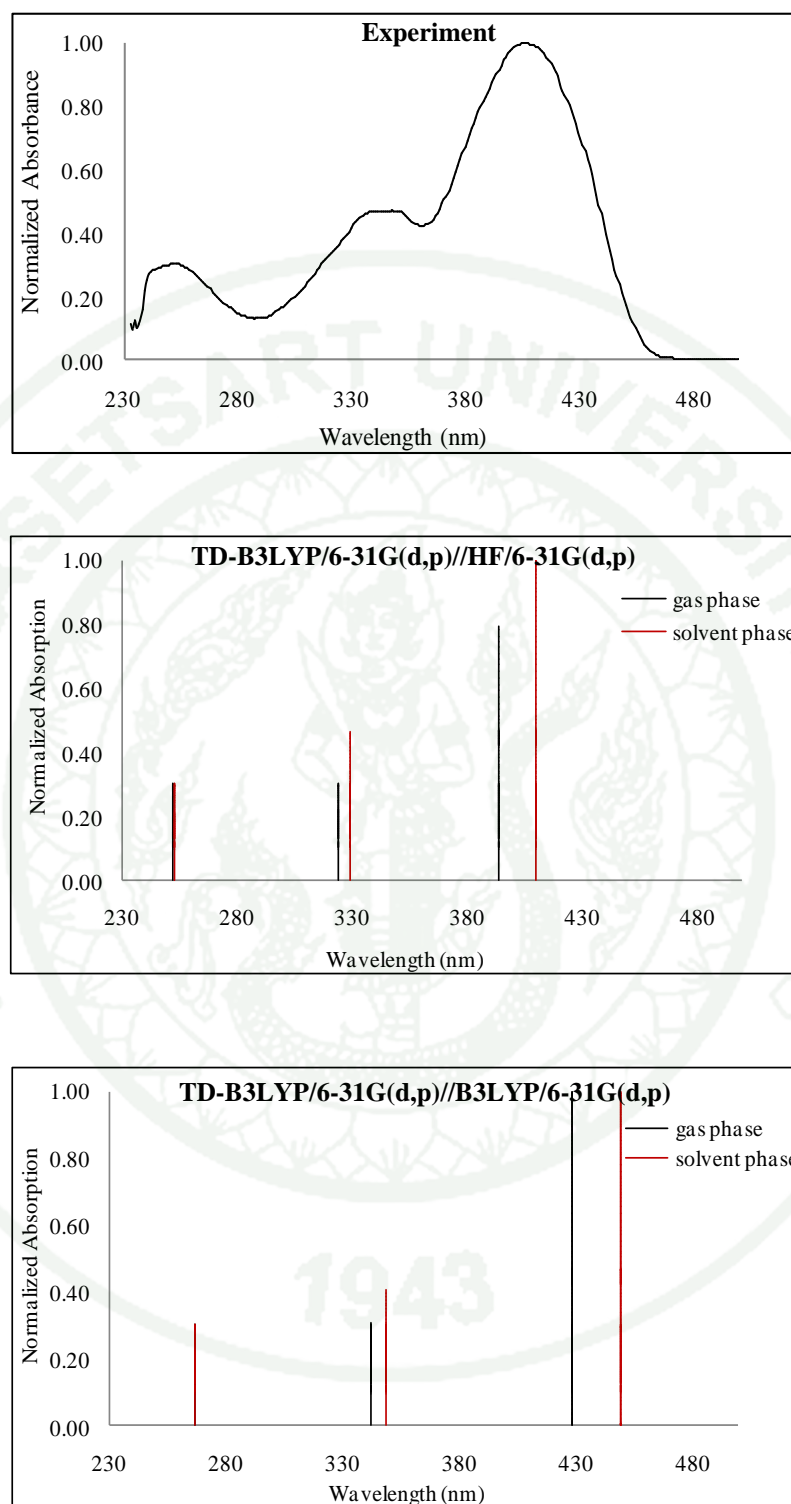


**Figure 17** Absorption spectra of MEH-ThV obtained from the experimental in  $\text{CHCl}_3$  solution and calculated using TD-B3LYP/6-31G(d,p) in gas phase (black line) and PCM model in  $\text{CHCl}_3$  solution (red line) with optimization at HF/6-31G(d,p) and B3LYP/6-31G(d,p) methods.

## 2. Ground state and Excited state Structural Properties

In 2005, Gabański and coworker obtained a model macromonomer namely 1,4-diethoxy-2,5-bis-[2-(thien-2-yl)ethenyl]benzene in three pure stereoisomeric of *EE*, *EZ* and *ZZ* forms, which the *EZ* isomer was not suitable for crystallography. This structure is similar with the MEH-ThV molecule, but the alkoxy groups at C2 and C5 positions on phenylene ring are different. Therefore, stereoisomer can be obtained as three possibility isomers (*EE*-, *EZ*- and *ZZ*-) of both molecules, as shown in Figure 5 and 6, respectively.. The vinylene unit was fixed the torsion angle at 0 or 180 degrees corresponding to *E*- form, whereas *Z*- conformation was located at 30 or 150 degree. Which it will be defined structures by excellent model systems that can be used to study conformation of all structures corresponding to the experimental results. In order to understand structural properties of stereoisomers, the ground state ( $S_0$ ) and the first singlet excited state ( $S_1$ ) geometries, bond length, bond angle and torsion angle, of MEH-ThV and MEH-ThV-CN geometries were investigated.

### 2.1 Ground state and Excited state Structural Properties of *EE*-, *EZ*- and *ZZ*-MEH-ThV

All calculations of the three stereoisomers of MEH-ThV structures were full optimized by using *ab initio* method with HF and DFT method with B3LYP hybriide at 6-31G(d,p) level of basis set for the ground state optimized geometries ( $S_0$ ) and TD-B3LYP/dft-SV(P) level of the first singlet excited state optimized geometries ( $S_1$ ), as listed in Table 5. The structural parameters in term of bond length were considered on backbone structure while the bond angle and torsion angle were studied only for vinylene bridge position as well as conformational isomer of all stereoisomers.

**Table 5** Fully optimization of structural parameters of *EE*-, *EZ*- and *ZZ*-MEH-ThV with the  $S_0$  and  $S_1$  geometries obtained from HF/6-31G(d,p) and TD-B3LYP/dft-SV(P) methods, respectively (bond length in angstrom and angle in degrees).

Structural parameters	<i>EE</i>		<i>EZ</i>		<i>ZZ</i>	
	$S_0$	$S_1$	$S_0$	$S_1$	$S_0$	$S_1$
Bond length						
C1-C2	1.34	1.37	1.34	1.38	1.34	1.38
C2-C3	1.43	1.42	1.43	1.41	1.43	1.41
C3-C4	1.35	1.38	1.35	1.40	1.35	1.41
C4-C5	1.46	1.45	1.46	1.43	1.47	1.43
C5-C6	1.33	1.35	1.33	1.38	1.33	1.39
C6-C7	1.47	1.47	1.48	1.43	1.48	1.43
C7-C8	1.40	1.40	1.40	1.43	1.39	1.42
C8-C9	1.38	1.39	1.38	1.38	1.38	1.39
Bond angle						
C4-C5-C6	125.2	133.3	125.2	130.7	131.4	133.3
C5-C6-C7	128.9	131.0	129.0	130.9	129.3	131.0
Torsion angle						
C4-C5-C6-C7	-178.2	-179.4	-178.2	-179.9	-5.9	-20.2
BLA	0.0800	0.0575	0.0825	0.0150	0.0875	0.0150

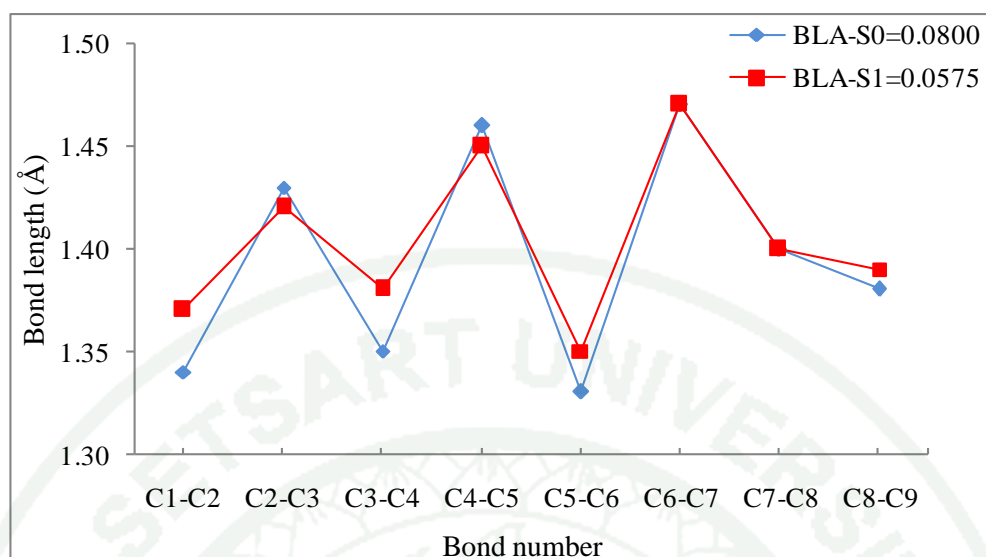


**Figure 18** Optimized bond length and bond length alternation (BLA) of *EE*-MEH-ThV of the  $S_0$  and  $S_1$  geometries as obtained from HF/6-31G(d,p) and TD-B3LYP/dft -SV(P) methods, respectively.

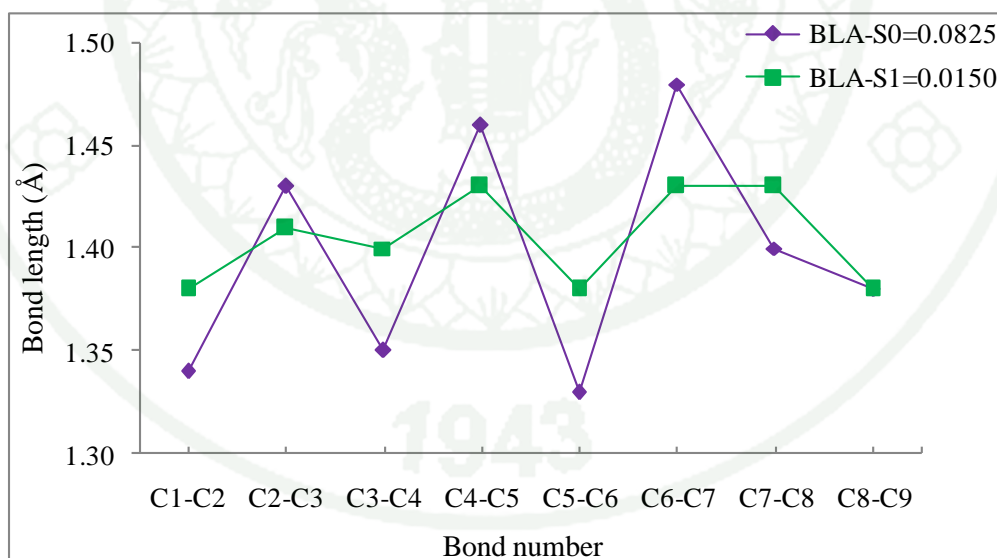


**Figure 19** Optimized bond length and bond length alternation (BLA) of *EZ*-MEH-ThV of the  $S_0$  and  $S_1$  geometries as obtained from HF/6-31G(d,p) and TD-B3LYP/dft -SV(P) methods, respectively.



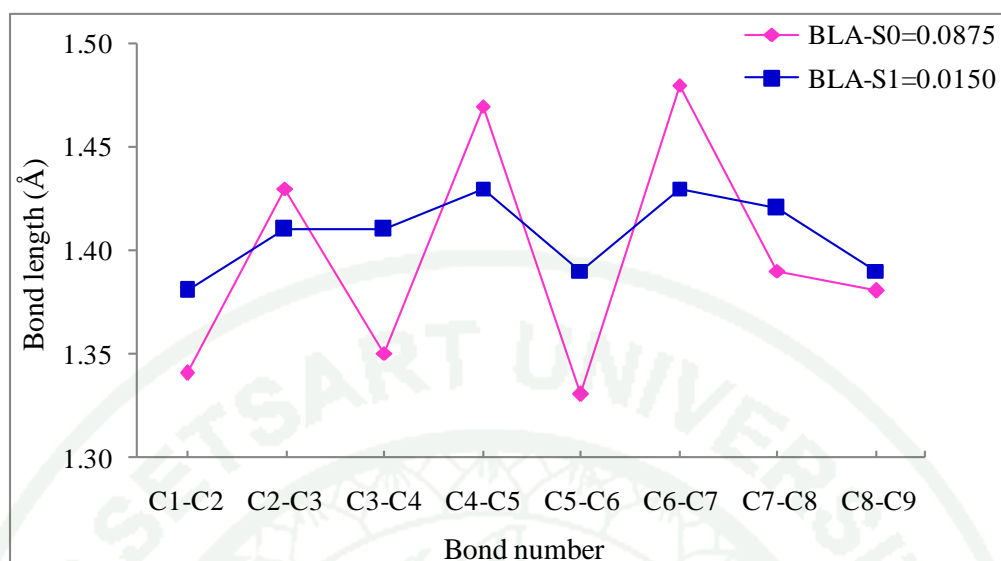


**Figure 20** Optimized bond length and bond length alternation (BLA) of ZZ-MEH-ThV of the  $S_0$  and  $S_1$  geometries as obtained from HF/6-31G(d,p) and TD-B3LYP/dft-SV(P) methods, respectively.

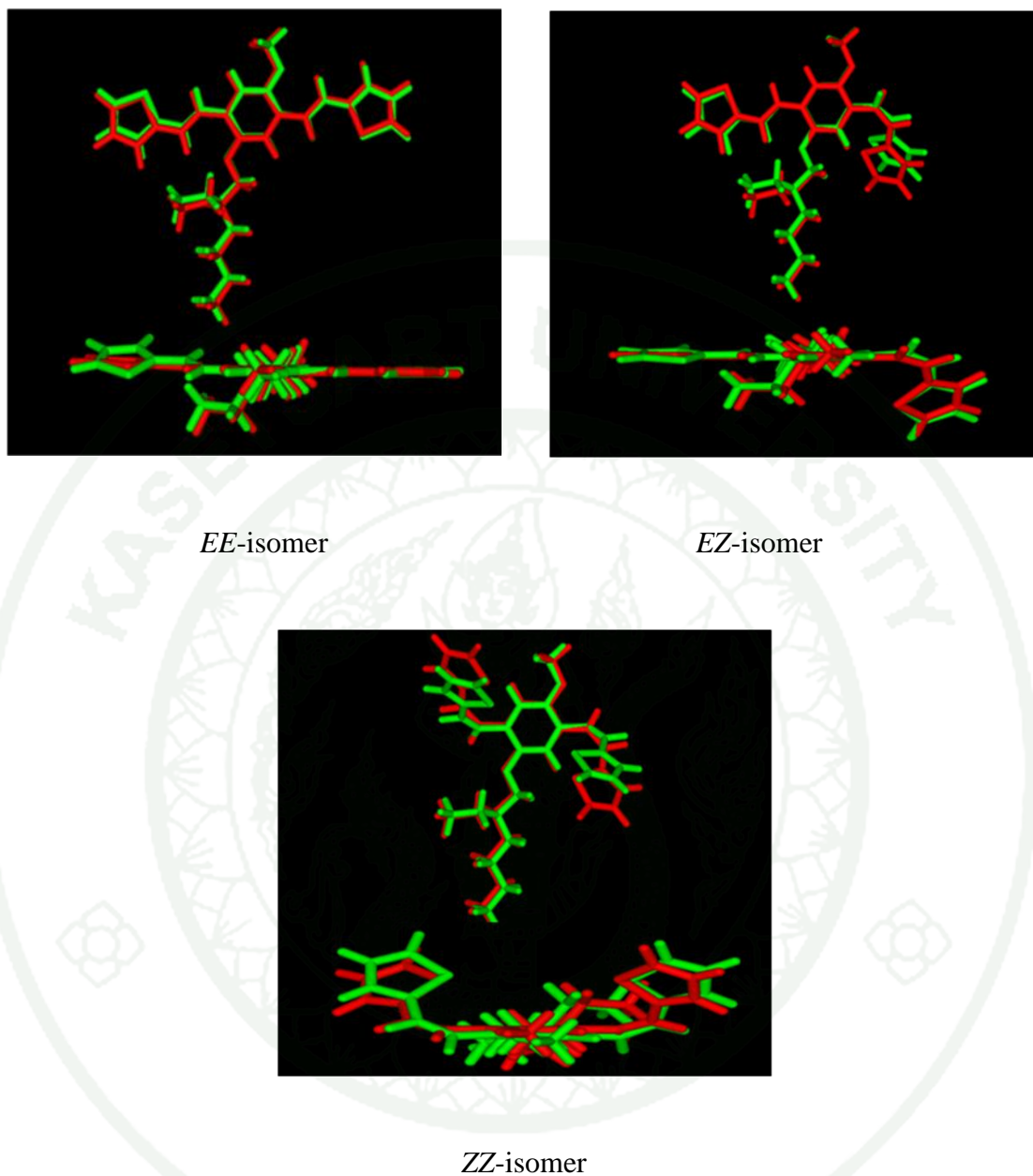


**Figure 21** Optimized torsion angle of *EE*-, *EZ*- and *ZZ*-MEH-ThV of the ground state ( $S_0$ ) (green line) and the first singlet excited state ( $S_1$ ) geometries (red line) as obtained from HF/6-31G(d,p) and TD-B3LYP/dft -SV(P) methods, respectively.

The bond lengths in thienyl fragment do not vary as the conjugated chain are elongated indicating that the bond lengths of C3-C4, C4-C5, C5-C6, and C6-C7 in vinylene unit change. The single bond C4-C5 and C6-C7 of the ground state geometries ( $S_0$ ) are shorter than that the bond lengths of excited state geometries ( $S_1$ ), while the double bond C3-C4 and C5-C6 in  $S_0$  are longer than that the bond length of  $S_1$  of *EE*-, *EZ*- and *ZZ*- stereoisomers, as shown in Figure 18, 19 and 20, respectively. The bond length variation of the thienyl fragments leads to the stronger conjugation effects compared and results in the relaxation of single bonds and strengthening of double bonds.

The BLA of *EE*-, *EZ*- and *ZZ*- stereoisomers of the ground state ( $S_0$ ) are slightly larger than first singlet excited state ( $S_1$ ). For instance, the *EE*-isomer optimized geometries of the ground state ( $S_0$ ) lead to increase of the BLA value by 0.08, whereas the first singlet excited state ( $S_1$ ) is decreased of 0.06. From positive sign of BLA of three stereoisomers suggests that, in the excited state, the molecules become more aromatic-like, as seen clearly in Figure 16.

Investigation of the bond angles of from  $S_0$  geometries (around 125.0-129.0 degrees) slightly larger than  $S_1$  geometries (around 130.0-133.0 degrees). The calculated bond angles of all isomers in  $S_0$  geometries are close to 120.0 degree, which indicated that the all  $S_0$  geometries structures are hardly changed with the increase of the chain lengths (Liu *et al.*, 2007). The torsion angles of the ground state and the lowest singlet excited-state optimized geometries are given in Figure 21. The torsion angle between  $S_0$  geometries represented in green color and  $S_1$  geometries represented as red color, compared on the geometrical optimization at  $S_0$  and  $S_1$  geometries. The torsion angles C4-C5-C6-C7 of three isomers are slightly significant twists within about -15.0 degree between adjacent phenylene and the two adjacent thienyl indicating that the  $\pi$  conjugated structure are obtained due to the cooperation with two thienyl-based electron donating moieties. The results indicated that the bond length, bond angle and torsion angle of both stereoisomers at  $S_1$  geometries become closed to planar structure (Chidthong *et al.*, 2007).

## 2.2 Comparison on the absorption properties of *EE*-, *EZ*- and *ZZ*-MEH-ThV with the experimental data

The calculated  $S_0 \rightarrow S_1$  absorption energies, transition stated (H denoted HOMO and L is LUMO) and oscillator strength of the three isomers of MEH-ThV molecule and the corresponding experimental values are presented in Table 6. All transition consists of one-electron transitions mainly from HOMO to LUMO (H $\rightarrow$ L). The TDDFT results show that the absorption spectra of *EE*-MEH-ThV (410.27, 329.91 and 253.82 nm) is agreed well with the experimental spectra (407, 348 and 252 nm) in chloroform solution which this absorption spectra in gas phase and PCM model in chloroform solution is slightly differ from the experimental data. The excitation energies calculated by TDDFT of *EE*-, *EZ*- and *ZZ*-MEH-ThV corresponding to the absorption wavelength are underestimated when compared to the maximum wavelength from experimental results, as shown in Figures 22, 23 and 24, respectively. The theoretical absorption spectrum of the *EE*-isomer compound consists of closely separated three peaks with large oscillator strength, the highest oscillator strength ( $\pi$ - $\pi^*$  transition) of each stereoisomers calculated by TD-B3LYP/6-31G(d,p) method which are compared to the experimental absorption spectra. On the other hand, the calculated absorption wavelength of *EZ*- and *ZZ*-MEH-ThV in both gas phase and solvent phase differ from the corresponding experimental values. For *EE*-isomer, it was similar to MEH-ThV compounds, showing three distinct bands with higher intensity in absorption spectra. This is in good agreement with the experimental measurements.

**Table 6** The lowest excitation energies in eV and oscillator strength ( $f$ ) (values in parentheses) both in gas phase and solvent phase (in  $\text{CHCl}_3$ ) using TD-B3LYP/6-31G(d,p) method and absorption spectra of experimental data in  $\text{CHCl}_3$  solution for the *EE*-, *EZ*- and *ZZ*-MEH-ThV geometries.

Molecules	states	TD-B3LYP/6-31G(d,p)//HF/6-31G(d,p)				Experiment
		Transition	$E_{ex}$	$\lambda_{abs}$	$f$	$\lambda_{abs}$ (nm)
		States	(eV)	(nm)		
<b><i>EE-isomer</i></b>						
Gas phase	$S_0 \rightarrow S_1$	H $\rightarrow$ L (81%)	3.14	394.89	1.2454	
	$S_0 \rightarrow S_3$	H-2 $\rightarrow$ L (58%)	3.82	324.11	0.2283	
	$S_0 \rightarrow S_9$	H-2 $\rightarrow$ L+1 (66%)	4.90	252.78	0.2034	
Solvent phase	$S_0 \rightarrow S_1$	H $\rightarrow$ L (85%)	3.02	410.27	1.4434	407
	$S_0 \rightarrow S_2$	H-1 $\rightarrow$ L (89%)	3.76	329.91	0.3676	348
	$S_0 \rightarrow S_9$	H-2 $\rightarrow$ L+1 (82%)	4.88	253.82	0.2102	252
<b><i>EZ-isomer</i></b>						
Gas phase	$S_0 \rightarrow S_1$	H $\rightarrow$ L (84%)	3.29	376.31	0.6316	
	$S_0 \rightarrow S_4$	H-2 $\rightarrow$ L (70%)	4.16	297.77	0.2045	
	$S_0 \rightarrow S_9$	H-3 $\rightarrow$ L (35%)	4.90	252.78	0.1030	
Solvent phase	$S_0 \rightarrow S_1$	H $\rightarrow$ L (87%)	3.22	384.91	0.7887	
	$S_0 \rightarrow S_2$	H-1 $\rightarrow$ L (74%)	3.82	324.66	0.1395	
	$S_0 \rightarrow S_8$	H-3 $\rightarrow$ L (26%)	4.86	254.91	0.1168	
<b><i>ZZ-isomer</i></b>						
Gas phase	$S_0 \rightarrow S_1$	H $\rightarrow$ L (90%)	3.46	358.48	0.2729	
	$S_0 \rightarrow S_4$	H-2 $\rightarrow$ L (81%)	4.21	294.31	0.1291	
	$S_0 \rightarrow S_5$	H-1 $\rightarrow$ L (82%)	4.52	274.19	0.1300	
Solvent phase	$S_0 \rightarrow S_1$	H $\rightarrow$ L (91%)	3.43	361.44	0.3569	
	$S_0 \rightarrow S_4$	H-2 $\rightarrow$ L (84%)	4.18	296.87	0.1957	
	$S_0 \rightarrow S_5$	H-1 $\rightarrow$ L+1 (87%)	4.51	274.99	0.1434	



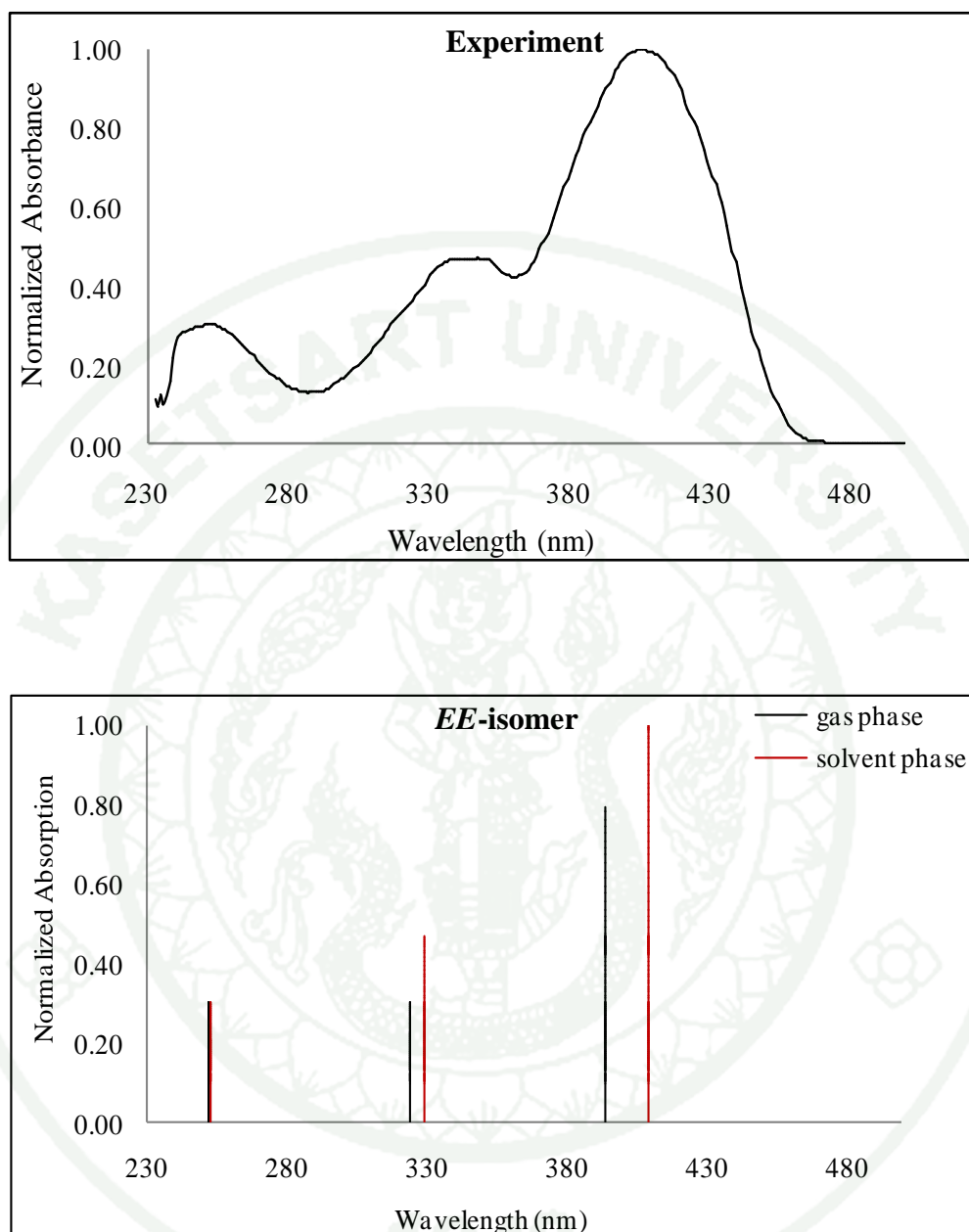


**Figure 22** Absorption spectra of *EE*-MEH-ThV obtained from the experimental in chloroform solution and calculated using TD-B3LYP/6-31G(d,p) in gas phase (black line) and PCM model (red line).

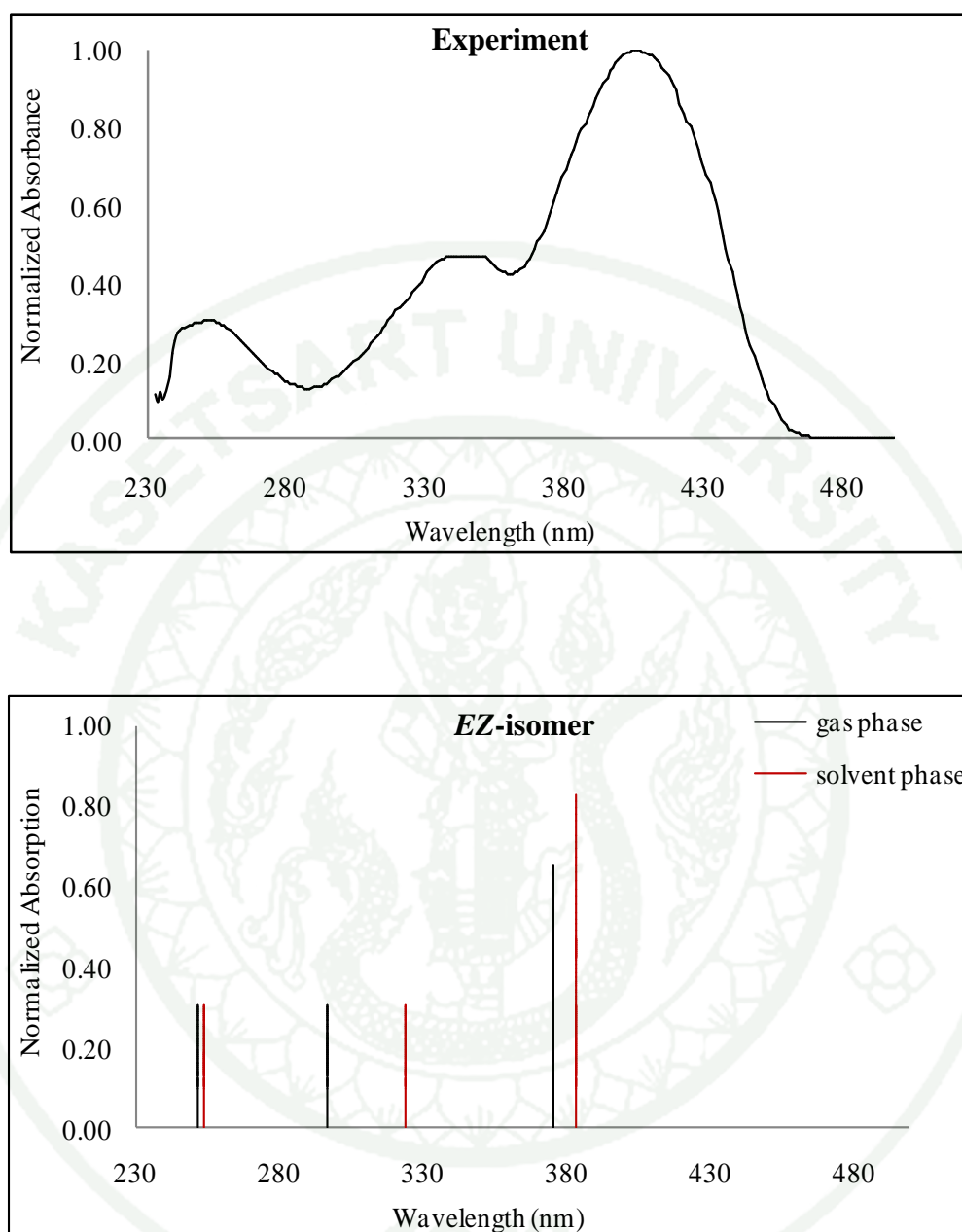


**Figure 23** Absorption spectra of *EZ*-MEH-ThV obtained from the experimental in chloroform solution and calculated using TD-B3LYP/6-31G(d,p) in gas phase (black line) and PCM model (red line).

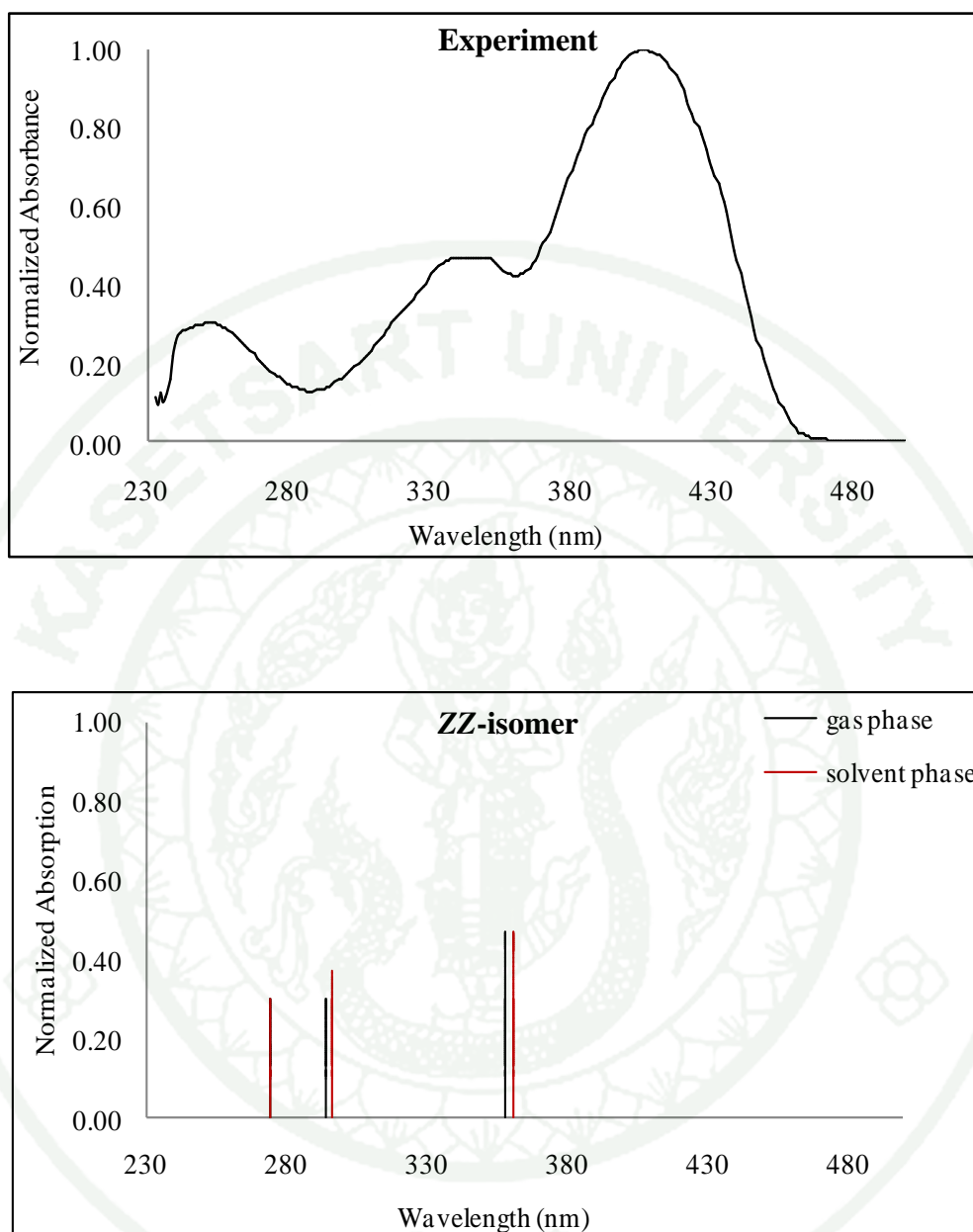


**Figure 24** Absorption spectra of ZZ-MEH-ThV obtained from the experimental in chloroform solution and calculated using TD-B3LYP/6-31G(d,p) in gas phase (black line) and PCM model (red line).

2.3 Ground state and Excited state Structural Properties of *EE*-, *EZ*- and *ZZ*-MEH-ThV-CN

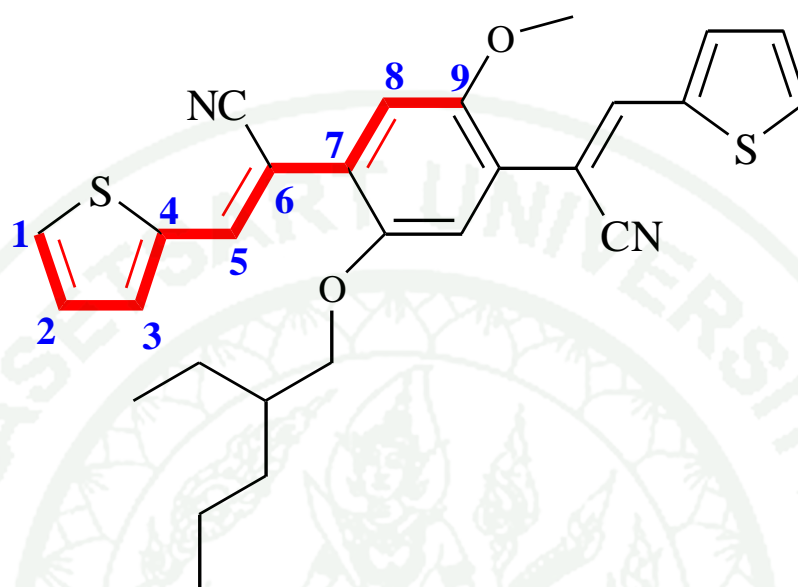


**Figure 25** Schematic represents the bond number on backbone structure of MEH-ThV-CN molecule.

**Table 7** Fully optimization of structural parameters of *EE*-, *EZ*- and *ZZ*-MEH-ThV-CN with the  $S_0$  and  $S_1$  geometries obtained from HF/6-31G(d,p) and TD-B3LYP/dft-SV(P) methods, respectively (bond length in angstrom and angle in degrees).

Structural parameters	<i>EE</i>		<i>EZ</i>		<i>ZZ</i>	
	$S_0$	$S_1$	$S_0$	$S_1$	$S_0$	$S_1$
Bond length						
C1-C2	1.35	1.39	1.35	1.38	1.35	1.38
C2-C3	1.42	1.41	1.42	1.41	1.43	1.41
C3-C4	1.36	1.42	1.36	1.40	1.36	1.41
C4-C5	1.46	1.41	1.46	1.42	1.46	1.42
C5-C6	1.34	1.42	1.33	1.39	1.33	1.40
C6-C7	1.49	1.50	1.48	1.46	1.50	1.48
C7-C8	1.39	1.39	1.40	1.41	1.39	1.39
C8-C9	1.38	1.42	1.38	1.40	1.38	1.42
Bond angle						
C4-C5-C6	131.0	130.2	131.1	130.8	131.1	133.6
C5-C6-C7	118.6	118.7	124.9	125.5	126.3	117.4
Torsion angle						
C4-C5-C6-C7	-179.2	-167.6	-179.0	-179.9	-5.8	-14.5
BLA	0.0775	0.0300	0.0750	0.0275	0.0850	0.0375



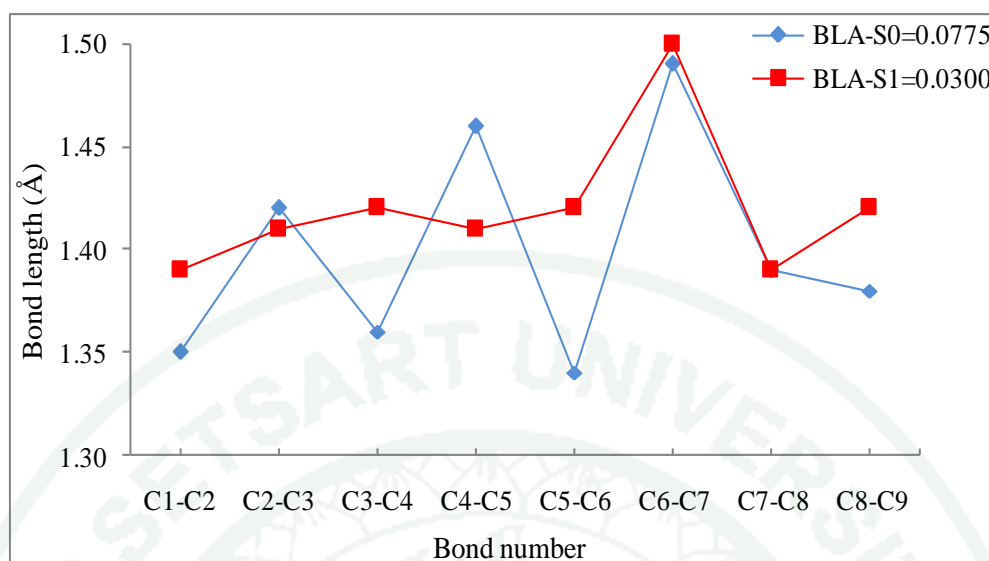


**Figure 26** Optimized bond length and bond length alternation (BLA) of *EE*-MEH-ThV-CN of the  $S_0$  and  $S_1$  geometries as obtained from HF/6-31G(d,p) and TD-B3LYP/dft-SV(P) methods, respectively.

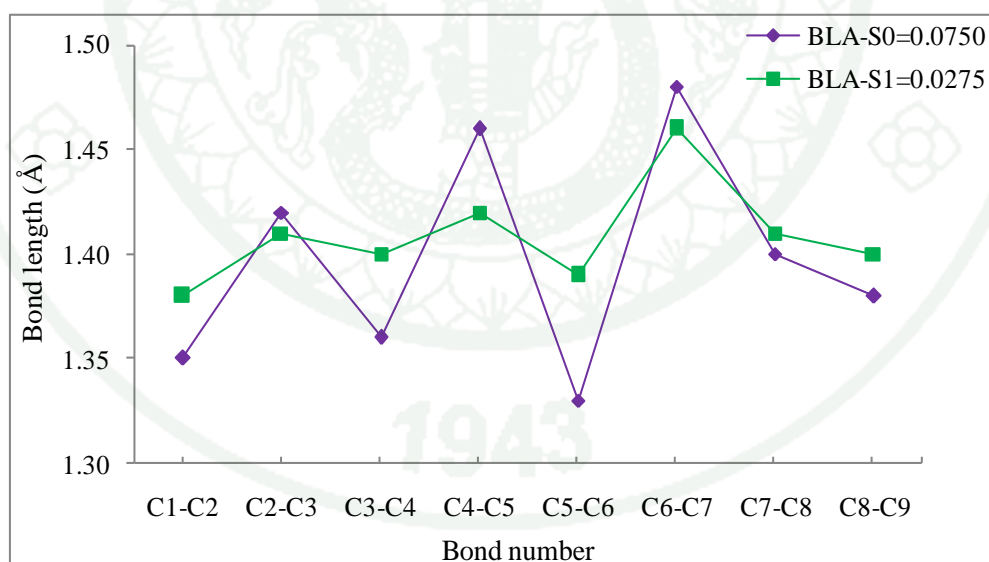


**Figure 27** Optimized bond length and bond length alternation (BLA) of *EZ*-MEH-ThV-CN of the  $S_0$  and  $S_1$  geometries as obtained from HF/6-31G(d,p) and TD-B3LYP/dft-SV(P) methods, respectively.

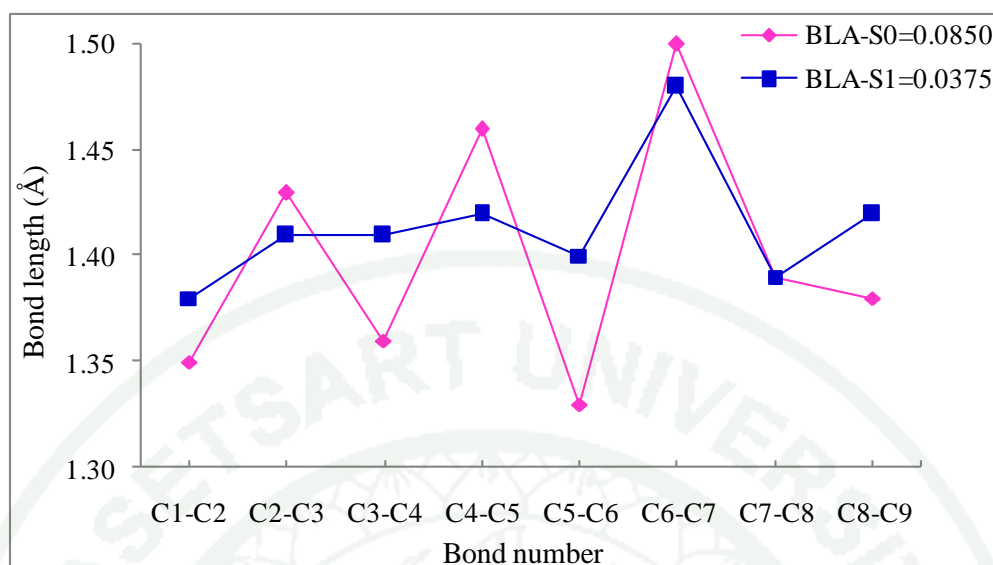


**Figure 28** Optimized bond length and bond length alternation (BLA) of ZZ-MEH-ThV-CN of the  $S_0$  and  $S_1$  geometries as obtained from HF/6-31G(d,p) and TD-B3LYP/dft-SV(P) methods, respectively.

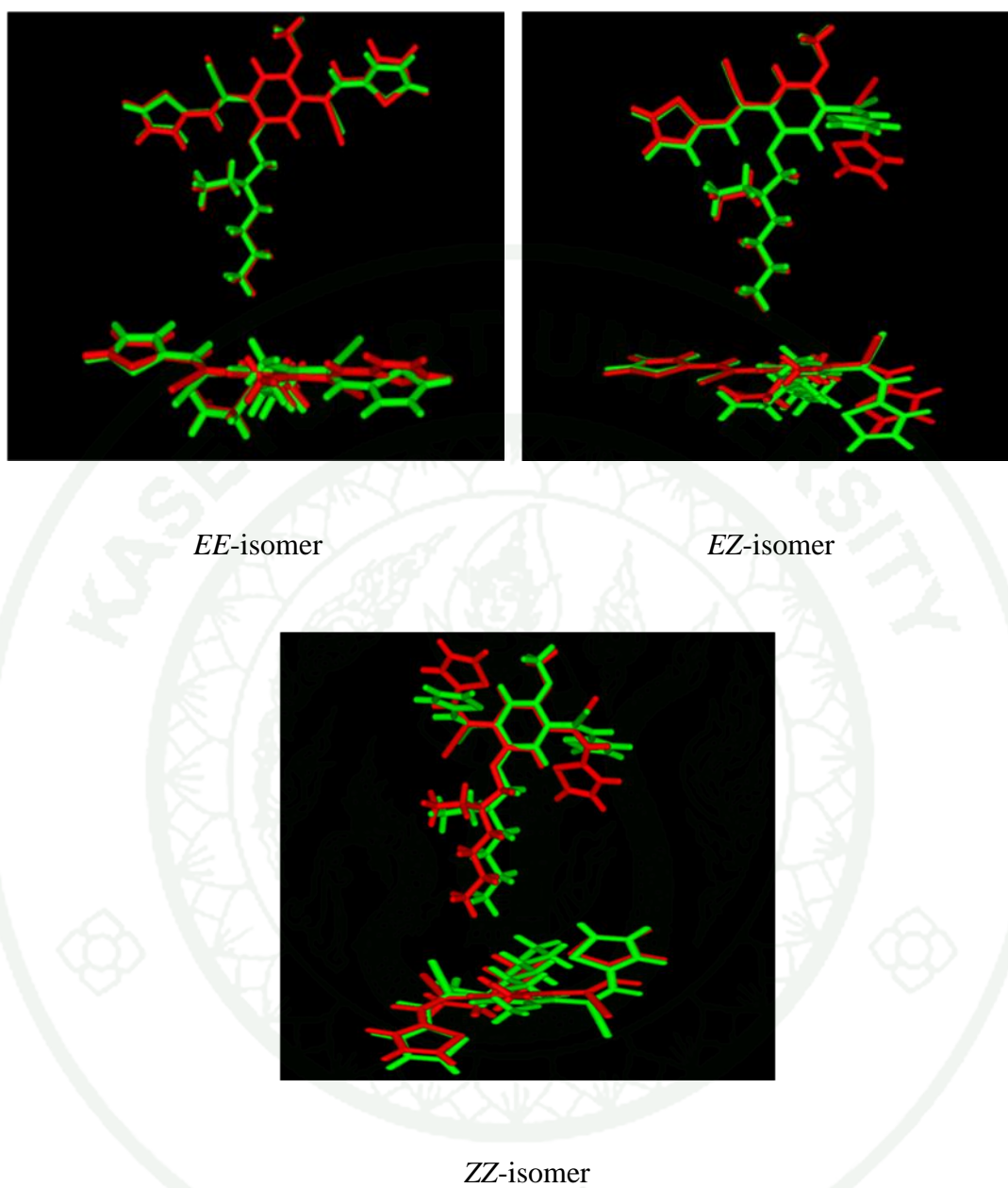


**Figure 29** Optimized torsion angle of *EE*-, *EZ*- and *ZZ*-MEH-ThV-CN of the ground state ( $S_0$ ) (green color) and first singlet excited state ( $S_1$ ) geometries (red color) as obtained from HF/6-31G(d,p) and TD-B3LYP/dft-SV(P) methods, respectively.

The optimized geometry structures of three isomers of MEH-ThV-CN were considered on main chain molecule of calculated bond length (Figure 25), while angles were attributed at vinylenes units. A comparison of the C-C and C=C bond lengths along with the conjugation between the  $S_0$  and  $S_1$  state geometries of the *EE*-, *EZ*- and *ZZ*-isomers of the MEH-ThV-CN compounds are shown in Figures 26, 27 and 28, respectively. It was found that the C5-C6 bond length in the  $S_0$  geometries is decreased and the lengths of the other bonds are increased of all isomers. In the  $S_0$  state, the carbon-carbon bond alternation exists for both the single and double bonds, but this bond alternation relaxes in the  $S_1$  state. Since the excitation is relatively localized in the central unit and thienyl unit, the prominent changes occur in the vinylenes unit. For the *EE*-isomer, the changes in bond length of single bond is 1.35 Å for C1-C2, C3-C4 and C5-C6, while the other changes in bond length are within 1.39-1.50 Å. The double bond lengths increase with the changes being localized toward the centre of the molecule are C6-C7 bond length in the lowest singlet excited state ( $S_1$ ) geometries of 1.5 degree. The structures of the ground state and the lowest singlet excited-state optimized geometries are given for the changes bond lengths of *EZ*- and *ZZ*-isomers similarly with the *EE*-isomer geometry. The geometry changes, as obtained from HF calculations, are found in all stereoisomers which BLA associated with the carbon-carbon conjugated bond for the ground and singlet excitations states for the central rings was estimated. It found that the BLA significantly changes in the excited states compared to the ground states, in the *EE*-, *EZ*- and *ZZ*-isomers, decreasing from 0.0775, 0.0750 and 0.0850 Å in  $S_0$  geometries to 0.0300, 0.0275 and 0.0375 Å in  $S_1$  geometries. These results indicate that the center of the aromatic-like is located at the linking bonds between the backbone units, as seen in Figure 30.

The torsional angles (C4-C5-C6-C7), both of ground and excited state have been investigated for the MEH-ThV-CN molecule. The torsion angles of the stereoisomers are presented in Table 7 for the ground ( $S_0$ ) and the lowest excited state ( $S_1$ ) of three stereoisomers. The optimized structures of all molecules in the ground states are generally more distorted than the structures in the excited states. It was found twisted conformations with torsional angles around -167.6 and -14.5 degrees for both *EE*- and *ZZ*-isomers, as shown in Figure 29. The effect was due to steric

hindrance and electronegativity of the cyano group which electron withdrawing groups can twist the inter-ring torsion angle. As a result of cyano group is electron-accepting capabilities and induces torsion in molecule.

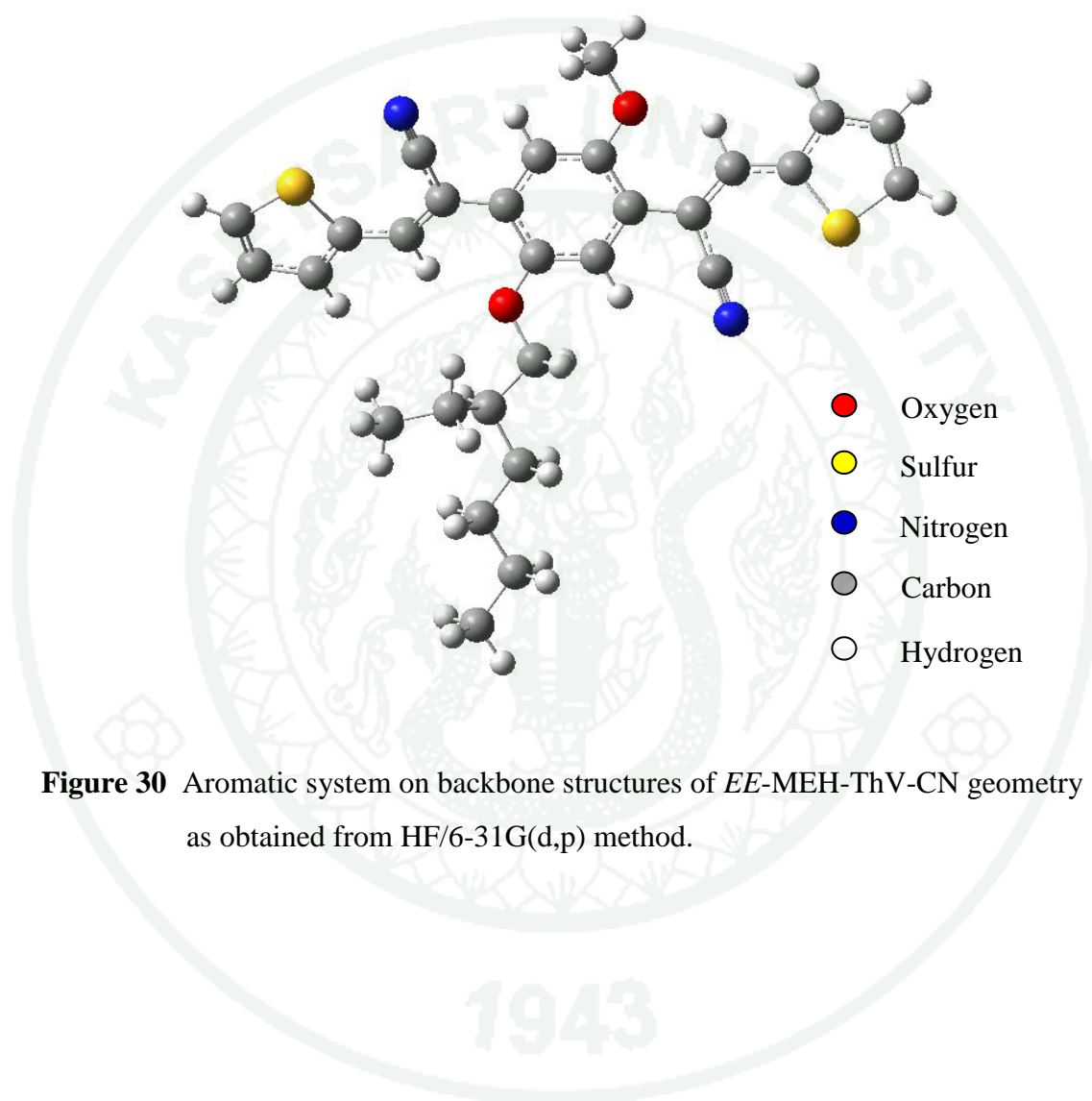


**Figure 30** Aromatic system on backbone structures of *EE*-MEH-ThV-CN geometry as obtained from HF/6-31G(d,p) method.



## 2.4 Comparison on the absorption properties of *EE*-, *EZ*- and *ZZ*-MEH-ThV with the experimental data

From our calculated electronic transitions with TD-B3LYP calculation compared with the experimental data, the TDDFT and experimental spectra of *EE*-, *EZ*- and *ZZ*-MEH-ThV-CN molecules are listed in Table 8. It is clear that the calculated absorption wavelength in solvent phase of chloroform solution of *ZZ*-isomers is blue-shifted with values of 18.42, 57.51 and 7.00 nm with experimental data, while the calculated absorption spectra of *EE*- (26.31, 4.23 and 9.21 nm) and *EZ*-isomer (17.85, 9.89 and 34.29 nm) are red shift with experimental results. According to Figure 31, both experimental and TDDFT data exhibit three transitions with the highest of the oscillator strength. It can be seen that our calculated values of the absorption spectra of *EE*-MEH-ThV-CN (406.31, 334.16 and 284.94 nm) are good agreement with the experimental spectra (393, 335 and 281 nm) in chloroform solution. Moreover, our compared the absorption wavelength in an aqueous solvent condition in chloroform solution by polarizable continuum model (with PCM model) as well, as calculated within Gaussian03 software package. The results show that the differences in wavelengths between the solvent phase and the gas phase are less than 10 nm, suggesting that the solvatochromic effect is inappreciable in this system. The presence of solvent can slightly increase the absorption spectra (419.31, 340.23 and 290.21 nm) and gives a good agreement with the experimental results in *EE*-isomer. On the other hand, the calculated absorption wavelength of *EZ*- (Figure 32) and *ZZ*-MEH-ThV-CN (Figure 33) of both gas phase and solvent phase differ from the corresponding experimental values.

**Table 8** The lowest excitation energies in eV and oscillator strength ( $f$ ) (values in parentheses) in gas phase and solvent phase (in  $\text{CHCl}_3$ ) using TD-B3LYP/6-31G(d,p) method and absorption spectra of experimental data in  $\text{CHCl}_3$  solution for the *EE*-, *EZ*- and *ZZ*-MEH-ThV-CN geometries.

Molecules	states	TD-B3LYP/6-31G(d,p)//HF/6-31G(d,p)				Experimental
		Transition	$E_{ex}$	$\lambda_{abs}$	$f$	$\lambda_{abs}$ (nm)
		States	(eV)	(nm)		
<b><i>EE-isomer</i></b>						
Gas phase	$S_0 \rightarrow S_1$	H $\rightarrow$ L (86%)	3.05	406.31	0.5702	
	$S_0 \rightarrow S_3$	H-1 $\rightarrow$ L (87%)	3.71	334.16	0.5293	
	$S_0 \rightarrow S_6$	H-2 $\rightarrow$ L+1 (77%)	4.35	284.94	0.3376	
Solvent phase	$S_0 \rightarrow S_1$	H $\rightarrow$ L (89%)	2.96	419.31	0.6838	393
	$S_0 \rightarrow S_3$	H-1 $\rightarrow$ L (90%)	3.64	340.23	0.6277	336
	$S_0 \rightarrow S_6$	H-2 $\rightarrow$ L+1 (81%)	4.72	290.21	0.3338	281
<b><i>EZ-isomer</i></b>						
Gas phase	$S_0 \rightarrow S_1$	H $\rightarrow$ L (62%)	2.92	424.95	0.2789	
	$S_0 \rightarrow S_5$	H-2 $\rightarrow$ L+1 (45%)	3.87	320.67	0.2925	
	$S_0 \rightarrow S_6$	H-2 $\rightarrow$ L+1 (45%)	4.10	302.67	0.3177	
Solvent phase	$S_0 \rightarrow S_1$	H $\rightarrow$ L (68%)	3.02	410.85	0.1373	
	$S_0 \rightarrow S_3$	H-1 $\rightarrow$ L (66%)	3.58	345.89	0.3091	
	$S_0 \rightarrow S_6$	H-2 $\rightarrow$ L+1 (64%)	3.93	315.29	0.6104	
<b><i>ZZ-isomer</i></b>						
Gas phase	$S_0 \rightarrow S_3$	H $\rightarrow$ L (84%)	4.06	305.48	0.1174	
	$S_0 \rightarrow S_5$	H-1 $\rightarrow$ L+1 (36%)	4.20	289.78	0.2567	
	$S_0 \rightarrow S_6$	H-1 $\rightarrow$ L+1 (34%)	4.30	288.24	0.3420	
Solvent phase	$S_0 \rightarrow S_3$	H-1 $\rightarrow$ L (86%)	4.02	308.28	0.3648	
	$S_0 \rightarrow S_6$	H-2 $\rightarrow$ L+1 (74%)	4.20	294.79	0.5670	
	$S_0 \rightarrow S_7$	H $\rightarrow$ L+2 (68%)	4.40	281.57	0.1193	

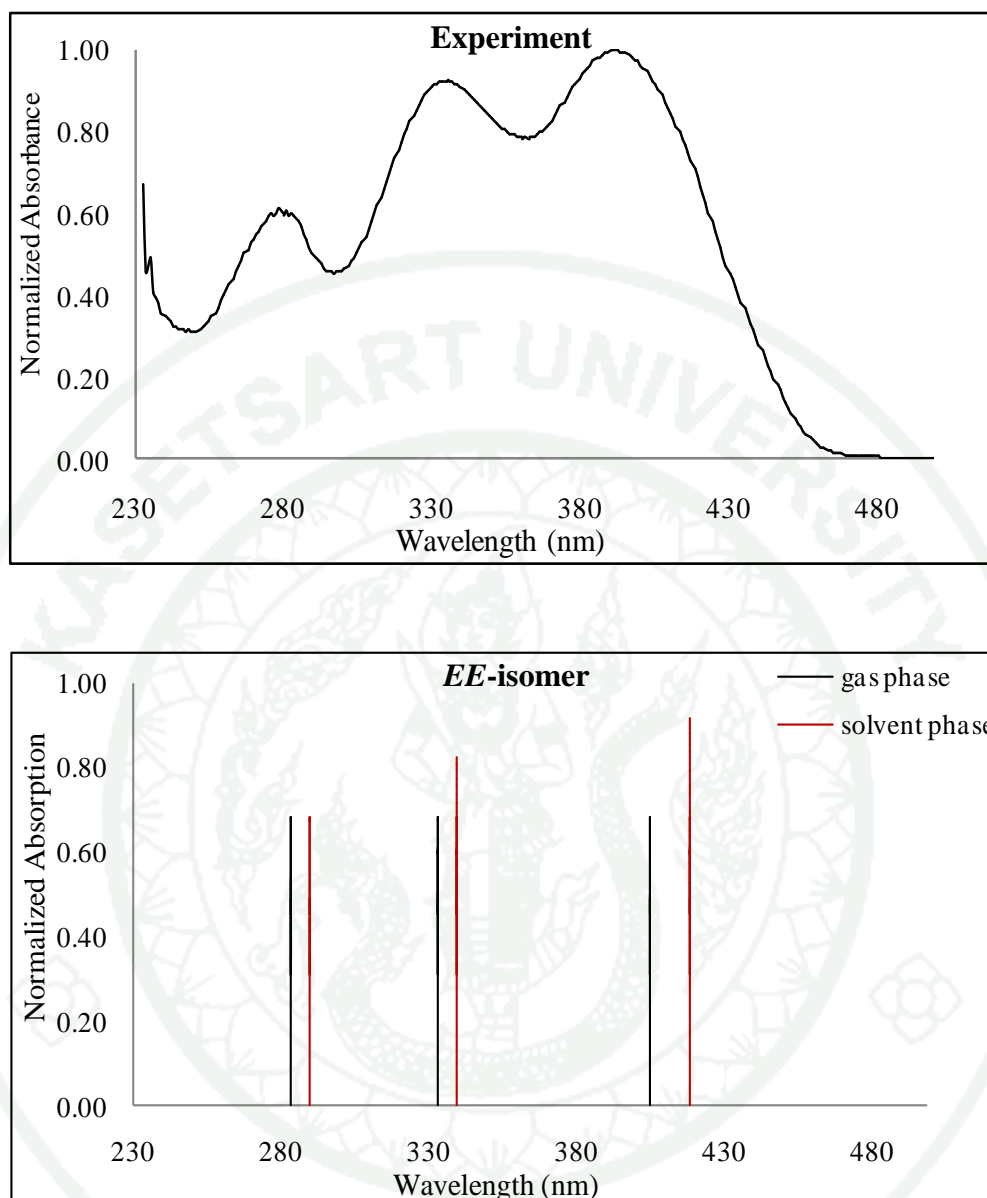


**Figure 31** Absorption spectra of *EE*-MEH-ThV-CN obtained from the experimental in chloroform solution and calculated using TD-B3LYP/6-31G(d,p) in gas phase (black line) and PCM model (red line).

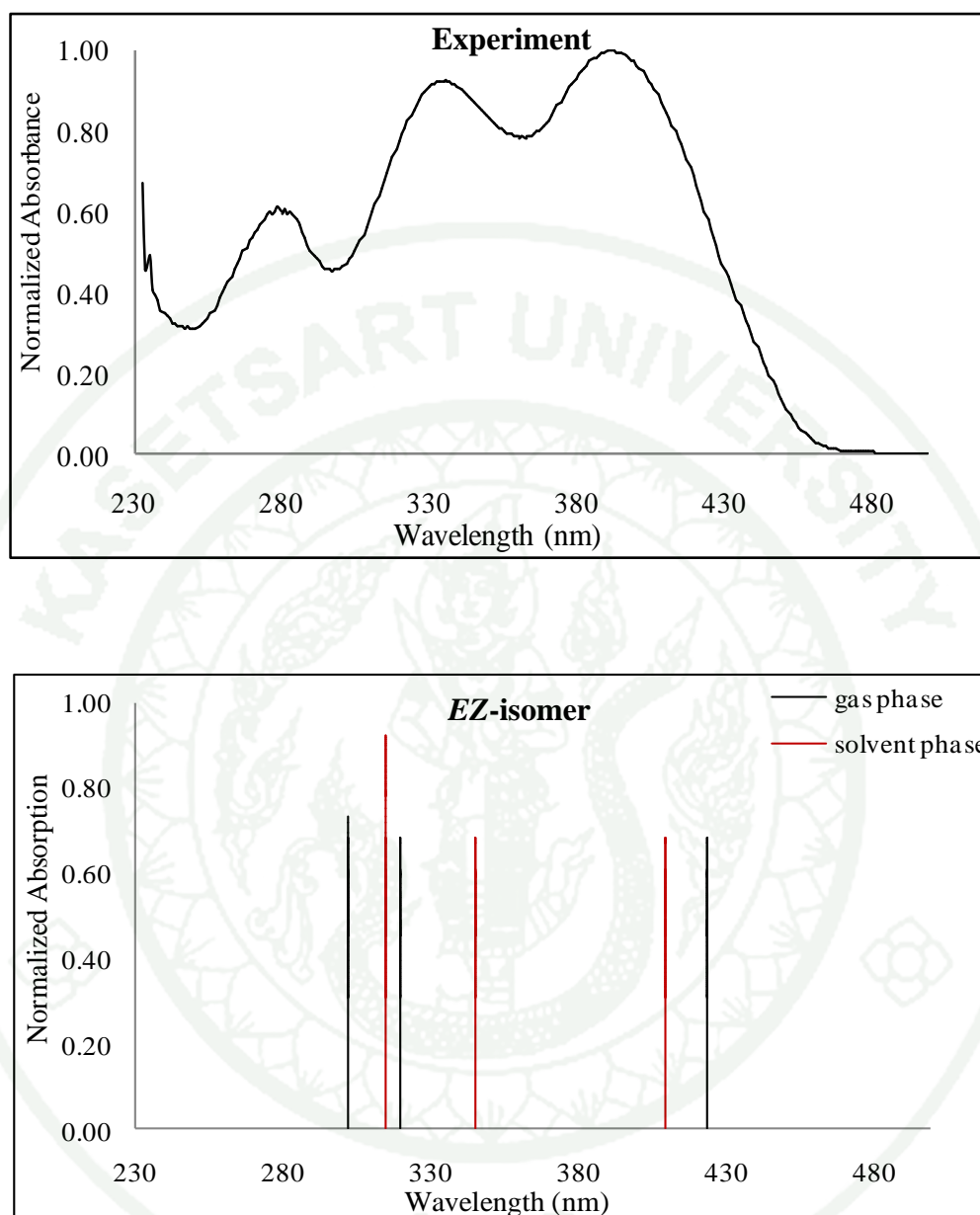


**Figure 32** Absorption spectra of *EZ*-MEH-ThV-CN obtained from the experimental in chloroform solution and calculated using TD-B3LYP/6-31G(d,p) in gas phase (black line) and PCM model (red line).

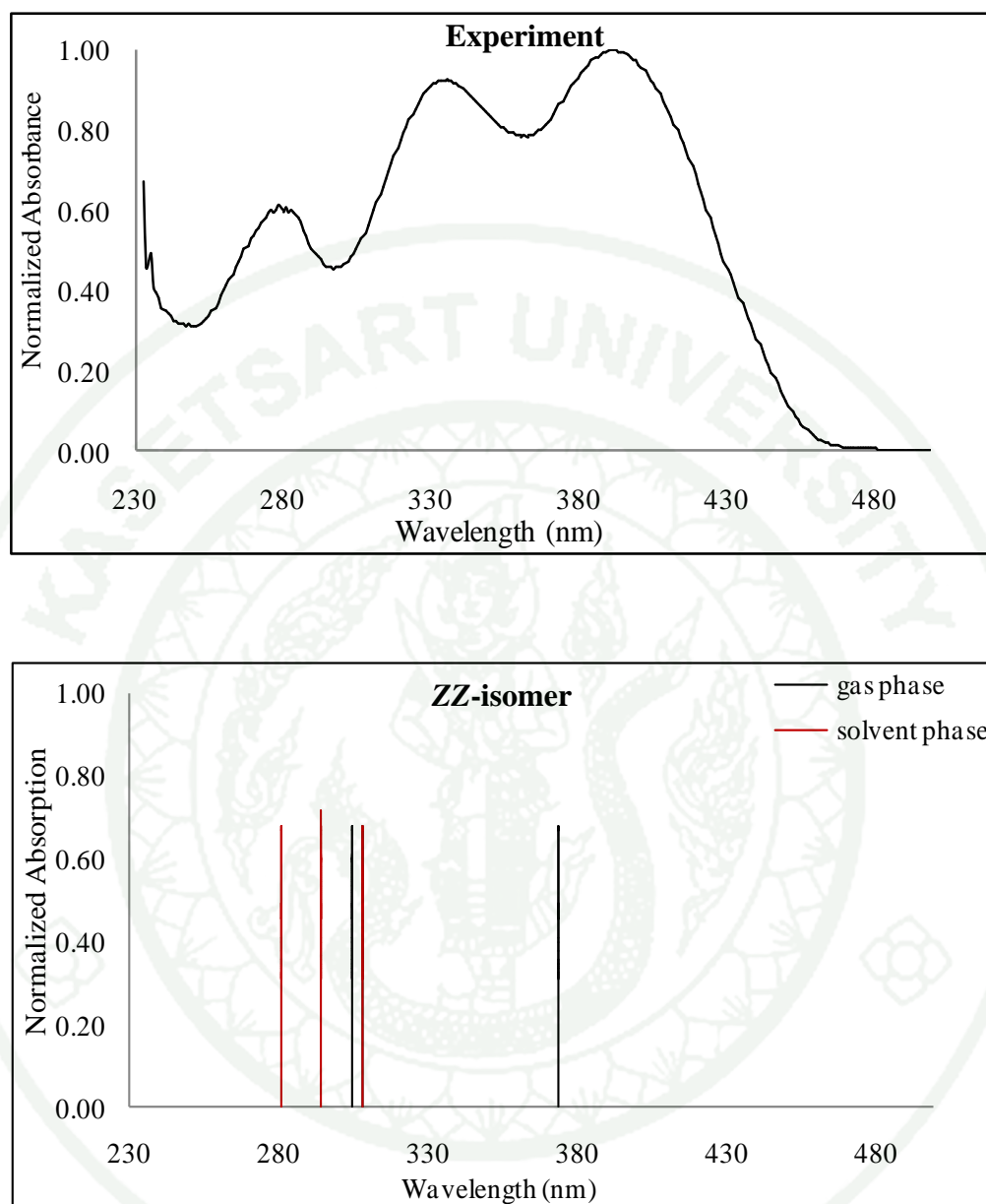


**Figure 33** Absorption spectra of ZZ-MEH-ThV-CN obtained from the experimental in chloroform solution and calculated using TD-B3LYP/6-31G(d,p) in gas phase (black line) and PCM model (red line).



### 3. Electronic Properties

#### 3.1 Absorption Properties

In order to understand the physical origin of optical transitions for the selected excitation energies, it is useful to examine the relevant (the highest) occupied and the lowest unoccupied molecular orbitals that play a dominant role. The HF/6-31G(d,p) method was used on the basis of the ground state optimized structures to compute vertical electron excitation energies, the highest occupied molecular orbital (HOMO) and the lowest unoccupied molecular orbital (LUMO), absorption wavelength and oscillator strength ( $f$ ) of all stereoisomer were investigated in this work. The calculated energies and absorption wavelength are compared with the experimental data in chloroform solution and quantum chemical calculation at TD-B3LYP/6-31G(d,p) method optimized with HF/6-31G(d,p) level. The electronic transitions are described in detail below in term of the contribution to the excited state which the excitation take place.

For the lowest excitation energy, the electron is excited from the highest occupied molecular orbitals (HOMO) to the lowest unoccupied molecular orbital (LUMO). This transition is  $\pi \rightarrow \pi^*$  character arising exclusively from  $S_0 \rightarrow S_1$  electronic transition mainly composed by HOMO  $\rightarrow$  LUMO transition. However, the orbital presentation of the next transitions is different with respect to the substitution. In the HOMO and next HOMO of *EE*-MEH-ThV molecule, the vinyl double bonds form bonding orbitals, and the single bonds linking the phenyl ring with the vinyl double bond are antibonding. In the LUMO, the vinyl single bonds are antibonding and the single bonds are bonding on the backbone structure. The next HOMO and LUMO orbitals are located at the vinyl-vinylene moiety, as seen in Figure 34.

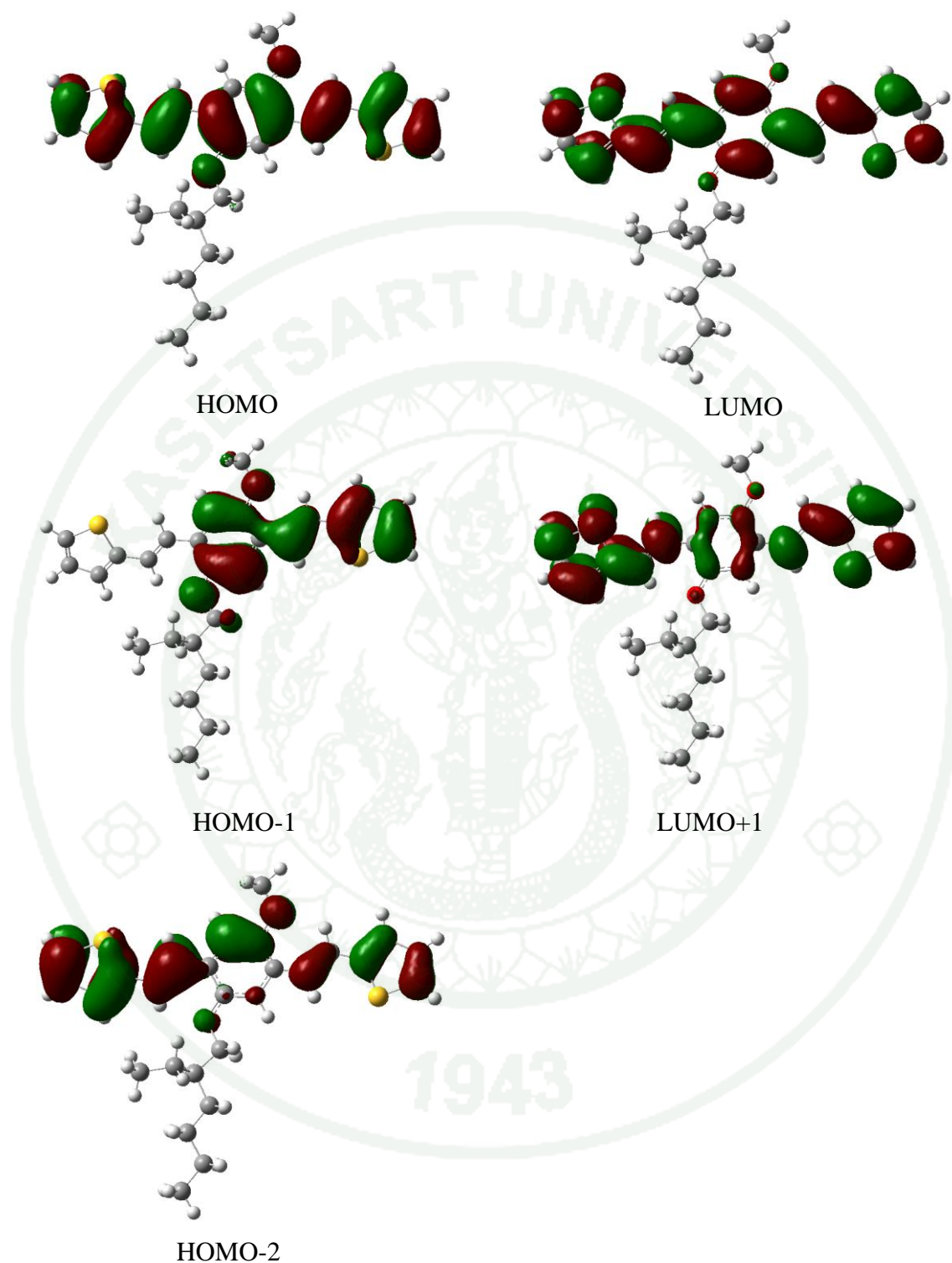


**Figure 34** Plots of the TD-B3LYP/6-31G(d,p) molecular orbitals contributing significantly to the lowest energy transitions of studied molecules in *EE*-MEH-ThV conformation. H denotes HOMO and L is LUMO.

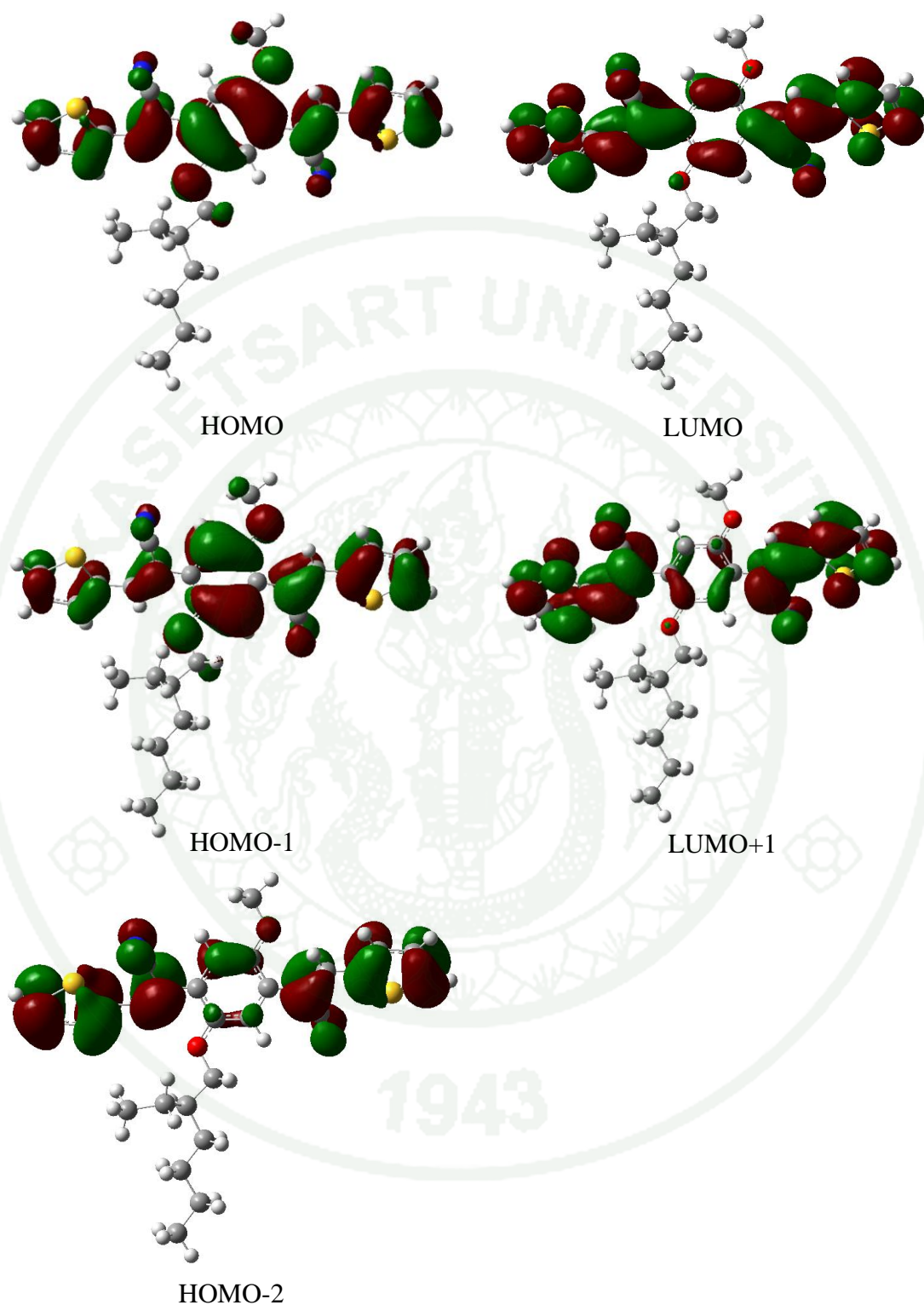


**Figure 35** Plots of the TD-B3LYP/6-31G(d,p) molecular orbitals contributing significantly to the lowest energy transitions of studied molecules in *EE*-MEH-ThV-CN conformation. H denotes HOMO and L is LUMO.

The molecular orbitals (MOs) relevant for the three low-lying excited states for the *EE*-MEH-ThV-CN compounds are shown in Figure 35. The HOMO is localized on the backbone structures. The alkoxy methoxy substitution on the phenyl ring also has a small contribution to the  $\pi^*$  conjugation. The LUMO contains localization on the main chain structure and cyano substitution group on vinylene unit, as a typical for  $\pi$ - $\pi^*$  transition in conjugated system.

### 3.2 Emission Properties

The emission calculations are performed by vertical de-excitation of the two compounds of *EE*-MEH-ThV and *EE*-MEH-ThV-CN molecules with the TD-B3LYP/dft-SV(P) method in their first singlet excited state, followed by using the resulting geometries to perform TD-DFT calculations employing the B3LYP/dft-SV(P) method from the singlet ground state. In Table 9 indicated that the calculated fluorescence wavelength of *EE*-MEH-ThV molecule is 450.05 and 347.60 nm for  $S_1$  with the largest oscillator strength arising from LUMO $\rightarrow$ HOMO corresponding to  $\pi^*$ - $\pi$  de-excitation and it is close to the experimental results of 463 and 383 nm. The luminescence peak at 458 and 403 nm of experimental spectra is close to the *EE*-MEH-ThV-CN geometry using TD-DFT method (450.05 and 347.60 nm). There is slightly deviation between the calculated fluorescence and the experimental result because the different environment for the system. The experimental emission wavelengths are measured in a chloroform solution, while the theoretical model is a gas phase system. The solution surrounding that as it is may be affecting the emission to some extent. Moreover, it is due to the planar geometry structure, the  $\pi$ - $\pi$  interactions may exist in the solid state and solvent.

**Table 8** The emission energies in eV and oscillator strength (values in parentheses) for ***EE-MEH-ThV*** and ***EE-MEH-ThV-CN*** geometries. The values written in italics stand for the excitation contributions in percentage involved in each calculated transition (H denoted HOMO and L is LUMO) using TD-B3LYP/dft-SV(P) method.

Molecules	states	TD-B3LYP/dft-SV(P)				Experimental $\lambda_{em}$ (nm)
		Transition States	$E_{em}$ (eV)	$\lambda_{em}$ (nm)	$f$	
<i>EE-MEH-ThV</i>	$S_1 \rightarrow S_0$	L $\rightarrow$ H (98%)	2.58	480.15	1.2486	<b>458</b>
	$S_2 \rightarrow S_0$	L+1 $\rightarrow$ H (53%)	3.18	390.02	0.3275	<b>403</b>
<i>EE-MEH-ThV-CN</i>	$S_2 \rightarrow S_0$	L+1 $\rightarrow$ H (92%)	2.75	450.05	0.7977	<b>463</b>
	$S_3 \rightarrow S_0$	L+1 $\rightarrow$ H-1 (70%)	3.57	347.60	0.3935	<b>383</b>



Absorption and fluorescence wavelengths difference should also lead to Stokes-shifts difference (Stokes, 1958). Therefore, evaluate the Stokes-shift as the differences  $\Delta\lambda = \lambda_{\text{em}} - \lambda_{\text{abs}}$ . The TD-B3LYP/dft-SV(P) values exhibit Stokes shift of about 43.74 and 13.44 nm for *EE*-MEH-ThV-CN and it is lower than those for *EE*-MEH-ThV of 69.88 and 60.11 nm, as summarized in Table 10. This result demonstrates that the transition of *EE*-MEH-ThV structure is more relaxed than those of *EE*-MEH-ThV-CN upon excitation. These results also show that the electronic excitation leads to the formation of an aromatic-like structure.

**Table 10** The calculation absorption ( $\lambda_{\text{abs}}$ ), emission wavelength ( $\lambda_{\text{em}}$ ) in gas phase and Stoke shift of the *EE*-MEH-ThV and *EE*-MEH-ThV-CN as obtained from TD-B3LYP/6-31G(d,p) and TD-B3LYP/dft-SV(P) methods, respectively.

Molecules	$\lambda_{\text{abs}}$ (nm)	$\lambda_{\text{em}}$ (nm)	Stoke shift (nm)
<i>EE</i> -MEH-ThV	410.27	480.15	69.88
	329.91	390.02	60.11
<i>EE</i> -MEH-ThV-CN	406.31	450.05	43.74
	334.16	347.60	13.44

### 3.3 Fluorescence Energy and Radiative Lifetime

Fluorescence energies and radiative lifetime computed with the TD-B3LYP/dft-SV(P) method using  $S_1$  optimized geometries of both the stereoisomer of *EE*-MEH-ThV and *EE*-MEH-ThV-CN are summarized in Table 10. According to Table 11, it is shown that the fluorescence energies of *EE*-MEH-ThV-CN and *EE*-MEH-ThV are red shifts from the excitation energies. Fluorescence energies of *EE*-MEH-ThV (2.58 and 3.18 eV) are slightly lower than *EE*-MEH-ThV-CN molecule (2.75 and 3.57 eV). Radiative lifetimes were calculated on the basis of fluorescence energy and oscillator strengths according to the following equation

$$\tau = \frac{c^3}{2(E_{flu})^2 f}$$

Where  $c$  is the velocity of light,  $E_{flu}$  is the fluorescence transition energies and  $f$  is oscillator strength. The lifetimes of these molecules are slightly different about 1.05 ns. The lifetime of the structure with cyano groups on vinylene linkage is 3.82 ns, which the radiative lifetime of *EE*-MEH-ThV molecule (2.77 ns) is lower than *EE*-MEH-ThV-CN because of the low relaxation time at excited state, the emission of *EE*-MEH-ThV is faster than that *EE*-MEH-ThV-CN molecule. It can be concluded that their low radiative lifetime can produce useful fluorescent emission (Tirapattur *et al.*, 2003; Jenekhe *et al.*, 2001; Schenning *et al.*, 2002; Pålsson *et al.*, 2002; Sun *et al.*, 2000).

**Table 11** Calculated fluorescence energies ( $E_{flu}$ ), oscillator strength and radiative lifetime of the *EE*-MEH-ThV and *EE*-MEH-ThV-CN as obtained from TD-B3LYP/dft-SV(P) calculations. Geometries first singlet excited stated ( $S_1$ ) were optimized at TD-B3LYP/dft-SV(P) level.

Molecules	TD-B3LYP/dft-SV(P)		
	$E_{flu}$ (eV)	Oscillator strength	Radiative Lifetime (ns)
<i>EE</i> -MEH-ThV	2.58	1.2486	2.77
<i>ZZ</i> -MEH-ThV-CN	2.75	0.7977	3.82

## CONCLUSION

The syntheses of two classes of cyano-containing based-MEH-ThV-CN and MEH-ThV monomer have been carried out. Both types of compound were synthesized via Knoevenagel condensation and the alkoxy side chain-base structures are soluble in common organic solvents such as chloroform, tetrahydrofuran, dichloromethane and dimethyl sulfoxide. These compounds were confirmed by  $^1\text{H}$ -NMR,  $^{13}\text{C}$ -NMR, TGA, LC-MS, UV-Vis and fluorescence measurements. The thermal stability of MEH-ThV (349.63 °C) is higher than that of MEH-ThV-CN (323.00 °C), suggesting that its dialkoxy side chain and the electron-donating thienyl group retard thermal degradation effectively while the electron-acceptor group-base molecule is not stable leads to easily decompose. The TGA results indicated that the MEH-ThV molecule is thermally stable enough to be used as electroluminescence materials in light-emitting devices. The absorption behavior of MEH-ThV-CN (281, 335 and 393 nm) and MEH-ThV (252, 348 and 407 nm) and optical band gap energies with the absorption onset are 3.06 and 2.93 eV, respectively. The electron-withdrawing cyano groups on the vinylene moiety next to the thienyl group can further give blue shifts in the absorption and emission spectra. The photophysical properties of MEH-ThV-CN exhibited as green-yellow light emission, while MEH-ThV exhibited as green light emission. It is noteworthy that can be used as new luminescence materials in the fabrication of OLED-based full-color displays. An electrochemical energy gap of MEH-ThV-CN and MEH-ThV incompatible with the optical energy gap due to the discrepancy is caused by the insulating effect of the side chains during the electrochemical process.

To confirm the optimized geometry, the structure of MEH-ThV from various methods was calculated the electronic properties using TD-B3LYP/6-31G(d,p) method with PCM to include the chloroform solvation effect and compared with the experimental absorption band of this molecule in chloroform solvent. The structural geometry result obtained from HF/6-31G(d,p) method is closer to the DFT with B3LYP/6-31G(d,p) method. In this study, there are not the structural parameters with X-ray crystallography. Therefore, optical spectra of MEH-ThV was investigated to

confirm the configuration for ground state geometry optimized with HF and B3LYP methods. The excitation result of the structural geometry obtained from HF/6-31G(d,p) method is closer to the experimental data than that of the structural geometry obtained from B3LYP/6-31G(d,p) method. Thus, in this study TD-B3LYP/6-31G(d,p)//HF/6-31G(d,p) method and the coplanar ground state geometry of MEH-ThV was selected to investigate the structural parameters and electronic properties of the substitutions of the vinylene unit by electron-accepting (CN) and electron-donating (thienyl) group of MEH-ThV and MEH-ThV-CN molecules.

The electron-withdrawing cyano group of MEH-ThV-CN exhibits the nonplanar structure because the conformation was distorted from the electron repulsion. MEH-ThV is the planar structure than that MEH-ThV-CN geometry. The absorption properties were investigated using TD-B3LYP/dft-SV(P) method. The obtained results indicated that the  $\lambda_{\max}$  based on *EE*-isomer of MEH-ThV is close to the experimental data in chloroform solution. The excitations (406.31, 334.16 and 284.94 nm) and fluorescence wavelength (450.05 and 347.60 nm) calculated by the TD-B3LYP/6-31G(d,p) and TD-B3LYP/dft-SV(P) methods of *EE*-MEH-ThV-CN are agreement with the experimental measurements. Radiative lifetimes were calculated on the basis of fluorescence energy and oscillator strengths. Radiative lifetime of *EE*-MEH-ThV molecule (2.77 ns) is lower than *EE*-MEH-ThV-CN because the emission of *EE*-MEH-ThV is faster than *EE*-MEH-ThV-CN molecule causing of the low relaxation time at excited state. It can be concluded that their low radiative lifetime can produce useful fluorescent emission faster than that.

## LITERATURE CITED

- Ahlrichs, R., M. Bär, M. Häser, H. Horn and C. Kölmel. 1989. Electronic structure calculations on workstation computers: the program system TURBOMOLE, **Chemical Physics Letters** 162(3): 165-169.
- Becke, A.D. 1993. Density-functional thermochemistry. III. The role of exact exchange. **The Journal of Chemical Physics** 98(7):5648-5652.
- Bongini, A. and A. Bottoni. 1999. A Theoretical investigation of the torsional potential in 3,3'-dimethyl-2,2'-bithiophene and 3,4'-dimethyl-2,2'-bithiophene: A comparison between HF, MP2, and DFT theory. **The Journal of Physical Chemistry A** 103(34):6800-6804.
- Bradley, D.D.C., A.R. Brown, P.L. Burn, J.H. Burroughes, R.H. Friend, A.B. Holmes, K.D. Mackay and R.N. Marks. 1991. Light emission from poly(p-phenylene vinylene): A comparison between photo- and electro-luminescence. **Synthetic Metals** 43(1-2):3135-3141.
- Bransden, B.H and C. J. Joachain. 1983. Physics of atoms and molecules. **Longman Group Limited**, New York, 377.
- Braun, D. and A.J. Heeger. 1991. Visible light emission from semiconducting polymer diodes. **Applied Physics Letters** 58(18):1982-1984.
- Burroughes, J.H., D.D.C. Bradley, A.R. Brown, P.N. Marks, K. Mackay, R.H. Friend, P.L. Burns and A.B. Holmes. 1990. Light-emitting diodes based on conjugated polymers. **Nature** 347(6293):539-541.
- Cao, Y., I.D. Parker, G. Yu, C. Zhang and A.J. Heeger. 1999. Improved quantum efficiency for electroluminescence in semiconducting polymers. **Nature** 397(6718):414-415.



- Chen, Z.K., W. Huang, L.H. Wang, E.T. Kang, B.J. Chen, C.S. Lee and S.T. Lee. 2000. A family of electroluminescent silyl-substituted poly(*p*-phenylenevinylene)s: Synthesis, characterization, and structure property relationships. **Macromolecules** 33(24):9015-9025.
- Choi, W.-S. and M.-K. Kim. 2004. Effect of small liquid crystal molecules on the driving voltage of cholesteric liquid crystal displays. **Displays** 25(5):195-199.
- Cleave, V., G. Yahiolu, P.L. Barny, R.H. Friend and N. Tessler. 1999. Harvesting singlet and triplet energy in polymer LEDs. **Advanced Materials** 11(4):285-288.
- Corral, C., D. Sempere-Torres, M. Revilla and M. Berenguer. 2000. A semi-distributed hydrological model using rainfall estimates by radar. Application to Mediterranean basins. **Physics and Chemistry of the Earth, Part B: Hydrology, Oceans and Atmosphere** 25(10-12):1133-1136.
- Correia, H.M.G. and M.M.D. Ramos. 2003. Modeling charge transport properties of cyano-substituted PPV. **Materials Science and Engineering: C** 23(6-8):773-777.
- Ding, A.L., J. Pei, Z.K. Chen, Y.H. Lai and W. Huang. 2000. Synthesis and characterization of a new yellow-green light-emitting polymer - poly{1,4-bis[3-(4'-butylphenyl)thienyl]-2,5-di(2'-ethylhexyloxy)phenylene}. **Thin Solid Films** 363(1-2):114-117.
- Egbe, D.A.M., T. Kietzke, B. Carbonnier, D. Muhlbacher, H.-H. Horhold, D. Neher and T. Pakula. 2004. Synthesis, characterization, and photophysical, electrochemical, electroluminescent, and photovoltaic properties of yne-containing CN-PPVs. **Macromolecules** 37(24):8863-8873.

Egbe, D.A.M., L.H. Nguyen, B. Carbonnier, D. Muhlbacher and N.S. Sariciftci.

2005. Thiophene-containing poly(arylene-ethynylene)-alt-poly(arylene-vinylene)s: Synthesis, characterisation and optical properties. **Polymer** 46(23):9585-9595.

Francl, M.M., W.J. Pietro, W.J. Hehre, J.S. Binkley, M.S. Gordon, D.J. DeFrees and J.A. Pople. 1982. Self-consistent molecular orbital methods. XXIII. A polarization-type basis set for second-row elements. **The Journal of Chemical Physics** 77(7):3654-3665.

Frisch, M.J., G.W. Trucks, H.B. Schlegel, G.E. Scuseria, M.A. Robb, J.R. Cheeseman, J.A. Montgomery Jr., T. Vreven, K.N. Kudin, J.C. Burant, J.M. Millam, S.S. Iyengar, J. Tomasi, V. Barone, B. Mennucci, M. Cossi, G. Scalmani, N. Rega, G.A. Petersson, H. Nakatsuji, M. Hada, M. Ehara, K. Toyota, R. Fukuda, J. Hasegawa, M. Ishida, T. Nakajima, Y. Honda, O. Kitao, H. Nakai, M. Klene, X. Li, J.E. Knox, H.P. Hratchian, J.B. Cross, V. Bakken, C. Adamo, J. Jaramillo, R. Gomperts, R.E. Stratmann, O. Yazyev, A.J. Austin, R. Cammi, C. Pomelli, J.W. Ochterski, P.Y. Ayala, K. Morokuma, G.A. Voth, P. Salvador, J.J. Dannenberg, V.G. Zakrzewski, S. Dapprich, A.D. Daniels, M.C. Strain, O. Farkas, D.K. Malick, A.D. Rabuck, K. Raghavachari, J.B. Foresman, J. V. Ortiz, Q. Cui, A.G. Baboul, S. Clifford, J. Cioslowski, B.B. Stefanov, G. Liu, A. Liashenko, P. Piskorz, I. Komaromi, R.L. Martin, D.J. Fox, T. Keith, M.A. Al-Laham, C.Y. Peng, A. Nanayakkara, M. Challacombe, P. M.W. Gill, B. Johnson, W. Chen, M.W. Wong, C. Gonzalez and J.A. Pople. 2004. **Gaussian**. Inc, Wallingford CT.

Grozema, F.C. and J.M. Warman. 2005. Highly mobile electrons and holes on polyfluorene chains formed by charge scavenging in pulse-irradiated trans-decalin solutions. **Radiation Physics and Chemistry** 74(3-4):234-238.

- Gustafsson G., Y. Cao, G.M. Treacy, F. Klavetter, N. Colaneri and A.J. Heeger. 1992. Flexible light-emitting diodes made from soluble conducting polymers. **Nature** 357(6378):477-479.
- Han, Y.-K. and S.U. Lee. 2004. Time-dependent density-functional calculations of  $S[0] \rightarrow S[1]$  transition energies of poly(p-phenylene vinylene). **The Journal of Chemical Physics** 121(1):609-611.
- Heeger, A.J. et al., MacDiarmid, A.G. et al., Shirakawa, H. et al. 1977. Electrical conductivity in doped polyacetylene. **Journal Physical Review Letters** 39(17):1098-1101.
- Ho, C.-C., K.-M. Yeh and Y. Chen. 2004. Luminescent poly(1,4-phenylene vinylene-4,4'-biphenylene vinylene)s containing oligo(ethylene oxide) or hexyloxy side groups. **Polymer** 45(26):8739-8749.
- Hou, J., Z.a. Tan, Y. Yan, Y. He, C. Yang and Y. Li. 2006. Synthesis and photovoltaic properties of two-dimensional conjugated polythiophenes with bi(thienylenevinylene) side chains. **Journal of the American Chemical Society** 128(14):4911-4916.
- \_\_\_\_\_, C. Yang, J. Qiao and Y. Li. 2005. Synthesis and photovoltaic properties of the copolymers of 2-methoxy-5-(2'-ethylhexyloxy)-1,4-phenylene vinylene and 2,5-thienylene-vinylene. **Synthetic Metals** 150(3):297-304.
- Huang, Y.M., J.W.Y. Lam, K.K.L. Cheuk, W. Ge and B.Z. Tang. 2001. The role of the phenyl and biphenyl chromophores in the blue luminescent liquid crystalline polyacetylenes. **Materials Science and Engineering B** 85(2-3):242-246.

- Huo, L., J. Hou, C. He, M. Han and Y. Li. 2006. Synthesis, characterization and photovoltaic properties of poly{[1',4'-bis-(thienyl-vinyl)]-2-methoxy-5-(2'-ethylhexyloxy)-1,4-phenylene-vinylene}. **Synthetic Metals** 156(2-4):276-281.
- Hutchison, G.R., M.A. Ratner, and T.J. Marks. 2002. Accurate prediction of band gaps in neutral heterocyclic conjugated polymers. **Journal of Physical chemistry A** 106:10596-10605.
- Jacquemin, D. and E.A. Perpète. 2006. Ab initio calculations of the colour of closed-ring diarylethenes: TD-DFT estimates for molecular switches. **Chemical Physics Letters** 429(1-3):147-152.
- Jiu, T., Y. Li, H. Liu, J. Ye, X. Liu, L. Jiang, M. Yuan, J. Li, C. Li, S. Wang and D. Zhu. 2007. Brightly full-color emissions of oligo(*p*-phenylenevinylene)s: substituent effects on photophysical properties. **Tetrahedron** 63(15):3168-3172.
- Lee, C., W. Yang and R.G. Parr. 1988. Development of the Colle-Salvetti correlation-energy formula into a functional of the electron density. **Physical Review B** 37(2):785.
- Li, Y., Y. Cao, J. Gao, D. Wang, G. Yu and A.J. Heeger. 1999. Electrochemical properties of luminescent polymers and polymer light-emitting electrochemical cells. **Synthetic Metals** 99(3):243-248.
- Liu, Y., W. Hu, W. Qiu, Y. Xu, S. Zhou and D. Zhu. 2001. Organic field-effect transistors based on Langmuir-Blodgett films of substituted phthalocyanines. **Sensors and Actuators B: Chemical** 80(3):202-207.
- Liu, Y., M.S. Liu and A.K.-Y. Jen. 1999. Synthesis and characterization of a novel and highly efficient light-emitting polymer. **Acta Polymerica** 50(2-3):105-108.

- Malinsky, J.E., G.E. Jabbour, S.E. Shaheen, J.D. Anderson, A.G. Richter, T.J. Marks, N.R. Armstrong, B. Kippelen, P. Dutta and N. Peyghambarian. 1999. Self-assembly processes for organic LED electrode passivation and charge injection balance. **Advanced Materials** 11(3):227-231.
- Meeto, W., S. Suramitr, S. Vannarat and S. Hannongbua. 2008. Structural and electronic properties of poly(fluorene-vinylene) copolymer and its derivatives: Time-dependent density functional theory investigation. **Chemical Physics** 349(1-3):1-8.
- Miller, E.K., C.J. Brabec, H. Neugebauer, A.J. Heeger and N. Serdar Sariciftci. 2001. Polarized doping-induced infrared absorption in highly oriented conjugated polymers. **Chemical Physics Letters** 335(1-2):23-26.
- Ogundare, F.O. and M.L. Chithambo. 2008. The influence of optical bleaching on lifetimes and luminescence intensity in the slow component of optically stimulated luminescence of natural quartz from Nigeria. **Journal of Luminescence** 128(10):1561-1569.
- Péres, L.O., M.R. Fernandes, J.R. Garcia, S.H. Wang and F.C. Nart. 2006. Synthesis and characterization of chloro and bromo substituted p-phenylene vinylene homopolymers and alternating copolymers. **Synthetic Metals** 156(7-8):529-536.
- Poolmee, P., M. Ehara, S. Hannongbua and H. Nakatsuji. 2005. SAC-CI theoretical investigation on electronic structure of fluorene-thiophene oligomers. **Polymer** 46(17):6474-6481.
- Santos, L.F., R.C. Faria, L. Gaffo, L.M. Carvalho, R.M. Faria and D. Goñalves. 2007. Optical, electrochemical and electrogravimetric behavior of poly(1-methoxy-4-(2-ethyl-hexyloxy)-p-phenylene vinylene) (MEH-PPV) films. **Electrochimica Acta** 52(13):4299-4304.



- Saha, S., D.V.S. Muthu, D. Golberg, C. Tang, C. Zhi, Y. Bando and A.K. Sood. 2006. Comparative high pressure raman study of boron nitride nanotubes and hexagonal boron nitride. **Chemical Physics Letters** 421(1-3):86-90.
- Sheats, J.R., Y.-L. Chang, D.B. Roitman and A. Stocking. 1999. Chemical aspects of polymeric electroluminescent devices. **Accounts of Chemical Research** 32(3):193-200.
- Suramitr, S., T. Kerdcharoen, T. Srihirin and S. Hannongbua. 2005. Electronic properties of alkoxy derivatives of poly(para-phenylenevinylene), investigated by time-dependent density functional theory calculations. **Synthetic Metals** 155(1):27-34.
- Tan, Z.a., E. Zhou, Y. Yang, Y. He, C. Yang and Y. Li. 2007. Synthesis, characterization and photovoltaic properties of thiophene copolymers containing conjugated side-chain. **European Polymer Journal** 43(3):855-861.
- Tang, C.W. and S.A. VanSlyke. 1987. Organic electroluminescent diodes. **Applied Physics Letters** 51(12):913-915.
- Tomasi, J. and M. Persico. 1994. Molecular interactions in solution: An overview of methods based on continuous distributions of the solvent. **Chemical Reviews** 94(7):2027-2094.
- Tretiak, S., A. Saxena, R.L. Martin and A.R. Bishop. 2002. Conformational dynamics of photoexcited conjugated molecules. **Physical Review Letters** 89(9):097402.
- Vardeny, Z.V., A.J. Heeger and A. Dodabalapur. 2005. Fundamental research needs in organic electronic materials. **Synthetic Metals** 148(1):1-3.

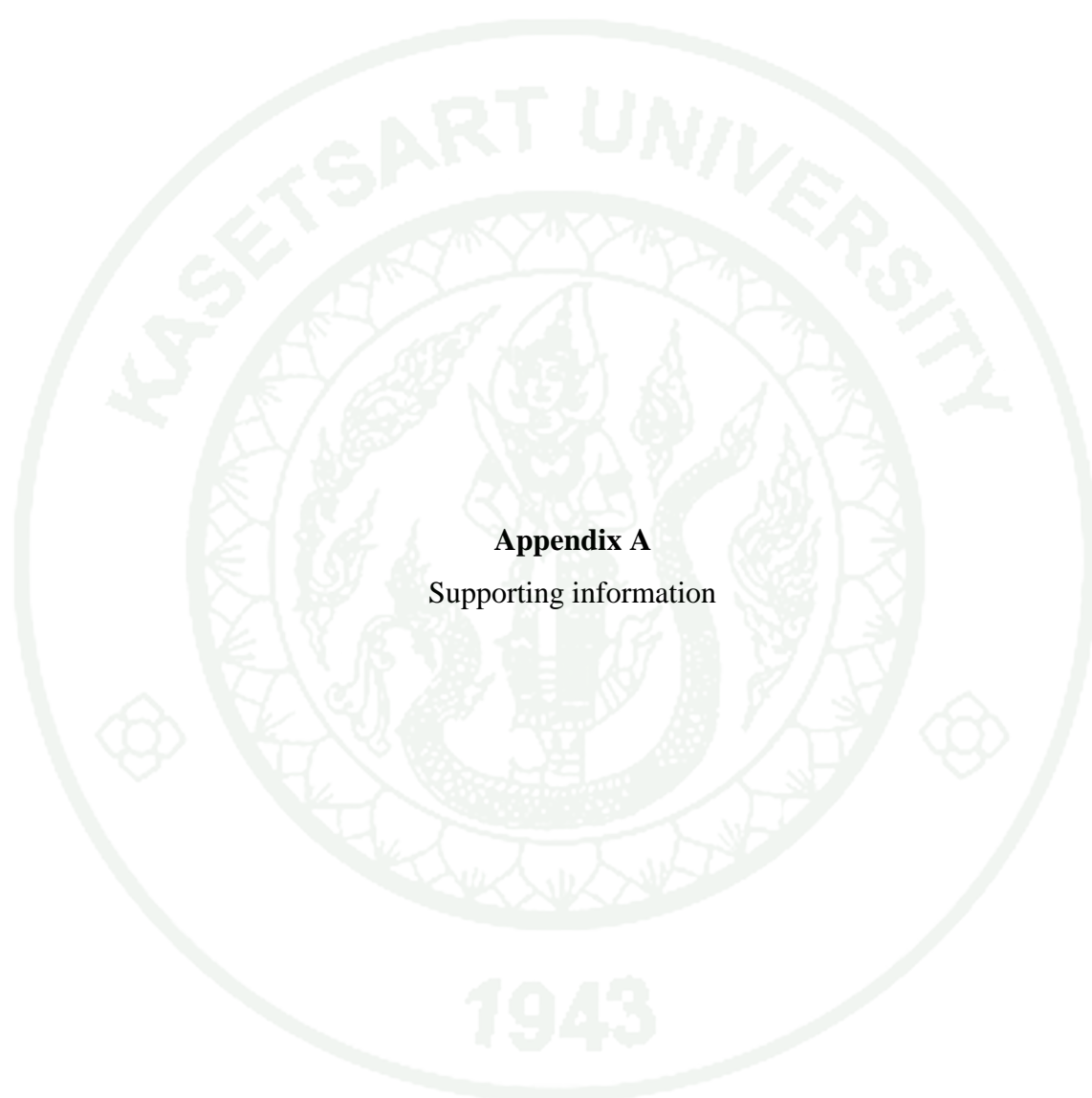
- Wen, S., J. Pei, Y. Zhou, P. Li, L. Xue, Y. Li, B. Xu and W. Tian. 2009. Synthesis of 4,7-diphenyl-2,1,3-benzothiadiazole-Based copolymers and their Photovoltaic applications. **Macromolecules** 42(14):4977-4984.
- Whitelegg, S.A., C. Giebeler, A.J. Campbell, S.J. Martin, P.A. Lane, D.D.C. Bradley, G. Webster and P.L. Burn. 2000. Optical studies of polymer light-emitting diodes using electroabsorption measurements. **Synthetic Metals** 111-112:241-244.
- Wu, F-I., D.S. Reddy, and C-F. Shu. 2003. Novel oxidazole-containing polyfluorene with efficient blue electroluminescence. *Chemistry of Materials* 15(1):269-274.
- Yamamoto, T., Q. Fang and T. Morikita. 2003. **Macromolecules** 36:4262.
- Xue, C. and F.-T. Luo. 2004. Novel *p*-phenylene-vinylene-dithienylene type copolymer: potential red-emitting materials. **Synthetic Metals** 145(1):67-73.
- Wagner, P., A.M. Ballantyne, K.W. Jolley and D.L. Officer. 2006. Synthesis and characterization of novel styryl-substituted oligothiénylenevinylenes. **Tetrahedron** 62(10):2190-2199.
- Xue, C. and F.-T. Luo. 2004. Novel *p*-phenylene-vinylene-dithienylene type copolymer: potential red-emitting materials. **Synthetic Metals** 145(1):67-73.
- Yook, K.S., S.O. Jeon, J.Y. Lee, K.H. Lee, Y.S. Kwon, S.S. Yoon and J.H. Yoon. 2009. High efficiency pure white organic light-emitting diodes using a diphenylaminofluorene-based blue fluorescent material. **Organic Electronics** 10(7):1378-1381.
- Yook, K.S., S.O. Jeon, C.W. Joo, J.Y. Lee, M.S. Kim, H.S. Choi, S.J. Lee, C.W. Han and Y.H. Tak. 2009. Highly efficient pure white phosphorescent organic light-emitting diodes using a deep blue phosphorescent emitting material. **Organic Electronics: physics, materials, applications** 10(4):681-685.

Zhu, M., T. Cui and K. Varahramyan. 2004. Experimental and theoretical investigation of MEH-PPV based Schottky diodes. **Microelectronic Engineering** 75(3):269-274.





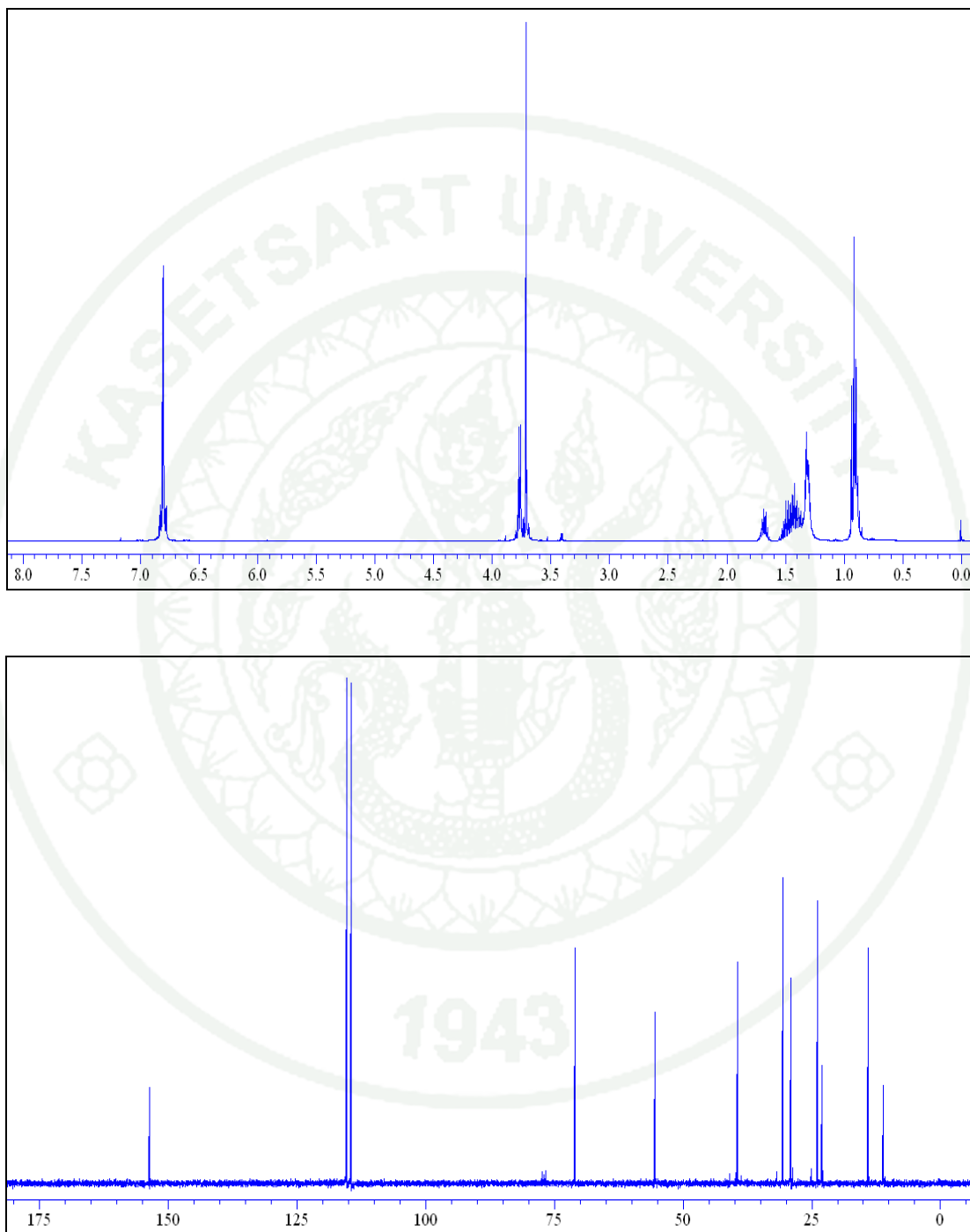
## APPENDICES



**Appendix A**  
Supporting information

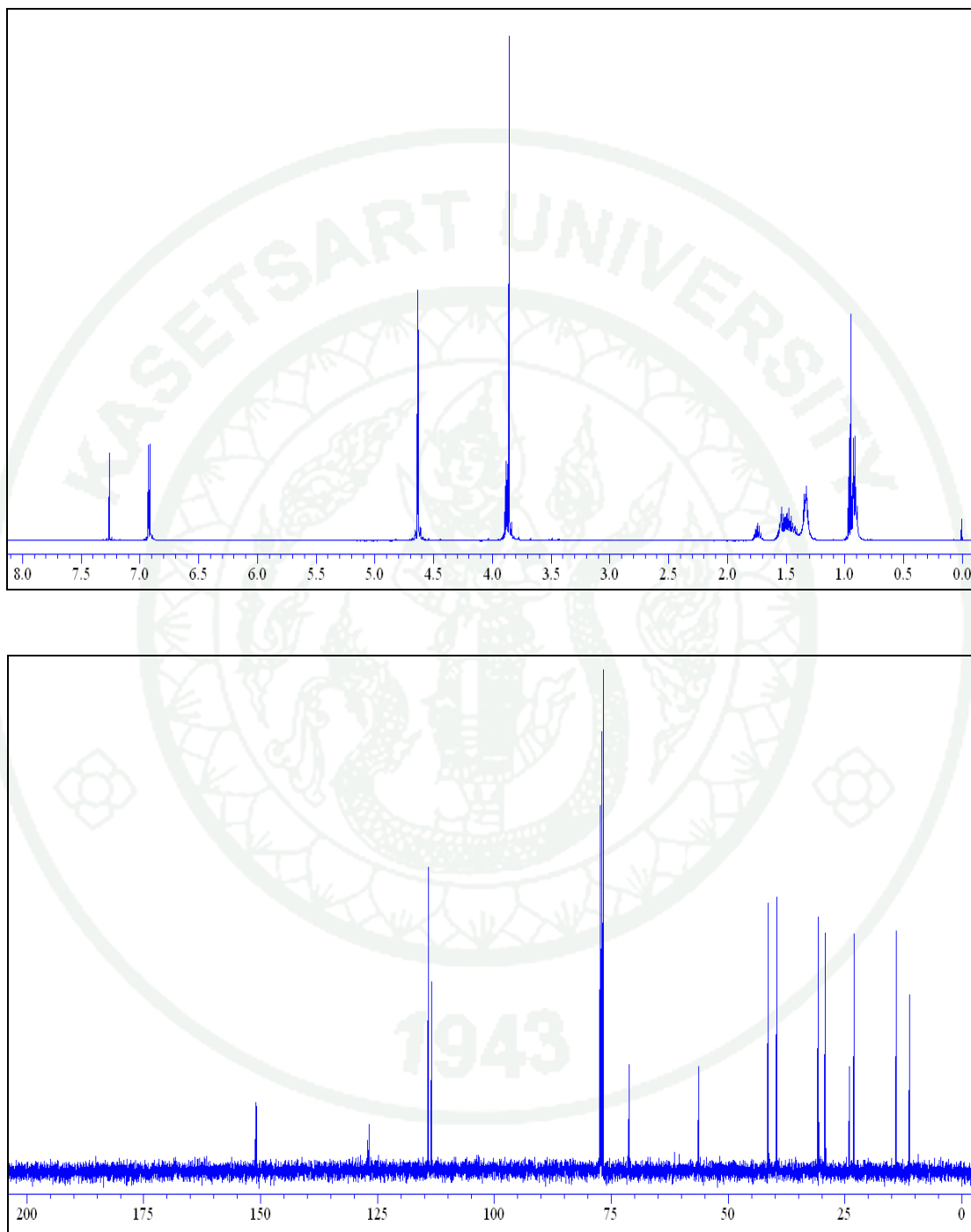


**1. 1-((2-Ethylhexyl)oxy)-4-methoxybenzene (C2)**



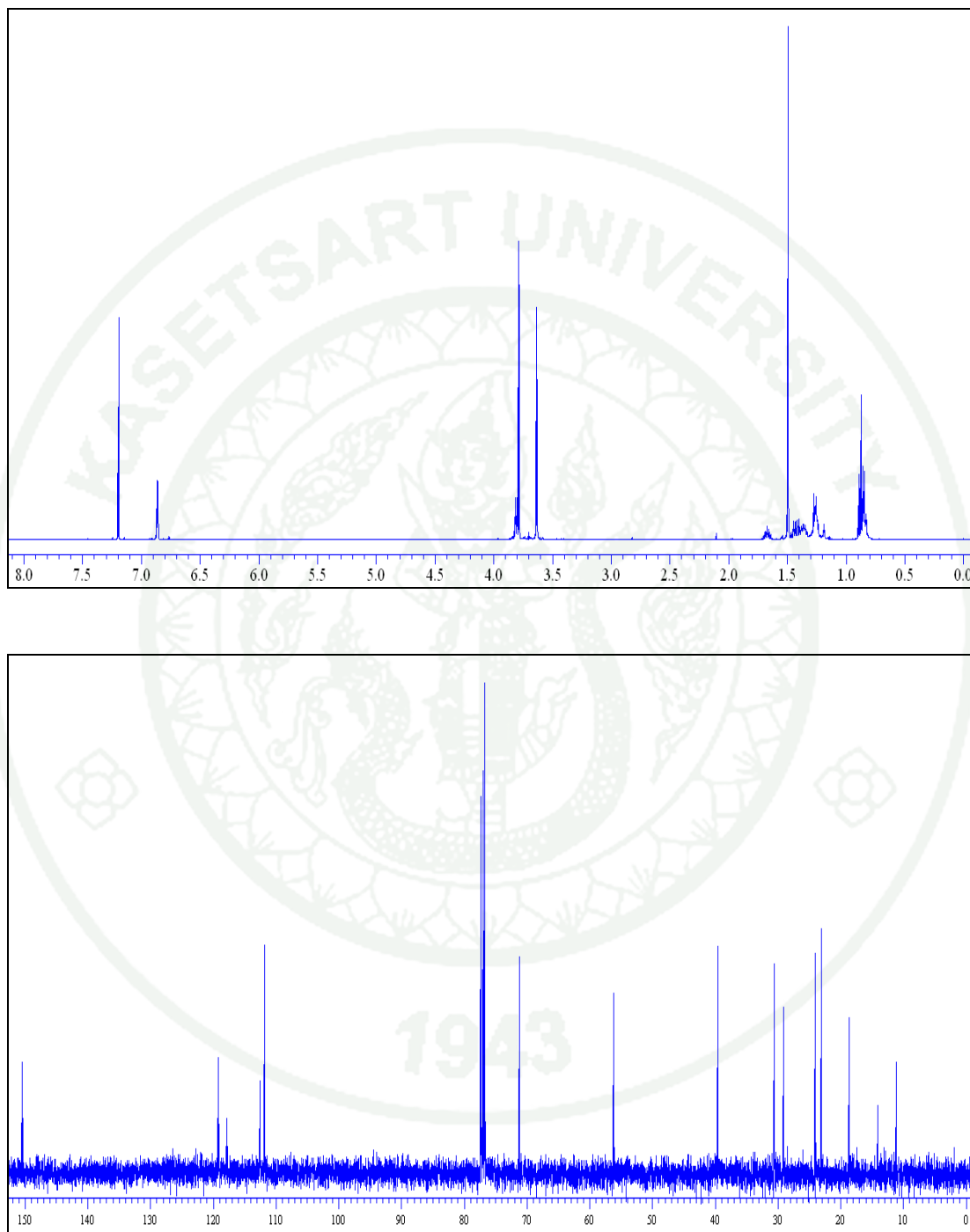
**Appendix Figure A1**  $^1\text{H}$ -NMR and  $^{13}\text{C}$ -NMR spectrum of C2.

2. 1,4-Bis(chloromethyl)-2-((2'-ethylhexyl)oxy)-5methoxybenzene (C3)



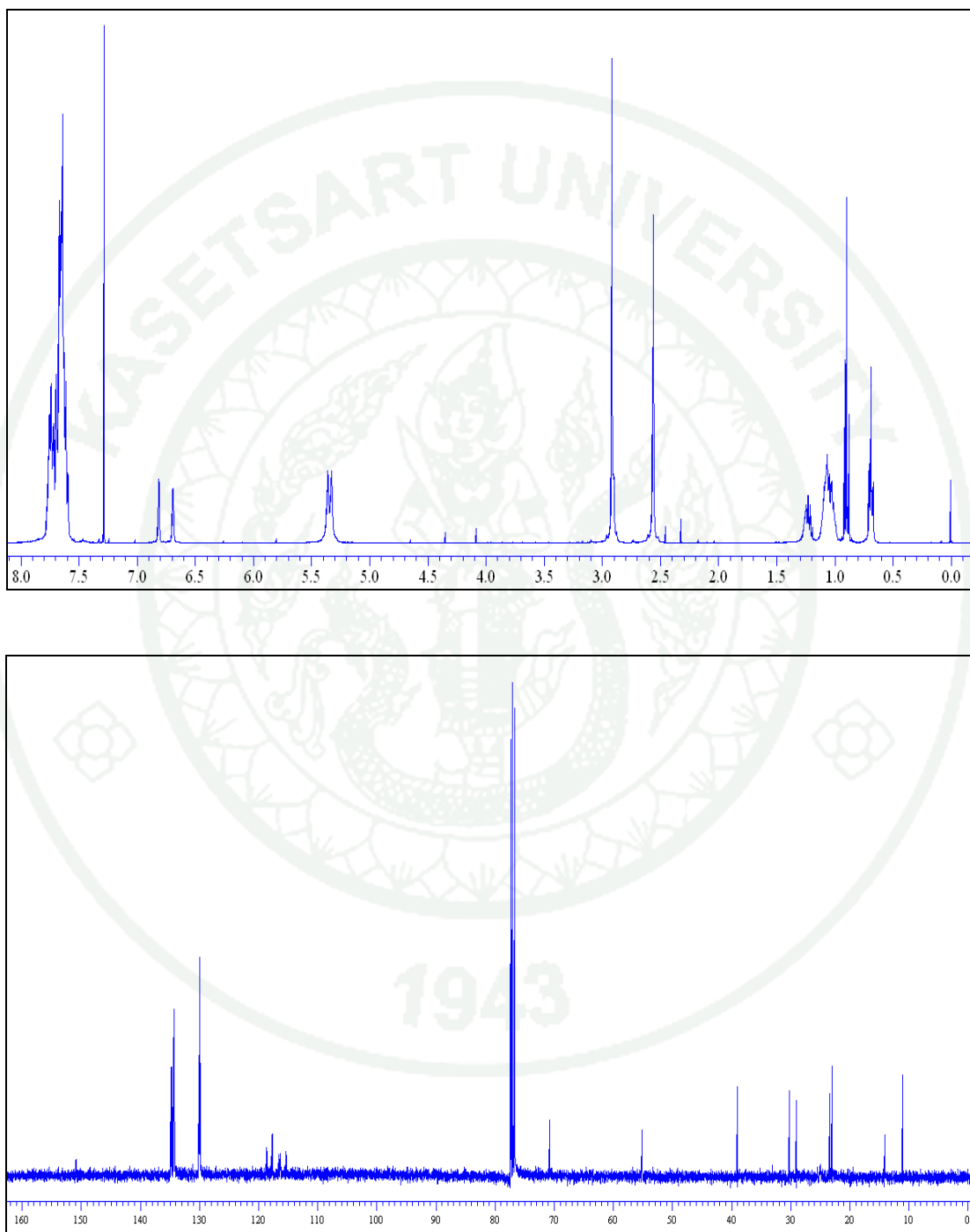
**Appendix Figure A2**  $^1\text{H}$ -NMR and  $^{13}\text{C}$ -NMR spectrum of C3.

**3. 1,4-Bis(cyanomethyl)-2-((2'-ethylhexyl)oxy)-5-methoxybenzene (C4)**



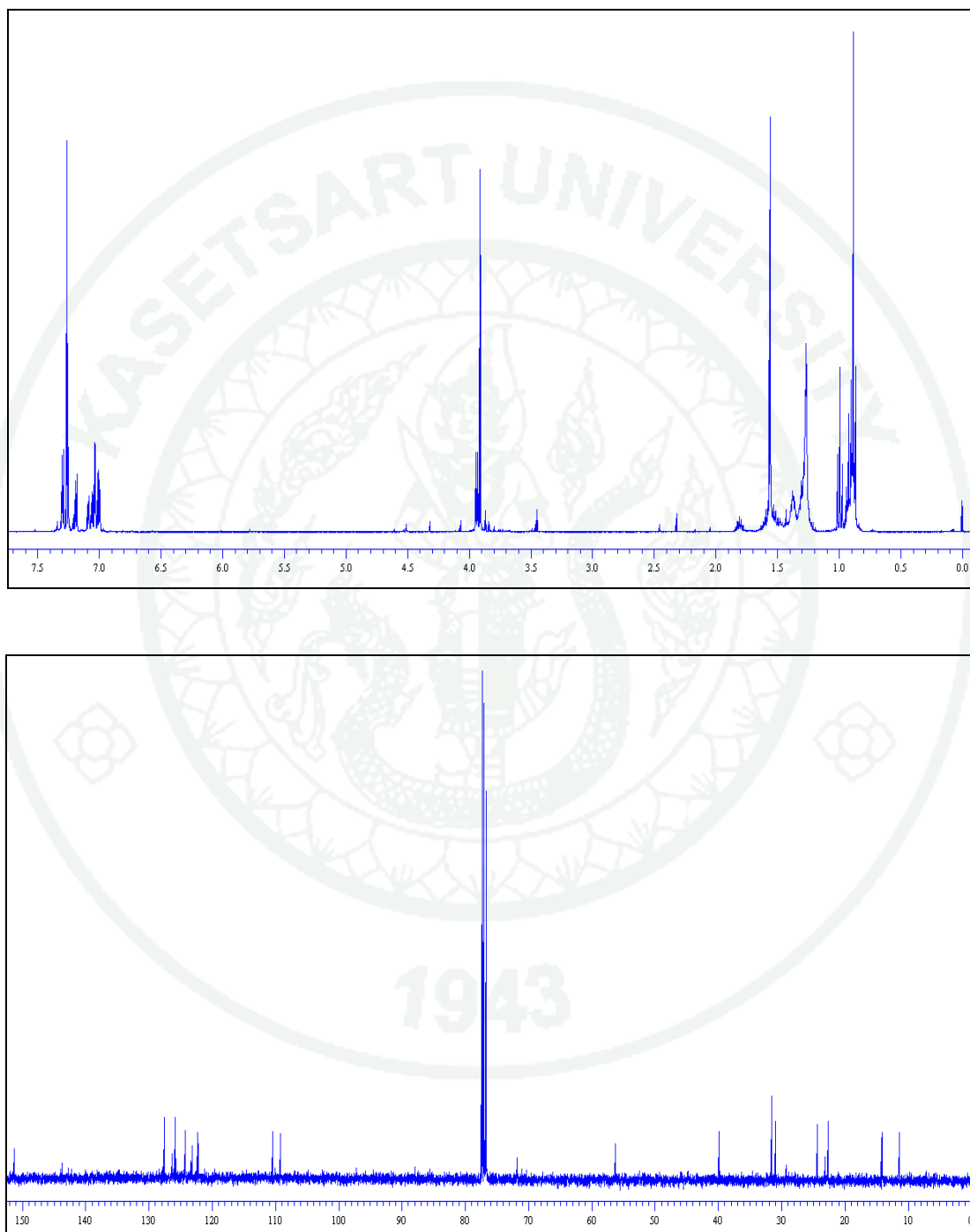
**Appendix Figure A3**  $^1\text{H}$ -NMR and  $^{13}\text{C}$ -NMR spectrum of C4.

**4. 1,4-Bis(triphenyl phosphine)-2-methoxy-5-(2-methylhexyloxy) benzene salt (C5)**



**Appendix Figure A4**  $^1\text{H}$ -NMR and  $^{13}\text{C}$ -NMR spectrum of C5.

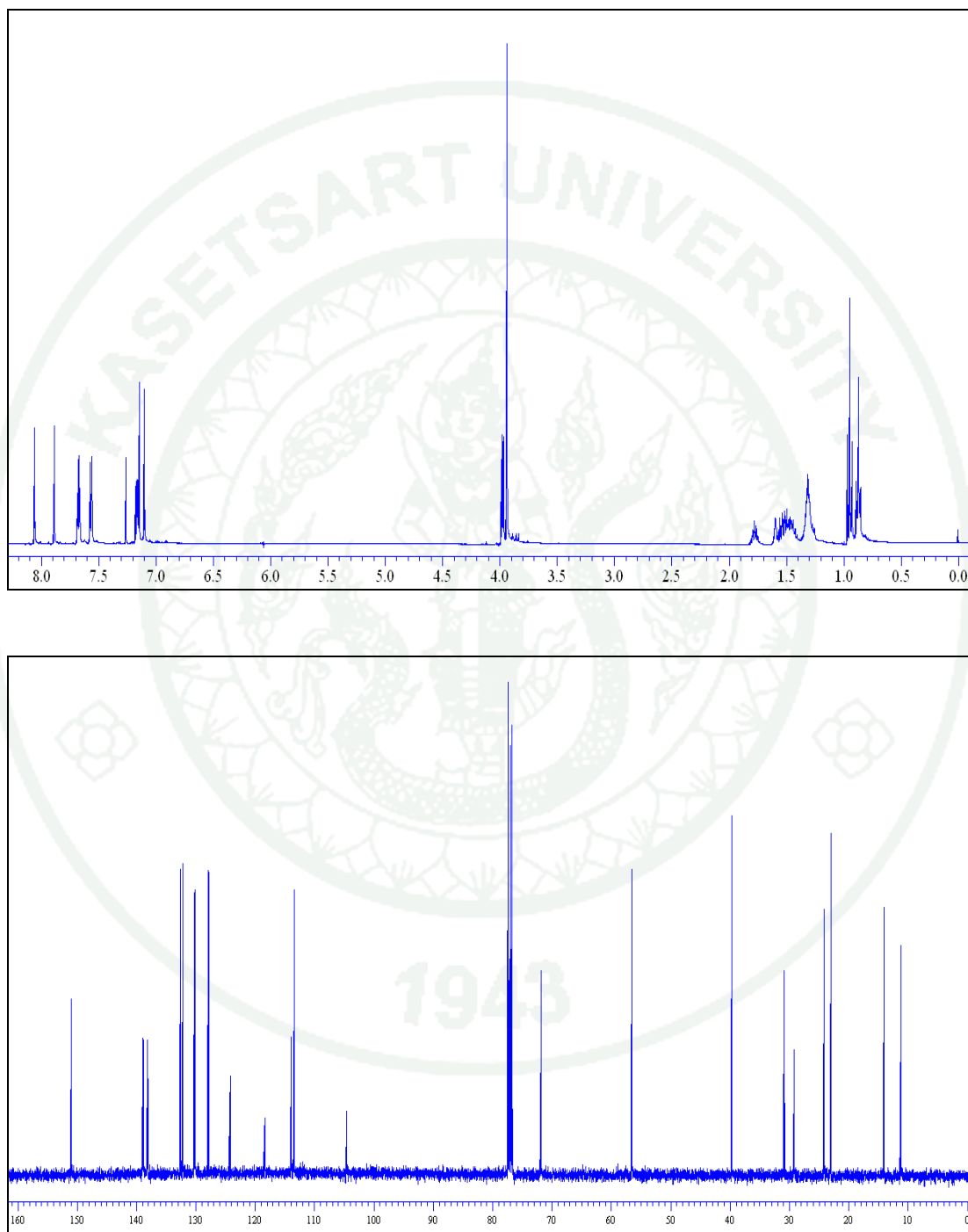
5. [1,4-Bis(thienyl-vinyl)]-2-methoxy-5-(2-methylhexyloxy)benzene  
(MEH-ThV)



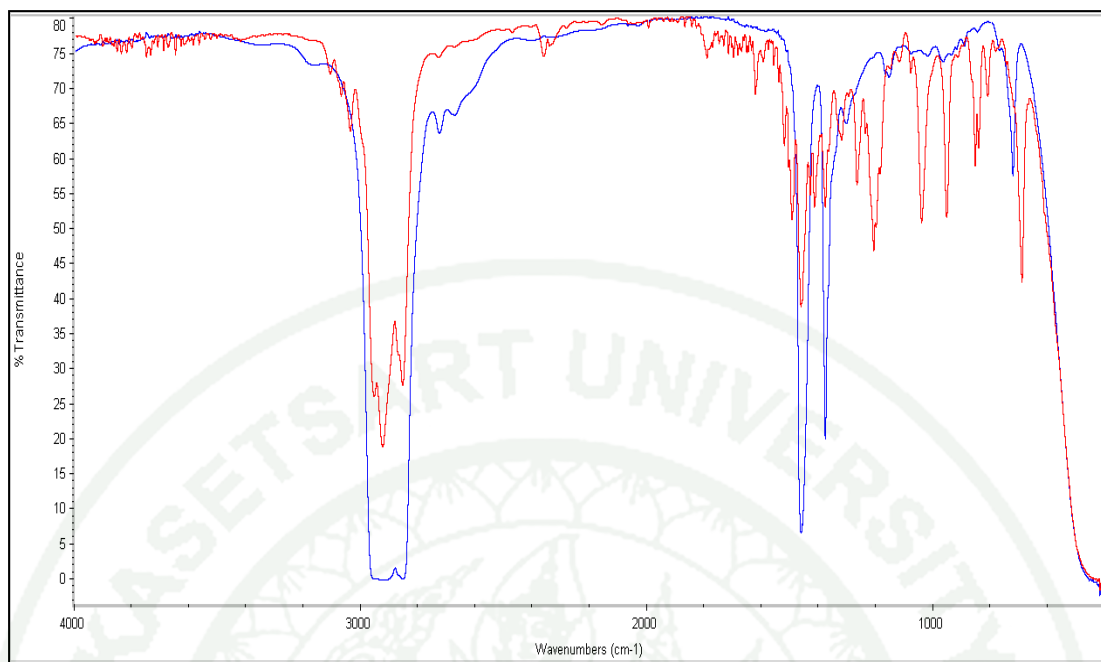
**Appendix Figure A5**  $^1\text{H}$ -NMR and  $^{13}\text{C}$ -NMR spectrum of MEH-ThV compound.



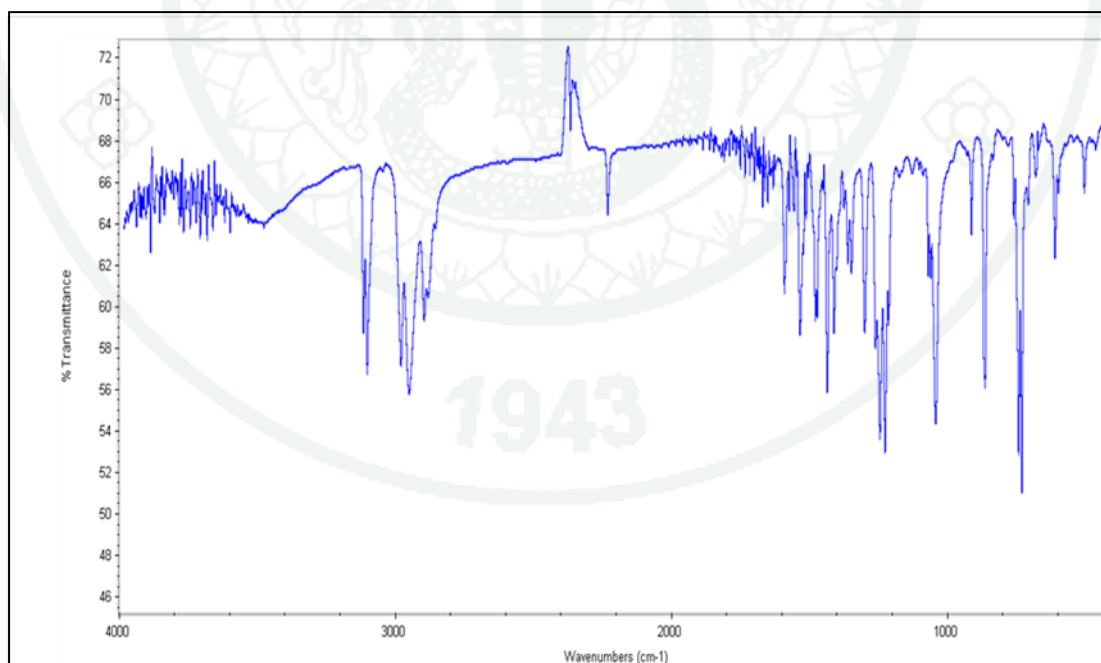
6. [1,4-Bis(thienyl-1,1'-cyanovinylene)]-2-methoxy-5-(2-methylhexyloxy) benzene (MEH-ThV-CN)



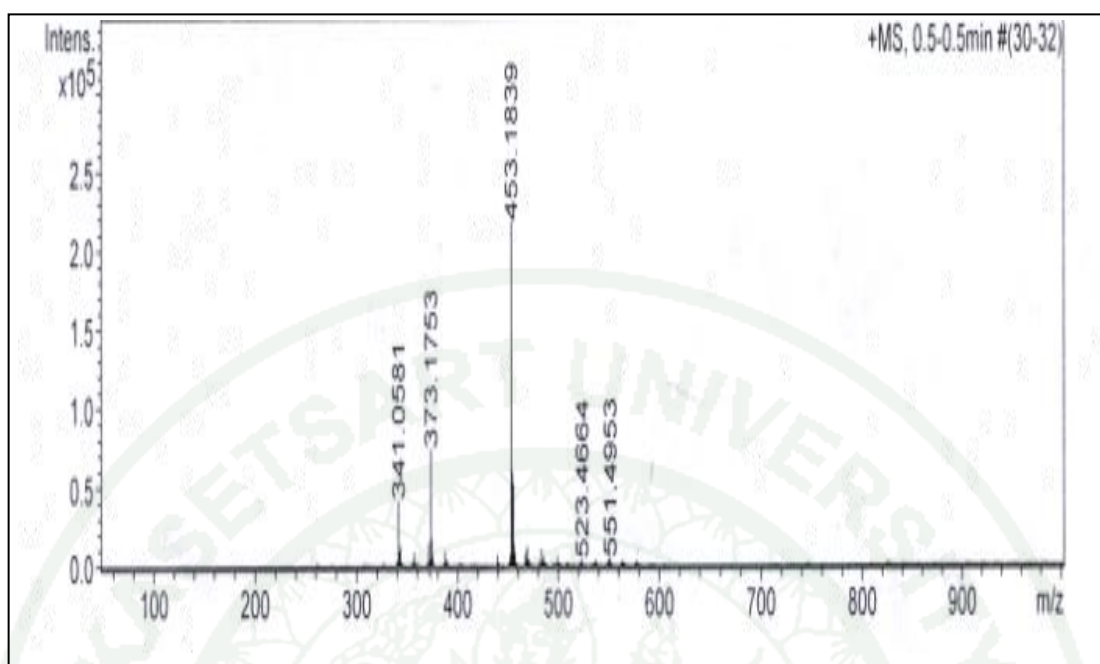
**Appendix Figure A6**  $^1\text{H}$ -NMR and  $^{13}\text{C}$ -NMR spectrum of MEH-ThV-CN compound.



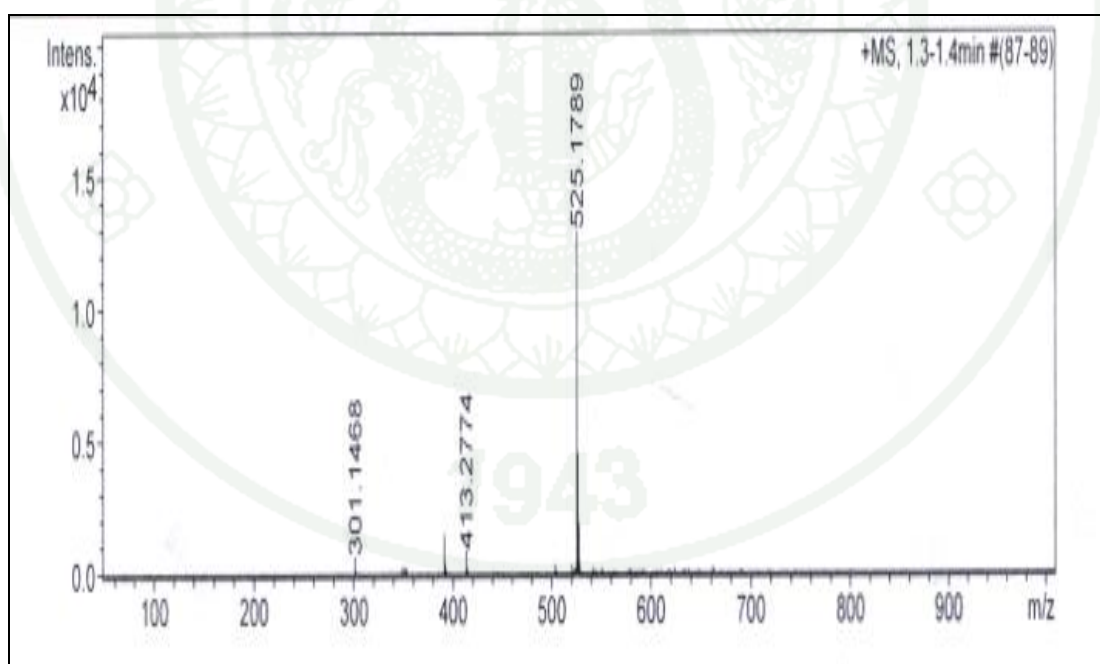
**Appendix Figure A7** FTIR spectrum of MEH-ThV compound (red line) and nujol mulls (blue line).



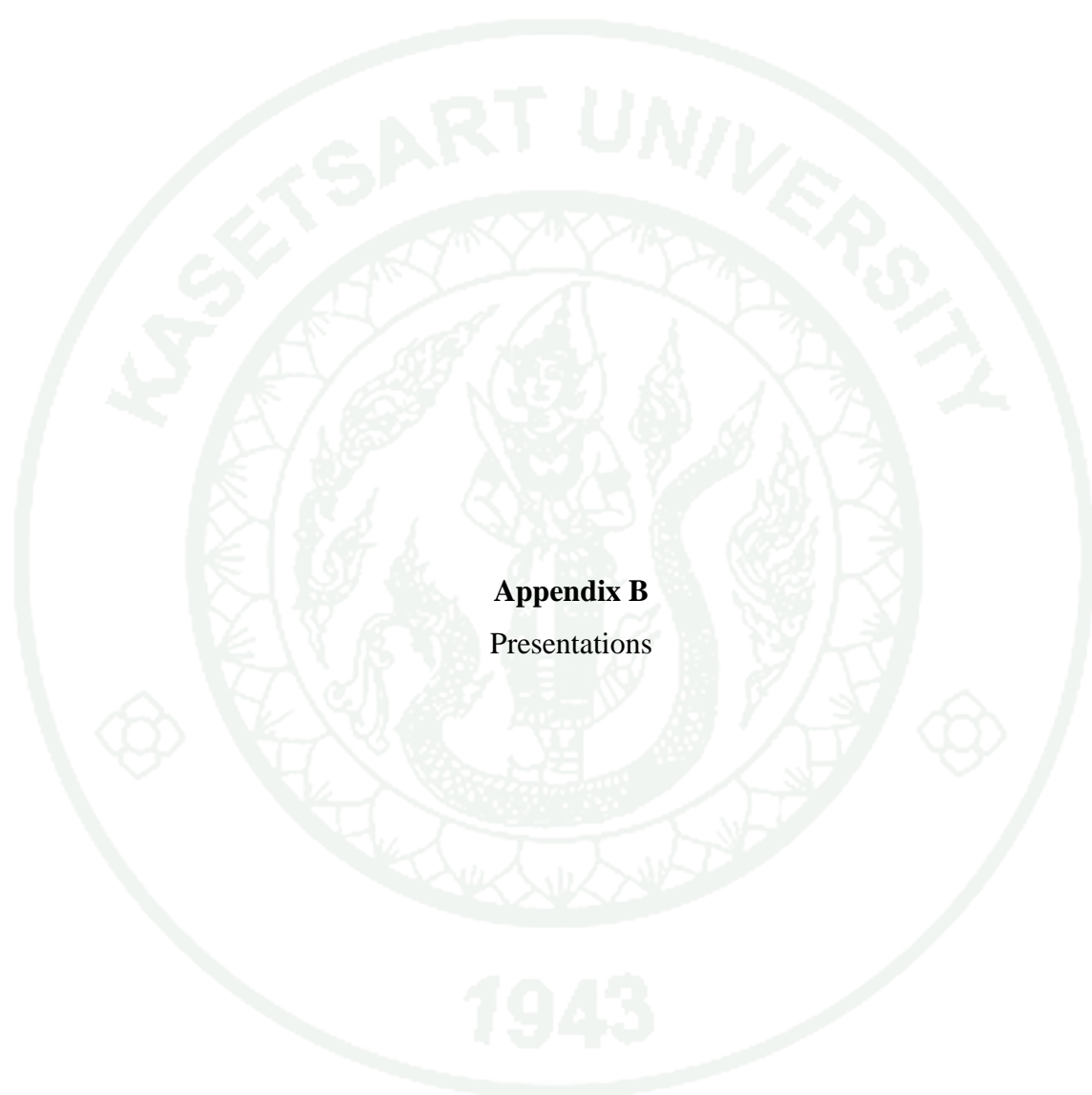
**Appendix Figure A8** FTIR spectrum of MEH-ThV-CN compound.



**Appendix Figure A9** MS spectrum of MEH-ThV compound.



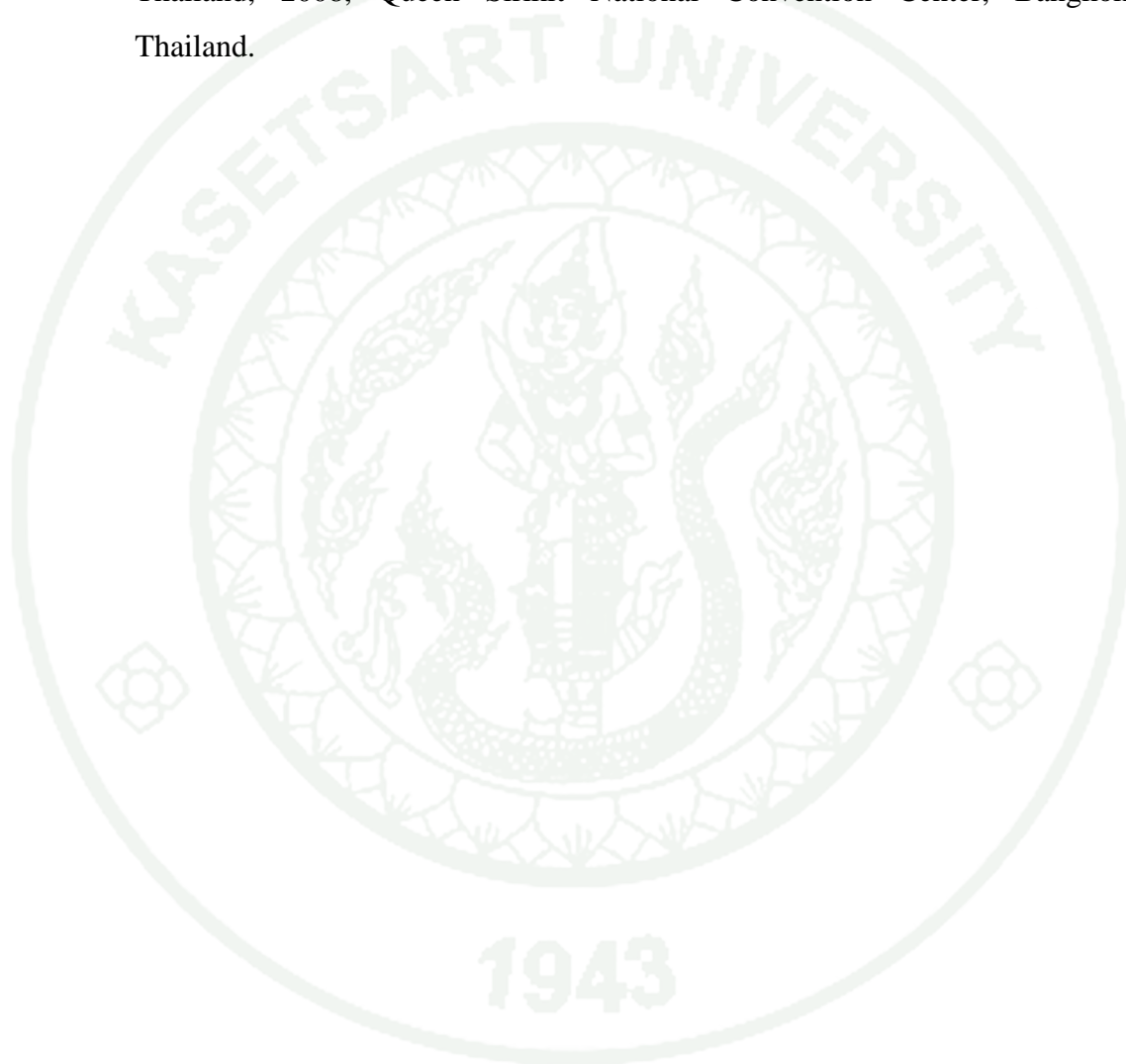
**Appendix Figure A10** MS spectrum of MEH-ThV-CN compound.



**Appendix B**  
Presentations

## 1. Poster Presentation

Suphawarat Phalinyot, Songwut Suramitr, Chuleeporn Luadthong and Supa Hannongbua. Theoretical studies of Poly(phenylene-vinylene) copolymer by substitutions to fuctional groups. 34<sup>th</sup> Congress on Science and Technology of Thailand, 2008, Queen Sirikit National Convention Center, Bangkok, Thailand.



การศึกษาโครงสร้างของพอลิ(ฟีนิลีน-ไวนิลีน)โคพอลิเมอร์ โดยมีการเติมหมู่ฟังก์ชัน ด้วยระเบียบวิธีทางเคมีควอนตัม

# THEORETICAL STUDIES OF POLY(PHENYLENE-VINYLENE) COPOLYMER BY SUBSTITUTIONS TO FUNCTIONAL GROUP

ศุภาวรัตน์ ผดิมยศ, ทรงวุฒิ สุรมิตร\*, สุภา หารหนองบัว

Suphawarat Phalinyot<sup>1,2</sup>, Songwut Suramit<sup>1,2\*</sup> and Supa Hannongbua<sup>1,2</sup>

<sup>1</sup>Department of Chemistry, Faculty of Science, Kasetsart University, Bangkok 10900, Thailand,

<sup>2</sup>Center of Nanotechnology, Kasetsart University, Bangkok 10900, Thailand,

\*E-mail: [fsciswsm@ku.ac.th](mailto:fsciswsm@ku.ac.th), Tel. +66 25 62 55 55 ext. 2227

**บทคัดย่อ:** ได้ศึกษาสมบัติของพอลิ(ฟีนิลีน-ไวนิลีน)โคพอลิเมอร์ (PPV) โดยที่มีการเติมหมู่ฟังก์ชัน ได้แก่ ไทโอเฟน, ไพโรล, คาร์บาโซล และ ฟลูออรีน โดยมีการศึกษาโครงสร้างและสมบัติทางแสงด้วยระเบียบวิธีทางเคมีคอมพิวเตอร์ โดยวิธี B3LYP/6-31G\* เพื่อให้โครงสร้างที่เสถียรที่สุดและพบว่าค่าความแตกต่างของแถบพลังงานของ (PPV)<sub>n</sub>, (PPV-Thiophene)<sub>n</sub>, (PPV-Pyrrole)<sub>n</sub>, (PPV- Carbazole)<sub>n</sub> และ (PPV-Fluorene)<sub>n</sub> เมื่อ  $n=\infty$  มีค่าเท่ากับ 2.08, 1.84, 2.03, 2.70 และ 2.78 eV และสามารถเรียงลำดับค่าความแตกต่างของแถบพลังงานของ (PPV-Thiophene)<sub>n</sub> > (PPV-Pyrrole)<sub>n</sub> > (PPV)<sub>n</sub> > (PPV-Carbazole)<sub>n</sub> > (PPV- Fluorene)<sub>n</sub> จะเห็นได้ว่า (PPV-Thiophene)<sub>n</sub> มีค่าความแตกต่างของแถบพลังงานต่ำที่สุด ทั้งนี้ (PPV-Thiophene)<sub>n</sub> จึงน่าที่จะมีสมบัติในการนำไฟฟ้าได้ดีที่สุดเมื่อเปรียบเทียบกับโครงสร้างทั้งสี่โคพอลิเมอร์ (PPV-Thiophene)<sub>n</sub> และจะได้นำไปทำการสังเคราะห์เพื่อศึกษาโครงสร้างทางผลึกของ (PPV-Thiophene)<sub>n</sub> ต่อไป

**Abstract:** Structure and energetic properties of poly(phenylene-vinylene) (PPV) copolymer with its derivatives have been studied, by quantum chemical calculations. Some functional groups (thiophene, pyrrole, carbazole and fluorene) were substituted on PPV to investigate the optical properties. All structures were optimized at the B3LYP/6-31G/\*\* level of calculations. Calculated energy gaps of (PPV)<sub>n</sub>, (PPV-Thiophene)<sub>n</sub>, (PPV-Pyrrole)<sub>n</sub>, (PPV-Carbazole)<sub>n</sub> and (PPV- Fluorene)<sub>n</sub>,  $n=\infty$  are 2.08, 1.84, 2.03, 2.70 and 2.78 eV, respectively. The energy gaps can be ordered as following; (PPV-Thiophene)<sub>n</sub> > (PPV-Pyrrole)<sub>n</sub> > (PPV)<sub>n</sub> > (PPV- Carbazole)<sub>n</sub> > (PPV- Fluorene)<sub>n</sub>. It was found that (PPV-Thiophene)<sub>n</sub> revealed the lowest energy gap. Therefore, the (PPV-Thiophene)<sub>n</sub> was supposed to a promising semiconductor material and will be further synthesized.





## Theoretical studies of poly(phenylene-vinylene) copolymer by substitutions to functional groups

Suphawarat Phalinyot<sup>1,2</sup>, Songwut Suramitr<sup>1,2\*</sup> and Supa Hannongbua<sup>1,2</sup>

<sup>1</sup>Department of Chemistry, Faculty of Science, Kasetsart University, Bangkok, 10900 Thailand

<sup>2</sup>Center of Nanotechnology, Kasetsart University, Bangkok, 10900 Thailand

\*E-mail: [sciswsm@ku.ac.th](mailto:sciswsm@ku.ac.th), Tel. +66 25 62 55 55 ext. 2227

### Introduction

Poly(phenylene-vinylene) (PPV) is one of the most important conductive polymers and PPV has been studied due to the interests in materials research because PPV based on high electrical conductivity, electroluminescence, photoluminescence and photoconductivity. In addition, PPV was combined with donor-acceptor. The electronic properties of PPV and its derivatives were changed. Therefore, in this work, we investigated the electronic and optical properties of these structural geometries by using quantum chemical calculations and comparison to available experimental data.

### Methodologies

The structure of the poly(phenylene-vinylene) (PPV) derivatives were optimized by HF and B3LYP level of theory and the standard 6-31G(d,p) basis set were used for HF and B3LYP levels calculations. The calculation HOMO-LUMO energy of geometry structures were studied by TD-DFT calculation base on ground state geometries. The excited state structures of all derivatives were optimized by TD-B3LP/6-31G(d,p) method. All calculations were performed using Gaussian03 program package.

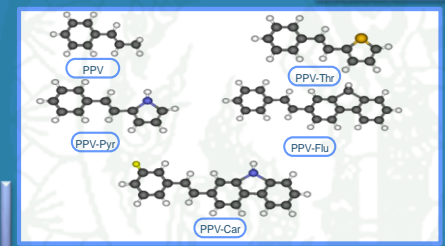


Fig. 1. Structural geometries of PPV and its derivatives.

### Results and discussion

#### Ground-state geometries

The optimized geometries parameter for the (PPV)<sub>n</sub> and its derivatives, (PPV-Thr)<sub>n</sub>, (PPV-Pyr)<sub>n</sub>, (PPV-Flu)<sub>n</sub>, and (PPV-Car)<sub>n</sub> have been calculated by using HF/6-31G(d,p) and B3LYP/6-31G(d,p) level, which the extrapolated energy gaps to infinite chain length ( $n \rightarrow \infty$ ) of structural geometries were summarized in Table 1. It was found that the results were calculated from HF/6-31G(d,p) method at  $n \rightarrow \infty$  are 3.26, 3.11, 3.14, 3.38 and 3.39 eV, respectively and energy gap at B3LYP/6-31G(d,p) method have given at 2.08, 1.84, 2.03, 2.70 and 2.78 eV, respectively, which (PPV)<sub>n</sub> from theoretical data is closer to the experimental data [1].

Table 1 The extrapolated energy gap of structural geometries of PPV and its derivatives.

PPV derivatives	Energy gap (eV)	
	HF/6-31G(d,p)	B3LYP/ 6-31G(d,p)
(PPV) <sub>n</sub>	3.26	2.08 (2.45) <sup>a</sup>
(PPV-Thr) <sub>n</sub>	3.11	1.84
(PPV-Pyr) <sub>n</sub>	3.14	2.03
(PPV-Flu) <sub>n</sub>	3.38	2.70
(PPV-Car) <sub>n</sub>	3.39	2.78

<sup>a</sup> Reference [1]

#### Acknowledgements :

This work was supported the Thailand Research Fund (TRF), Commission Higher Education (CHE), the National Center of Excellence for Petroleum, Petrochemicals, and Advanced Materials (NCE-PPAM), National Nanotechnology Center (NANOTEC), Laboratory and Applied Chemistry (LCAC) and Kasetsart University Research and Development Institute (KURDI) for research scholars.

Table 2 Absorption properties of all structural geometries.

Geometry	energy (eV)	electronic transition(%coefficient)	$\lambda_{\text{max}}$ TD-DFT(nm)	oscillator stragne
(PPV) <sub>n</sub>	n=1 4.59	H $\rightarrow$ L (65.04%)	287.32	0.10
	n=2 4.32	H-2 $\rightarrow$ L (65.14%)	269.84	0.46
	n=3 3.41	H $\rightarrow$ L (66.34%)	363.97	0.82
	n=4 3.10	H $\rightarrow$ L (66.54%)	400.43	1.42
	$n \rightarrow \infty$		454.00 <sup>b</sup>	
(PPV-Thr) <sub>n</sub>	n=1 4.23	H-1 $\rightarrow$ L (62.34%)	293.21	0.54
	n=2 3.20	H $\rightarrow$ L (66.56%)	378.78	0.99
	n=3 3.02	H $\rightarrow$ L (66.26%)	411.19	1.67
	n=4 2.93	H $\rightarrow$ L (64.73%)	422.97	2.17
(PPV-Pyr) <sub>n</sub>	n=1 3.92	H $\rightarrow$ L (59.27%)	316.35	0.46
	n=2 3.32	H $\rightarrow$ L (66.43%)	373.65	1.27
	n=3 3.08	H-1 $\rightarrow$ L (66.98%)	403.08	1.70
	n=4 2.97	H $\rightarrow$ L (65.15%)	417.82	1.84
(PPV-Flu) <sub>n</sub>	n=1 4.00	H-1 $\rightarrow$ L (64.92%)	310.11	0.72
	n=2 3.14	H $\rightarrow$ L (67.07%)	394.89	1.16
	n=3 3.16	H $\rightarrow$ L (60.78%)	392.79	2.54
	n=4 3.13	H $\rightarrow$ L (55.17%)	396.48	3.48
(PPV-Car) <sub>n</sub>	n=1 4.01	H-2 $\rightarrow$ L (65.01%)	308.89	0.55
	n=2 3.28	H $\rightarrow$ L (66.42%)	377.78	1.43
	n=3 3.19	H $\rightarrow$ L (59.34%)	388.43	2.42
	n=4 3.15	H $\rightarrow$ L (50.98%)	393.20	3.22

<sup>b</sup> Reference [2], measured in dichloromethane.

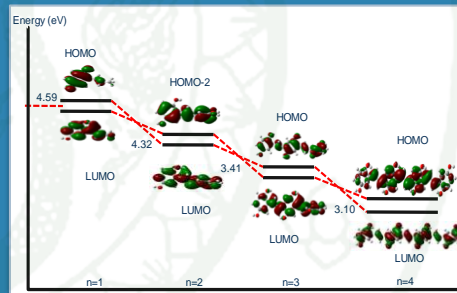


Fig. 2. Molecular orbitals (HOMO-LUMO) for (PPV)<sub>n</sub> oligomers.

#### Electronic properties

The vertical excitation energies for non-planar conformations of PPV and its derivatives using TD/B3LYP/6-31G(d,p) approach were summarized in table 2. The wave length of PPV oligomers at theoretical is closer to the experimental result, which it was observed in dichloromethane. The HOMO and LUMO of (PPV)<sub>n</sub> oligomers (Fig. 2) at  $n=1$ , 2, 3 and 4 oligomers are 65.04 IH $\rightarrow$ L>, 65.14IH-2 $\rightarrow$ L>, 66.34 IH $\rightarrow$ L> and 66.54IH $\rightarrow$ L> transitions, respectively.

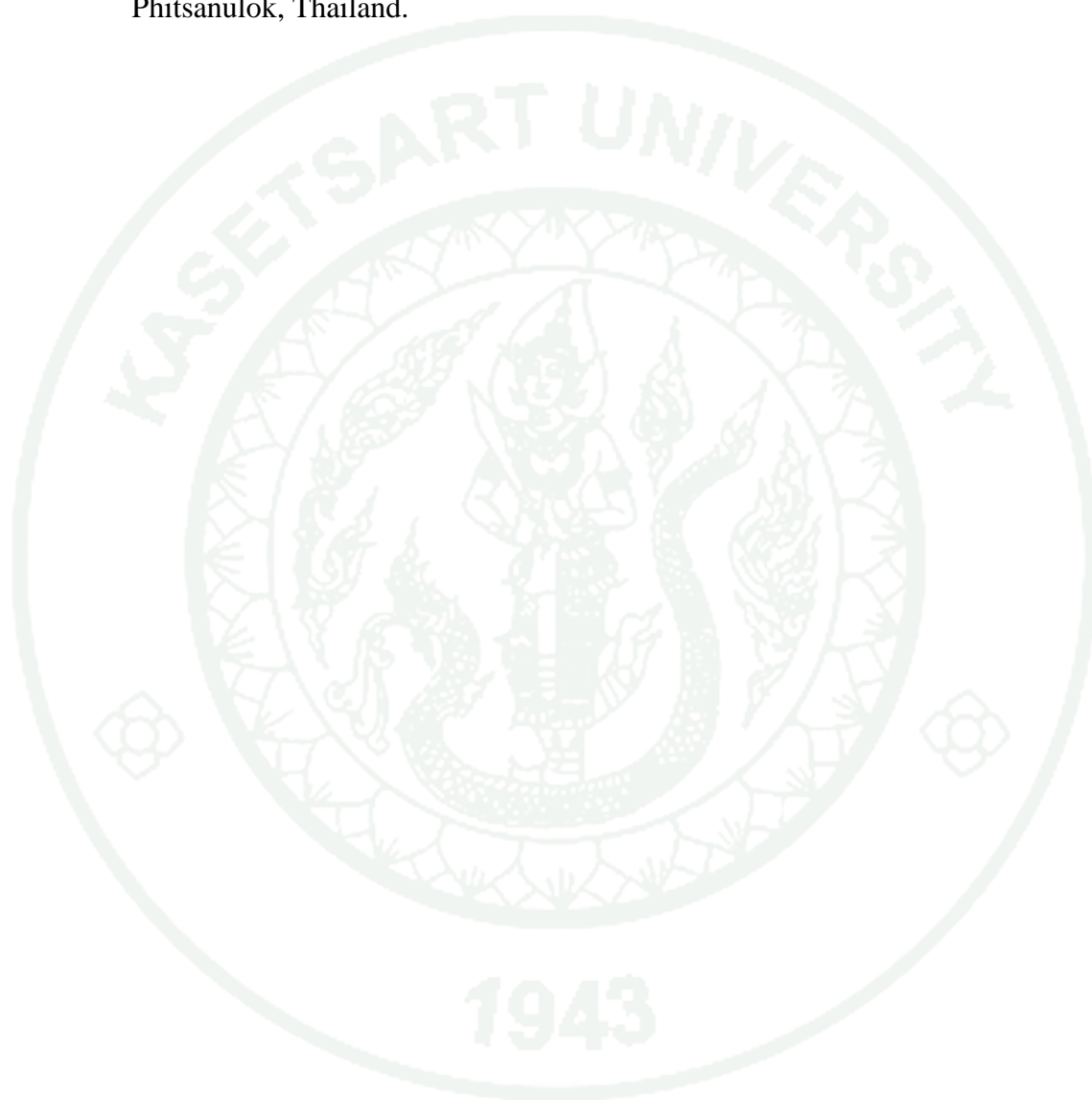
#### Conclusions

The structures of all oligomers were fully geometries optimized employing the HF and DFT level to non-planar conformations because the steric effect of vinylene group. Moreover, the structural of (PPV-Thr)<sub>n</sub> revealed the lowest extrapolate energy gap. Therefore, the (PPV-Thr)<sub>n</sub> was supposed to be a promising semiconductor material and will be further synthesized.

#### References :

1. Lagowski, J. B. *Theo Chem*, **2002**, 589-590, 125-137.
2. Schenning, A. P. H. J.; Tsipis, A. C.; Meskers, S. C. J.; Beljonne, D.; Meijer, E. W.; Brédas, J. L. *Chem. Mater.*, **2002**, 14, 1362-1368.
3. Suramitr, S.; Kerakiat, K.; Srihirin, T.; Hannongbua, S. *Synth.Met.*, **2005**, 155, 27-34.

Suphawarat Phalinyot, Songwut Suramitr, Chuleeporn Luadthong and Supa Hannongbua. Electronic properties of *p*-Methoxy phenylene-vinylene derivatives, investigated by Quantum Chemical Calculations. Pure and Applied Chemistry International Conference of Thailand, 2009, Naresuan University, Phitsanulok, Thailand.



# ELECTRONIC PROPERTIES OF *p*-METHOXY PHENYLENE VINYLENE DERIVATIVES, INVESTIGATED BY QUANTUM CHEMICAL CALCULATION

Suphawarat Phalinyot<sup>1,2</sup>, Songwut Suramitr<sup>1,2\*</sup>, Chuleeporn Luadthong<sup>1,2</sup>  
and Supa Hannongbua<sup>1,2</sup>

<sup>1</sup>Department of Chemistry, Faculty of Science, Kasetsart University, Bangkok, 10900 Thailand

<sup>2</sup>Center of Nanotechnology, Kasetsart University, Bangkok, 10900 Thailand

\*E-mail: [fsciswsm@ku.ac.th](mailto:fsciswsm@ku.ac.th), Tel. +66 25 62 55 55 ext. 2227

**Abstract:** Geometries and energetic properties of *p*-methoxy phenylene-vinylene (MeO-PV) derivatives have been studied, based on quantum chemical calculations. Some of the key functional groups (thiophene (Th), pyrrole (Py), fluorene (Fl) and carbazole (Cz)) have been substituted on MeO-PV to investigate the optical properties. All structures have been optimized at the DFT method and the standard 6-31G(d) basis set has been used for B3LYP level of calculation. The electronic transitions of structural geometries have been studied by TD/B3LYP/6-31G(d) calculation based on ground state geometries. The results show that calculated energy gaps of MeO-PV-Th, MeO-PV-Py, MeO-PV-Fl and MeO-PV-Cz are 2.99, 3.00, 3.01 and 3.02 eV, respectively. Additionally, the energy gaps can be rearranged as following: MeO-PV-Th > MeO-PV-Py > MeO-PV-Fl > MeO-PV-Cz. The electronic transitions of all functional substituted compounds are mainly transferred from HOMO to LUMO. The absorption spectra of MeO-PV derivatives show broad absorption peaks covered the range from 300-580 nm. In addition, the main electronic contributions of MeO-PV-Th, MeO-PV-Py, MeO-PV-Fl and MeO-PV-Cz are  $S_0 \rightarrow S_1$  (63.13%),  $S_0 \rightarrow S_1$  (65.51%),  $S_0 \rightarrow S_1$  (65.54%) and  $S_0 \rightarrow S_1$  (62.98%), respectively.

## Introduction

Conducting polymer are an important class of organic semiconductors and may be useful for the construction of flat screen display[1], transistors[2], lasers[3], light-emitting diodes[4] and organic solar cells[5]. Among the numerous conducting polymers, poly(*p*-phenylene vinylene) (PPV) is by far the most extensively studied. PPV, an organic semiconductor with energy gap of 2.5 eV, which has been studied due to the much interests in materials research. Moreover, PPV is a polymer with attractive properties such as high electrical conductivity, electroluminescence, photoluminescence and photoconductivity.

Derivatives of poly(*p*-phenylene vinylene) (PPV) have been examined by attaching methoxy side groups onto the phenylene ring at the C<sub>3</sub> and C<sub>6</sub> (*p*-methoxy phenylene-vinylene (MeO-PV)), leading to an increase of both their solubility and stability. While cyano group substitution [6] on vinylene backbond effects the electronic and optical behaviour because of its electron-accepting capabilities and induces torsion in the molecule due to its size. Furthermore, changing the substitutions [7-9] of the *p*-phenylene vinylene, the

band gap can be fine-tuned the MeO-PV derivatives including thiophene (MeO-PV-Th), pyrrole (MeO-PV-Py), fluorene (MeO-PV-Fl) and carbazole (MeO-PV-Cz) as the donor. The structures of MeO-PV derivatives are shown in Fig. 1.

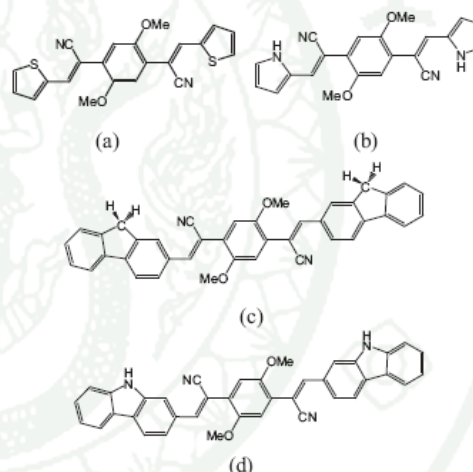


Figure 1. Structural geometries of (a) MeO-PV-Th, (b) MeO-PV-Py, (c) MeO-PV-Fl and (d) MeO-PV-Cz

Thus, the main objective of this work is to investigate structural, electronic properties *p*-methoxy phenylene-vinylene (MeO-PV) derivatives by using density functional theory method [10-14]. Then, the effects of the electron donor or acceptor ring based backbone on the electronic properties of MeO-PV derivatives were studied. The effects of the ring structure on the conformation and electronic properties are discussed in this study.

## Methods

The ground-state geometry and electronic structure of the studied *p*-methoxy phenylene-vinylene (MeO-PV) derivatives are optimized by means of the hybrid density functional theory (DFT) method at the B3LYP level of theory (Becke-style 3-parameter density functional theory with 6-31G(d) (6-31G basis set with



# Electronic Properties of *p*-Methoxy Phenylene Vinylene Derivatives, Investigated by Quantum Chemical Calculation



Suphawarat Phalinyot<sup>1,2</sup>, Songwut Suramitr<sup>1,2\*</sup>, Chuleeporn Luadthong<sup>1,2</sup> and Supa Hannongbua<sup>1,2</sup>

<sup>1</sup>Department of Chemistry, Faculty of Science, Kasetsart University, Bangkok, 10900 Thailand

<sup>2</sup>Center of Nanotechnology, Kasetsart University, Bangkok, 10900 Thailand

\*E-mail: [iscswsm@ku.ac.th](mailto:iscswsm@ku.ac.th), Tel. +66 25 62 55 55 ext. 2227

## Introduction

Poly(phenylene-vinylene) (PPV) is one of the most important conductive polymers. It has been studied due to the interests in materials research because PPV based on high electrical conductivity electro-luminescence, photoluminescence and photoconductivity. Therefore, the main objective of this work is to investigate structural and effects of the electron donor-acceptor based backbone on the electronic properties of *p*-methoxy phenylene-vinylene (MeO-PV) derivatives were studied by using quantum chemical calculations and comparison to available experimental data.

## Methods

The ground-state geometry and electronic structure of *p*-methoxy phenylene-vinylene (MeO-PV) derivatives, MeO-PV-Th, MeO-PV-Py, MeO-PV-Cz and MeO-PV-FI (in Figure 1) are optimized by using hybrid density functional theory (DFT) method at the B3LYP level of theory at 6-31G(d) basis set. Vertical excitation energies (absorption energy) were computed with TD-B3LYP/6-31G(d) method based on the ground state geometries. The results were compared with available experimental data. All calculations were performed on Gaussian 03 program package. In addition, electron density and UV spectrum have been studied by using GaussSum 2.0.6.0 program package.

## Results and discussion

### 1. Electronic properties

The geometry are optimized at the B3LYP/6-31G(d) level of theory. The obtained energy gap ( $E_g$ ) of MeO-PV derivatives (MeO-PV-Th, MeO-PV-Py, MeO-PV-FI and MeO-PV-Cz) are 2.99, 3.00, 3.01 and 3.02 eV, respectively. All structural geometries substituted by cyano groups on the MeO-PV backbone induce distortion in the molecule along the molecular plane. The distortion is large when the cyano groups are substituted on the vinylene moieties due to the electron-accepting.

## MeO-PV derivatives

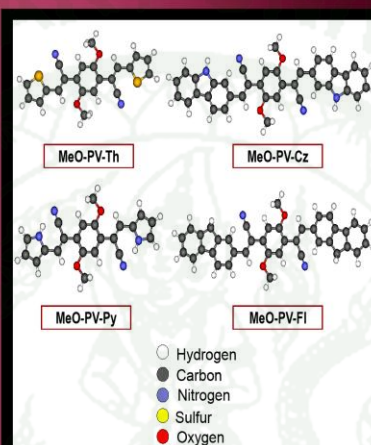


Figure 1. Structural geometries of MeO-PV-Th, MeO-PV-Py, MeO-PV-Cz and MeO-PV-FI.

Table 1 Electron density of MeO-PV-Th

Electronic transition	Energy (eV)	ThV1	CN1	MeO-PV	CN2	ThV2
L+1	-1.73	39	8	7	8	39
L	-2.32	37	3	19	3	37
H	-5.32	26	2	44	2	26
H-1	-6.18	10	1	77	1	10

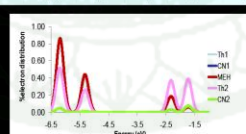


Figure 2. Electron density of MeO-PV-Th.

Table 2 Electronic transition of MeO-PV-Th

Structure	$E_g$ (eV)	$\lambda_{max}$ (nm)	Electronic transition	Oscillator strengths
MeO-PV-Th	2.99 (2.75)*	447 (450)*	H→L (63%)	0.99
MeO-PV-FI	3.00	464	H→L (65%)	1.70
MeO-PV-Cz	3.01	463	H→L (65%)	1.71
MeO-PV-Py	3.02	434	H→L (65%)	1.20

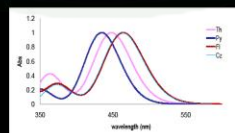


Figure 3. Absorption spectra of MeO-PV derivatives.

## References

- [1] S. Suramitr, T. Kerdcharoen, T. Srikiatthorn and S. Hannongbua, *Synth. Met.* 155 (2005), pp. 27-34.
- [2] V. Chernyak, S.N. Volkov and S. Mukamel, *J. Chem. Phys. A.* 105 (2001), pp. 1988-2004.
- [3] W. Meeto, S. Suramitr, S. Vannarat and S. Hannongbua, *Chem. Phys.* 349 (2008), pp. 1-8.

## Results and discussion

The injection of electrons to MeO-PV derivatives was substituted to both cyano groups and functional groups (Th, Py, FI and Cz) that lead to change in their electronic structures. From the results in Table 1 and Figure 2, the electron distribution of cyano groups and all functional groups are mainly transfer from HOMO to LUMO.

### 2. Absorption properties

The absorption transition energies ( $S_0 \rightarrow S_1$ ) were calculated by TD-B3LYP/6-31G(d) approaches using the ground state optimized geometries by B3LYP/6-31G(d) method. The electronic transition, energy gap, absorption wavelengths and oscillator strengths of MeO-PV derivatives were listed in Table 2. Experimentally, the MeO-PV-Th structure represent the absorption band. It was observed from THF solution at  $\lambda_{max}$  450 nm. While, the calculated absorption wavelengths is 447 nm, which is in strong agreement with the measured experimental data. Furthermore, UV spectrum of all structural geometries was summarized in Figure 3.

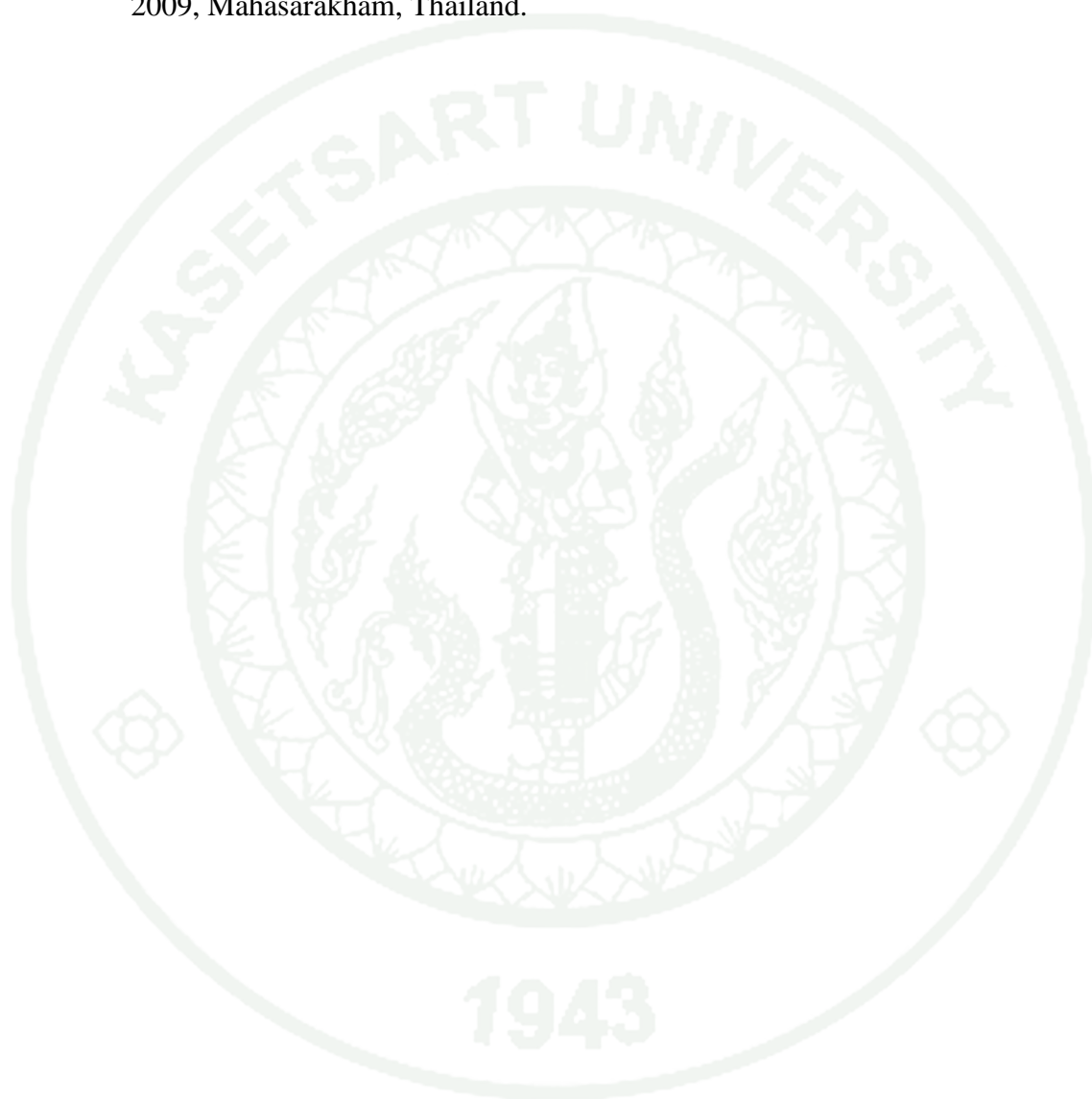
## Conclusion

The cyano groups and functional groups (Th, Py, FI and Cz) were substituted onto the MeO-PV as donor-acceptor lead to change electronic properties. In addition, molecular plan as non-planar has been distorted due to cyano groups substitution. The electronic transitions of all functional substituted compounds are mainly transferred from HOMO to LUMO. The absorption spectra of MeO-PV derivatives shown that broad absorption peaks covered the range from 300-580 nm. Comparisons with available experimental data demonstrated that TDDFT are a very reliable tool for investigating the electronic transitions of MeO-PV.

## Acknowledgements

This work was supported by the Thailand Research Fund (TRF), Commission Higher Education (CHE), the National Center of Excellence for Petroleum, Petrochemicals and Advanced Materials (NCE-PPAM), National Nanotechnology Center (NANOTEC), Laboratory and Applied Chemistry (LCAC) and Kasetsart University Research and Development Institute (KURDI) for research scholars.

Suphawarat Phalinyot, Songwut Suramitr, Chuleeporn Luadthong and Supa Hannongbua. Electronic Properties of 2-Methoxy-5-(2'-ethylhexyloxy)-1,4-phenylene-vinylene based Molecules : Synthesis and Quantum chemical calculations. 6<sup>th</sup> Thai Summer School of Computational Chemistry Workshop, 2009, Mahasarakham, Thailand.





19-22 October 2009

49

S1-P11

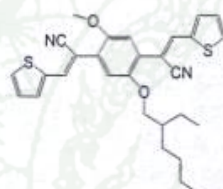
## Electronic Properties of 2-Methoxy-5-(2'-ethylhexyloxy)-1,4-phenylene-vinylene based Molecules : Synthesis and Quantum chemical calculations

Suphawarat Phalinvot,<sup>a,b</sup> Songwut Suramitr,<sup>a,b</sup> Chuleeporn Luadthong<sup>a,b</sup> and Supa Hannongbua<sup>a,b\*</sup>

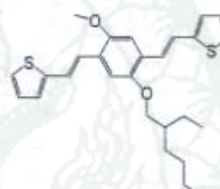
<sup>a</sup>Department of Chemistry, Faculty of Science, Kasetsart University, Jatuchak, Bangkok, Thailand 10900

<sup>b</sup>Center of Nanotechnology KU, and NANOTEC Center of Excellence at Kasetsart University, Kasetsart University, Jatuchak, Bangkok, Thailand 10900

\*E-mail: fscisph@ku.ac.th, Tel: +66-2-562-5555 ext 2140



MEH-ThV-CN



MEH-ThV

Two-based molecules [1',4'-Bis(thienyl-vinyl)]-2-methoxy-5-(2'-ethylhexyloxy)-1,4-phenylene vinylene (MEH-ThV) and [1',4'-Bis(thienyl-1,1'-cyanovinyl)]-2-methoxy-5-(2'-ethylhexyloxy)-1,4-phenylene vinylene (MEH-ThV-CN) were synthesized. The molecules, which contain both the phenyl, vinyl and thiophene moieties in the molecules were characterized by <sup>1</sup>H-NMR, FT-IR, and UV-visible spectrometry. Their compounds are readily soluble in common organic solvents, acetonitrile, THF and chloroform. All of these compounds exhibited strong absorption at around 383 nm which can be attributed to either the charge transfer between moieties segment of the molecules. The optical absorption spectra of two monomers were calculated using time-dependent density functional theory (TD-B3LYP/6-31G(d)//HF/6-31G(d)). It can be shown that the energy gap of MEH-ThV-CN and MEH-ThV are 3.87 and 3.38 eV and absorption maximum ( $\lambda_{max}$ ) are 385.85 and 394.39 nm, respectively, which corresponds to the available experimental optical absorption of MEH-ThV-CN (383.85 nm) in THF solution.

**Keywords:** [1',4'-Bis(thienyl-vinyl)]-2-methoxy-5-(2'-ethylhexyloxy)-1,4-phenylene vinylene (MEH-ThV), [1',4'-Bis(thienyl-1,1'-cyanovinyl)]-2-methoxy-5-(2'-ethylhexyloxy)-1,4-phenylene vinylene (MEH-ThV-CN), Hartree-fock (HF) and density function theory (DFT)

### Selected References:

1. Colladet, K.; Fourier, S.; Cleij, T. J.; Lutsen, L.; Gelan, J.; Vanderzande, D.; Huong Nguyen, L.; Neugebauer, H.; Sariciftci, S.; Aguirre, A.; Janssen, G.; Goovaerts, E. *Macromolecules*, 2007, 40, 65-72.
2. Hou, J.; Yang, C.; Qiao, J.; Li, Y. *Synth. Met.*, 2005, 150, 297-304.
3. Suramitr, S.; Kerdcharoen, T.; Srihirin, T.; Hannongbua, S. *Synth. Met.*, 2005, 155, 27-34.



# Electronic Properties of 2-Methoxy-5-(2'-ethylhexyloxy)-1,4-phenylene-vinylene based Molecules : Synthesis and Quantum chemical calculations



Suphawarat Phalinyot<sup>1,2</sup>, Songwut Suramit<sup>1,2\*</sup>, Chuleeporn Luadthong<sup>1,2</sup> and Supa Hannongbua<sup>1,2</sup>

<sup>1</sup>Department of Chemistry, Faculty of Science, Kasetsart University, Bangkok, 10900 Thailand

<sup>2</sup>Center of Nanotechnology, Kasetsart University, Bangkok, 10900 Thailand

\*E-mail: [fsciswsm@ku.ac.th](mailto:fsciswsm@ku.ac.th), Tel. +66 25 62 55 55 ext. 2227



## Introduction

Poly(2-methoxy-5-[2'-ethyl-hexyloxy]-phenylene vinylene (MEH-PPV) based on conjugated polymers with a optical gap 2.17 eV, which has been studied extensively because of it promising applications in light-emitting diodes (LEDs), field effect transistors (FETs), solid-state lasers, and photovoltaics. This is due to advantages of these materials as compared to inorganic semiconductors, including low weight, easy of processing, flexibility, and low fabrication cost. Furthermore, when an organic conjugated system combines with donor-acceptor groups or fused with other conjugated ring, its band gap may be further reduced. So, we interested in study the structures of (2-methoxy-5-[2'-ethyl-hexyloxy]-phenylene vinylene (MEH-PV) based molecules with donor-acceptor groups. In this work, our goal is observe by comparison between experimental and theoretical calculation. We synthesized and characterize of [1,4-Bis(thienyl-vinylene)]-2-methoxy-5-(2-methylhexyloxy)phenylene (MEH-ThV) and [1,4-Bis(thienyl-1,1'-cyanovinylene)]-2-methoxy-5-(2-methylhexyloxy)phenylene (MEH-ThV-CN). The structure consists of a central dialkoxyphenylene core (donor), para-disubstituted by two thiophene derivatives (donor) through a cyanovinylene linker (acceptor). Quantum chemical calculations are an important tool to investigated the relation between the optical properties of MEH-ThV and MEH-ThV-CN and comparison with the experimental results.

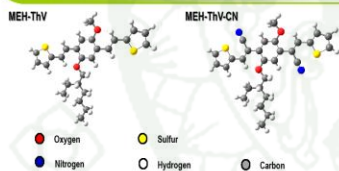


Figure 1. Molecular structures of MEH-ThV and MEH-ThV-CN.

## Experimental and Theoretical

### Synthesis and Characterization

The MEH-ThV-CN molecule was prepared from 1,4-Bis(chloromethyl)-2-((2'-ethylhexyloxy)-5-methoxybenzene, sodium cyanide in anhydrous DMF solution. The mixture was combined with thiophene-2-carbaldehyde, potassium tert-butoxide in methanol, next the crude product was recrystallized to obtain a pale yellow. The characterization were determined from <sup>1</sup>H-NMR, FT-IR and UV-Vis spectrometry.

### Computational details

We have been investigated the electronic properties of MEH-ThV and MEH-ThV-CN by using a quantum chemical calculations. The geometries were optimized by HF/6-31G(d) level. The absorption properties were calculated at TD-B3LYP/6-31G(d) level. All calculations have been performed using Gaussian03 program.

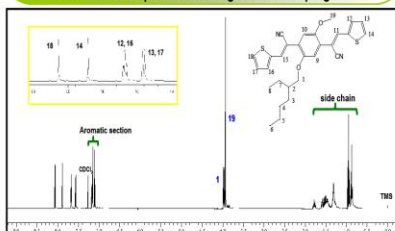


Figure 2. Spectrum <sup>1</sup>H-NMR of the MEH-ThV-CN molecule in CDCl<sub>3</sub> solvent.

### References

- Collard, K.; Fourier, S.; Cleij, T.J.; Lutsen, L.; Gelan, J.; Vanderzande, D.; Huang Nguyen, L.; Neugebauer, H.; Sanicifti, S.; Aguirre, A.; Janssen, G.; Goovaerts, E. *Macromolecules* **2007**, *40*, 65.
- Hou, J.; Yang, C.; Qiao, J.; Li, Y. *Synthetic Metals* **2005**, *150*, 297.
- Suramit, S.; Kerdrachon, T.; Srikhin, T.; Hannongbua, S. *Synthetic Metals* **2005**, *155*, 27.

## Results and Discussion

### 1. Synthesis and Characterization of the MEH-ThV-CN

The cyanogroup on the ary unit is the acceptor group, can be easily obtained by nucleophilic substitution. It was obtained with a yield of 90.38% as a white solid in Fig. 3 (a). Thiophene carboxaldehyde as the donor groups was prepared via a Knoevenagel condensation. The product was obtained as a pale orange (yield 58.43%), as shown in Fig. 3 (b). The <sup>1</sup>H-NMR spectrum confirms the MEH-ThV-CN structure (Fig. 2), exhibiting the chemical shift of alkyl chains at 0.85-1.808 ppm. The methoxy (CH<sub>3</sub>O-) <sup>1</sup>H and methyleneoxy protons (-CH<sub>2</sub>O-) <sup>1</sup>H appear at 3.95 ppm (3H, s) and 3.96 ppm (2H, d). The phenyl ring protons are found in the range of 7.09-7.17 ppm. The thiophene rings protons at 7.5-8.5 ppm. In the FT-IR spectrum of MEH-ThV-CN, the C≡N stretching band (2271 cm<sup>-1</sup>) and the %transmission peak at 3150 cm<sup>-1</sup> was assigned to C-H stretching of the aromatic ring (data is not show). MEH-ThV is under synthesized.

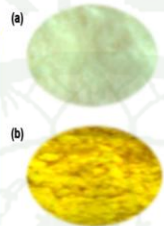


Figure 3. Compounds were substituted with (a) cyano groups (acceptor) and (b) thiophene rings (donor) or MEH-ThV-CN molecule.

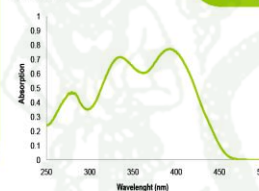


Figure 4. The absorption spectrum of the MEH-ThV-CN dilute in THF solution.

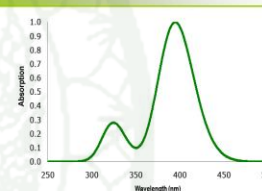


Figure 5. The absorption spectrum of the MEH-ThV-CN calculated from TD-B3LYP/6-31G(d) method.

Table 1: Electronic transition data ( $S_0 \rightarrow S_1$ ) of the MEH-ThV as obtained by TDDFT/B3LYP-6-31G(d) method

Conformation	Excited-state	Energy gap (eV)	Electronic transition (coefficient)	Wavelength	Oscillator strengths
MEH-ThV	$S_0 \rightarrow S_1$	3.14	H $\rightarrow$ L (0.64)	394.38	1.2513
	$S_0 \rightarrow S_2$	3.81	H-1 $\rightarrow$ L (0.55)	325.82	0.1392
	$S_0 \rightarrow S_3$	3.83	H-2 $\rightarrow$ L (0.50)	323.83	0.211
MEH-ThV-CN	$S_0 \rightarrow S_1$	3.25(3.23) <sup>a</sup>	H $\rightarrow$ L (0.69)	380.77(383.85) <sup>a</sup>	0.0628
	$S_0 \rightarrow S_2$	3.37	H $\rightarrow$ L+1 (0.69)	367.86	0.0074
	$S_0 \rightarrow S_3$	3.94	H-1 $\rightarrow$ L (0.66)	314.43	0.0478

Figure 6. Energy diagram of the MEH-ThV and MEH-ThV-CN

<sup>a</sup> Absorption band measured in THF solution

### 2. Electronic properties

The ground-state geometries of the MEH-ThV and MEH-ThV-CN was determined by a full optimization at HF/6-31G(d) method. The cyano groups are twisted (torsion angle > 50°) leading to non-planar structure, while the geometry of the MEH-ThV is planar along the main chain. The HOMO-LUMO energy level are shown in Fig. 6. The energy gap of MEH-ThV and MEH-ThV-CN be obtained are 3.38 and 3.87, respectively.

### 3. Absorption properties

The absorption transition energies ( $S_0 \rightarrow S_1$ ) were calculated by TD-B3LYP/6-31G(d). The electronic transition, energy gap, absorption wavelengths and oscillator strengths of both molecules were listed in Table 1. The absorption spectrum of MEH-ThV-CN from experiment is show in Fig. 4. It was observed in tetrahydrofuran (THF) solution at  $\lambda_{max}$  393 nm (3.23 eV) (Fig. 4). While, the calculated absorption wavelengths is 380 nm (3.23 eV) (table 1), which is in strong agreement with the measured experimental data.

## Conclusions

MEH-PPV based molecules were substituted with cyano groups (acceptor) and thiophene rings (donor) lead to change structures properties and electronic properties. In addition, molecular plan as non-planar has been distorted due to cyano groups substitution result in higher the energy gap of the MEH-ThV-CN higher than the MEH-ThV molecule. TDDFT are a very reliable tool for investigating the electronic transitions of the MEH-ThV-CN, due to it gives similar wavelength to the experimental.

### Acknowledgements

This work was supported by the Thailand Research Fund (RTA5080005), Kasetsart University Research and Development Institute (KURDI), Office of the Higher Education Commission, Ministry of Education, the National Center of Excellence for Petroleum, Petrochemicals, and Advanced Materials (NCE-PPAM), Large scale Simulation Research Laboratory (LSR), NECTEC, The Center of Nanotechnology, Kasetsart University, The 6<sup>th</sup> Thai Summer School of Computational Chemistry Workshop.

## 2. Proceeding

Suphawarat Phalinyot, Songwut Suramitr, Chuleeporn Luadthong and Supa Hannongbua. Electronic properties of *p*-Methoxy phenylene-vinylene derivatives, investigated by Quantum Chemical Calculations. Pure and Applied Chemistry International Conference of Thailand, 2009, Naresuan University, Phitsanulok, Thailand.

## 3. Oral Presentation

Suphawarat Phalinyot, Songwut Suramitr, Chuleeporn Luadthong and Supa Hannongbua. Electronic Properties Study for All Stereoisomers of [1',4'-Bis(thienyl-vinyl)]-2-methoxy-5-(2'-ethylhexyloxy)-1,4-phenylene vinylene by Quantum Chemical Calculations. 4<sup>th</sup> Asian Pacific Conference of Theoretical & Computational Chemistry, 2009, Port Dickson, Malaysia.



- S012 -

### Electronic Properties Study for All Stereoisomers of [1',4'-Bis(thienyl-vinyl)]-2-methoxy-5-(2'-ethylhexyloxy)-1,4-phenylene vinylene by Quantum Chemical Calculations

Suphawarat Phalinyot<sup>1,2</sup>, Songwut Suramitr<sup>1,2</sup>, Chuleeporn Luadthong<sup>1,2</sup>  
and Supa Hannongbua<sup>1,2\*</sup>

<sup>1</sup>Department of Chemistry, Faculty of Science, Kasetsart University, Jatuchak, Bangkok, Thailand 10900

<sup>2</sup>Center of Nanotechnology KU, and NANOTEC Center of Excellence at Kasetsart University, Kasetsart University, Jatuchak, Bangkok, Thailand 10900

\*E-mail: fscisph@ku.ac.th, Tel: +66-2-562-5555 ext 2140

Three stereoisomers, EE, EZ and ZZ isomers, of [1',4'-Bis(thienyl-vinyl)]-2-methoxy-5-(2'-ethylhexyloxy)-1,4-phenylene vinylene (MEH-ThV) were studied the structural and electronic properties. The optical absorption spectra of three stereoisomers were calculated by using time-dependent density functional theory (TD-B3LYP/6-31G(d,p)//B3LYP/6-31G(d,p)). In addition, spectrums 1H-NMR were calculated for exhibition of shielding or deshielding effects in each configuration. For the results we found that all of these compounds exhibited strong absorption in the visible region. EE isomer is red-shifted more than other structures. This can be attributed to either the charge transfer between moieties segment of the molecules.

#### References

1. Colladet, K.; Fourier, S.; Cleij, T. J.; Lutsen, L.; Gelan, J.; Vanderzande, D.; Huong Nguyen, L.; Neugebauer, H.; Sariciftci, S.; Aguirre, A.; Janssen, G.; Goovaerts, E. *Macromolecules* **2007**, *40*, 65.
2. Xue, C.; Luo, F.-T. *Synthetic Metals* **2004**, *145*, 67..
3. Suramitr, S.; Kerdcharoen, T.; Srihirin, T.; Hannongbua, S. *Synthetic Metals* **2005**, *155*, 27

## CURRICULUM VITAE

**NAME** : Miss Suphawarat Phalinyot

**BIRTH DATE** : July 31, 1984

**BIRTH PLACE** : Roi-Et, Thailand

**EDUCATION** : 

<u>YEAR</u>	<u>INSTITUTION</u>	<u>DEGREE/DIPLOMA</u>
2007	Maharakham University	B.Sc.(Chemistry)

**SCHOLARSHIP** :

- 1) Thailand Research Fund (RTA5080005)
- 2) Commission on Higher Education (CHE)
- 3) The Kasetsart University Research and Development Institute (KURDI), and National Nanotechnology Center (NANOTEC)
- 3) Postgraduate Education and Research Programs in Petroleum and Petrochemicals, and Advanced Materials (NCE-PPAM)
- 4) Kasetsart University Research and Development Institute (KURDI)